UNIVERSIDADE FEDERAL DE SANTA CATARINA
CENTRO TECNOLÓGICO
PROGRAMA DE PÓS-GRADUAÇÃO EM ENGENHARIA DE ALIMENTOS

Anderson Felipe Viana da Silva

MEMBRANE FUNCTIONALIZATION WITH TITANIUM DIOXIDE USING POLYDOPAMINE AS BINDING AGENT: ASSESSMENT OF THE SEPARATION OF OILY COMPOUNDS AND PHOTOCATALYTIC PERFORMANCE

Florianópolis
2023

Anderson Felipe Viana da Silva

MEMBRANE FUNCTIONALIZATION WITH TITANIUM DIOXIDE USING POLYDOPAMINE AS BINDING AGENT: ASSESSMENT OF THE SEPARATION OF OILY COMPOUNDS AND PHOTOCATALYTIC PERFORMANCE

Thesis subjected to the Graduate Program in Food Engineering from the Federal University of Santa Catarina as a requirement to obtain the degree Doctor (Dr.) in Food Engineering.
Advisor: Prof. Alan Ambrosi, Dr.
Co-advisors: Prof. Marco Di Luccio, Dr.
Prof. José Vladimir de Oliveira, Dr.

Florianópolis

2023

da Silva, Anderson Felipe Viana da Silva
MEMBRANE FUNCTIONALIZATION WITH TITANIUM DIOXIDE USING POLYDOPAMINE AS BINDING AGENT: ASSESSMENT OF THE SEPARATION OF OILY COMPOUNDS AND PHOTOCATALYTIC PERFORMANCE / Anderson Felipe Viana da Silva da Silva ; orientador, Alan Ambrosi Ambrosi, coorientador, Marco Di Luccio Di Luccio, coorientador, José Vladimir de Oliveira de Oliveira, 2023.
151 p.

Tese (doutorado) - Universidade Federal de Santa Catarina, Centro Tecnológico, Programa de Pós-Graduação em Engenharia de Alimentos, Florianópolis, 2023.

Inclui referências.

1. Engenharia de Alimentos. 2. Processos com membranas. 3. Modificação de membranas. 4. Emulsões oleosas. 5. Fotocatálise. I. Ambrosi, Alan Ambrosi. II. Di Luccio, Marco Di Luccio. III. de Oliveira, José Vladimir de Oliveira IV. Universidade Federal de Santa Catarina. Programa de Pós-Graduação em Engenharia de Alimentos. V. Título.

Anderson Felipe Viana da Silva

MEMBRANE FUNCTIONALIZATION WITH TITANIUM DIOXIDE USING POLYDOPAMINE AS BINDING AGENT: ASSESSMENT OF THE SEPARATION OF OILY COMPOUNDS AND PHOTOCATALYTIC PERFORMANCE

O presente trabalho em nível de Doutorado foi avaliado e aprovado, em 25 de agosto de 2023, pela banca examinadora composta pelos seguintes membros:

Prof.(a) Liliane Damaris Pollo, Dr.(a)
Universidade Federal do Rio Grande do Sul - UFRGS

Prof.(a) Ana Cláudia Vaz de Araújo, Dr.(a)
Universidade Federal Rural de Pernambuco - UFRPE

Prof.(a) Sergio Yesid Gómez González, Dr.(a)
Universidade Federal de Santa Catarina - UFSC

Certificamos que esta é a versão original e final do trabalho de conclusão que foi julgado adequado para obtenção do título de Doutor em Engenharia de Alimentos.

Documento assinado digitalmente
Jaciane Lutz Ienczak
Data: 17/11/2023 10:02:36-0300
CPF: ***.280.630-**
Verifique as assinaturas em https://v.ufsc.br

Coordenação do Programa de Pós-Graduação

Documento assinado digitalmente
Alan Ambrosi
Data: 17/11/2023 10:03:10-0300
CPF: ***.340.800-**
Verifique as assinaturas em https://v.ufsc.br

Prof. Alan Ambrosi, Dr.
Orientador

Florianópolis, 2023.

Dedico este trabalho inteiramente à minha amada família,
em especial à minha mãe e irmãos, que foram os maiores
incentivadores das minhas realizações e sonhos
Muito obrigado

ACKNOWLEDGMENT

À minha família, em especial à minha mãe Raquel, que sempre me dedicou muito amor, aos meus irmãos Alexsandra e Alison, e aos meus sobrinhos Isaak, Adam e Bryan, por emanarem felicidade e tornarem a família mais alegre. Sem o amor, o apoio e o encorajamento deles, este trabalho não seria possível. Agradeço por estarem sempre presentes em todos os momentos da minha vida e por serem a minha constante fonte de inspiração e força, mesmo com toda a distância que foi necessária neste momento. Muito obrigado por tudo.

Aos professores Dr. Alan Ambrosi, Dr. Marco Di Luccio e Dr. José Vladimir de Oliveira, por sua orientação e apoio durante a realização desta tese. Suas valiosas orientações, percepções e sugestões foram fundamentais para moldar minhas ideias e aprimorar a qualidade deste trabalho. Agradeço por dedicarem seu tempo, por compartilharem seus conhecimentos e por incentivarem meu crescimento como pesquisador.

A todos os meus amigos que me acompanharam nessa jornada durante esses últimos anos, em especial a Jonas da Silva, por ser meu amigo confidente e me auxiliar de maneira tão significativa nesta trajetória, se mostrando um farol nos momentos mais sombrios e me motivando a cada conquista. Essa jornada não seria a mesma sem os amigos que fiz, sem vocês esse trabalho não seria o mesmo.

Aos meus colegas do LABSEM por todos os momentos de descontração e ajuda no dia a dia no laboratório, em especial a Renata Vicente, por ser minha parceira no LABSEM e me ajudar tanto nos momentos de desespero. A jornada se tornou mais prazerosa com pessoas que me incentivavam e inspiravam ao meu redor.

A todos os meus professores que me acompanharam até hoje em toda minha vida acadêmica. Agradeço de forma especial à professora Dra. Ana Cláudia Vaz de Araújo, por ter sido a minha primeira orientadora e ter plantado a semente da pesquisa no meu coração, fazendo com que fosse possível eu me tornar o pesquisador que sou hoje.

Ao pessoal do LATESC, LINDEN, LEMA, LCME e da Central de análises, pela colaboração no uso de equipamentos e no processo de caracterização necessário.

Por fim, agradeço à banca pelas contribuições feitas ao trabalho, a Universidade Federal de Santa Catarina pela infraestrutura e à CAPES e ao CNPq, pelo auxílio financeiro e a bolsa concedida.

“A felicidade pode ser encontrada mesmo nas horas
mais difíceis, se você se lembrar de acender a luz”
Alvo Dumbledore

RESUMO

A contaminação dos corpos hídricos por compostos oleosos é um problema ambiental que vem ganhando espaço em pesquisas científicas nos últimos anos, uma vez que esses compostos normalmente encontram-se emulsionados no meio, dificultando a sua separação. Uma gama de processos físicos e químicos pode ser utilizada para minimizar ou evitar os efeitos adversos causados pela presença de compostos oleosos em águas residuais. O trabalho em questão busca obter uma membrana fotocatalítica para tratamento desses compostos, combinando a função fotocatalítica de um catalisador com a separação obtida com os processos com membranas, e então, otimizar o tratamento desse tipo de efluente. Este estudo investiga e demonstra um método prático de modificação da superfície da membrana de poli(fluoreto de vinilideno) (PVDF) com polidopamina (PDA) e TiO_2 para obter membranas fotocatalíticas. Para tanto, inicialmente uma membrana de PVDF foi modificada com concentrações de TiO_2 variando de 0,2 a 2,0% em massa. A deposição de TiO_2 foi confirmada por um pico característico de TiO_2 na análise de difração de raios-X (DRX). Micrografias de microscopia eletrônica de varredura (MEV) mostraram que o processo de modificação com PDA causou alguma obstrução dos poros. No entanto, a membrana modificada com 1,0% de TiO_2 apresentou a maior permeância à água, indicando que esta incorporação promoveu maior hidrofilicidade para a membrana. Posteriormente, o efeito de diferentes concentrações de PDA e TiO_2 na solução usada na modificação foi avaliado com relação à permeância à água, rejeição de TOC e capacidade de degradação fotocatalítica. Os resultados mostraram que a incorporação de PDA e TiO_2 conferiu propriedades anti-incrustantes à membrana, com permeância à água, rejeição de TOC e degradação fotocatalítica chegando a 781 kg h^{-1} bar^{-1} m^{-2}, 87% e 97%, respectivamente, ao utilizar concentração de DA de 0,92 g L^{-1}, uma quantidade de TiO_2 de 1,39% e uma velocidade de agitação de 106 rpm na modificação. Após o processo de autolimpeza fotocatalítica, a recuperação do fluxo atingiu 86%, indicando que a presença de TiO_2 melhorou as propriedades anti-incrustante da membrana. Essas descobertas sugerem que a incorporação de PDA e TiO_2 pode melhorar a separação de compostos oleosos, reduzir a incrustação e promover a autolimpeza a partir da modificação superficial da membrana. Este estudo fornece informações valiosas para o desenvolvimento de processos de separação, nos quais o uso de PDA e TiO_2 como modificadores de superfície pode ser uma estratégia eficaz para melhorar o desempenho e a durabilidade das membranas de PVDF em aplicações de tratamento de águas residuais oleosas.

Palavras-chave: Processos com membranas. Modificação de membranas. Dopamina. Titânia. Emulsões oleosas.

RESUMO EXPANDIDO

Introdução

A disposição inadequada de efluentes industriais contendo compostos oleosos é um problema ambiental preocupante. Diversas indústrias, como petroquímicas, metalúrgicas, alimentícias, de couro e acabamento de metais, produzem grandes volumes de efluentes oleosos, que podem conter gorduras, hidrocarbonetos e frações de petróleo. Esses compostos representam uma ameaça ao meio ambiente e à saúde humana devido à presença de substâncias tóxicas.

Os processos que utilizam membranas surgem como uma alternativa promissora aos métodos convencionais para a separação de diferentes compostos em efluentes industriais. Embora muitas aplicações já tenham sido desenvolvidas, há ainda desafios a serem superados para melhorar o desempenho de separação, a resistência à incrustação e a estabilidade das membranas. As técnicas fotocatalíticas são uma alternativa promissora para superar algumas dessas limitações. Nesse processo, um fotocatalisador produz radicais altamente reativos quando exposto a uma fonte de luz apropriada. Esses radicais podem degradar e/ou remover compostos tóxicos e incrustantes depositados na superfície da membrana. No entanto, a incorporação do catalisador à membrana ainda precisa ser amplamente estudada, pois existem muitos métodos com vantagens e desvantagens.

A modificação da superfície da membrana é uma das maneiras de melhorar a seletividade da membrana e incorporar diferentes materiais. Nos últimos anos, o uso de polidopamina (PDA) como agente de ligação entre a membrana e o material de modificação tem ganhado destaque. Essa técnica é inspirada nas secreções adesivas dos mexilhões, que formam uma forte interação com diferentes substratos em condições úmidas e pode ser utilizada com diversos materiais. O TiO_2 é um composto versátil, barato, estável, abundante e ecológico, amplamente descrito na literatura como tendo uma grande capacidade fotocatalítica e uma natureza hidrofílica, o que o torna ideal para modificações em membranas usadas na separação óleo/água.

Objetivo

Este estudo tem como objetivo apresentar um método alternativo de modificação de membrana polimérica usando PDA e TiO_2 para melhorar a hidrofilicidade da membrana e avaliar sua capacidade fotocatalítica de autolimpeza. Até o momento, não há relatos na literatura sobre a modificação da membrana de PVDF usando PDA e TiO_2 em uma única e simples etapa. Além disso, a investigação e otimização dos parâmetros de modificação da membrana de PVDF usando PDA e TiO_2 e a avaliação da capacidade fotocatalítica também não foram relatadas anteriormente.

Materiais e métodos

O processo de modificação das membranas foi realizado. Para isso, inicialmente foi preparada uma solução de cloridrato de dopamina em solução tampão Tris-HCl (pH 8,5, 50 mM) e adicionado em um erlenmeyer de 125 mL, logo em seguida o TiO_2 foi adicionado a essa solução e homogeneizado. A membrana de PVDF previamente preparada e cortada em discos (5 cm) foi então adicionada ao erlenmeyer, imersa na solução, levada ao agitador orbital (Solab, SL-223, Brasil) por 24 h na temperatura de 30 °C. Depois de completar o tempo de reação, a membrana foi enxaguada com água ultrapura para remover o excesso de solução não aderida à superfície, seca em estufa a 65 °C por 24h e armazenada para posterior caracterização.

Inicialmente foi avaliado o processo de modificação das membranas utilizando uma concentração de 2,0 g L^{-1} de dopamina e TiO_2 variando de 0,2 a 2,0% (m/v) e mantendo fixa a agitação do meio em 160 rpm. A superfície modificada das membranas foi caracterizada em relação à incorporação do TiO_2 a partir de análises de FTIR, DRX e MEV. A hidrofilicidade/hidrofobicidade das membranas obtidas a partir da molhabilidade. O desempenho de permeação das membranas frente a uma emulsão padrão também foi analisado.

Dentro dos resultados obtidos de forma efetiva inicialmente, os experimentos seguiram então variando as condições de modificação da superfície da membrana a partir de um delineamento composto central rotacional (DCCR) 2^3, tendo como fatores a concentração de dopamina (0,7 a 2,3 g L^{-1}), a concentração de TiO_2 (0,7 a 2,3% m/v) e a velocidade de agitação no processo de modificação (106 a 174 rpm). A superfície modificada das membranas foi caracterizada utilizando FTIR, DRX e MEV. Além disso, avaliou-se o desempenho de permeação das membranas frente a uma emulsão padrão e o desempenho das membranas na degradação de um contaminante padrão. A capacidade autolimpante da membrana com melhor resultado no DCCR também foi testada.

Resultados e discussão

A deposição de TiO_2 foi confirmada pela presença do pico característico de TiO_2 no difratograma de raios-X (DRX). As micrografias de microscopia eletrônica de varredura (MEV) mostraram que o processo de modificação com polidopamina causou uma certa obstrução dos poros. No entanto, observou-se que a membrana modificada com 1,0% de TiO_2 apresentou maior permeabilidade hidráulica do que a membrana pura, indicando que esta incorporação promoveu uma maior hidrofilicidade para a membrana.

Posteriormente, o efeito de diferentes concentrações de PDA e TiO_2, além da agitação do meio foi avaliado na modificação, com relação a permeabilidade hidráulica, rejeição de TOC e capacidade de degradação fotocatalítica. Os resultados mostraram que a incorporação de PDA e TiO_2 melhorou as propriedades anti-incrustante da membrana, com permeabilidade hidráulica atingindo 781 kg h^{-1} bar^{-1} m^{-2}, rejeição de TOC atingindo 87% e degradação fotocatalítica atingindo 97%. As condições utilizadas foram uma concentração de dopamina de 0,92 g L^{-1}, uma quantidade de TiO_2 de 1,39% e uma velocidade de agitação de 106 rpm.

Após o processo de autolimpeza fotocatalítica, a recuperação do fluxo atingiu 86%, indicando que a presença de TiO_2 conferiu propriedades anti-incrustantes à membrana. Os resultados experimentais sugerem que a incorporação de TiO_2 usando PDA aumenta a hidrofilicidade da membrana e melhora sua permeabilidade à água. Além disso, a incorporação de TiO_2 também leva à formação de espécies reativas de oxigênio, que, sob irradiação UV, podem efetivamente degradar os compostos orgânicos incrustados na superfície da membrana e melhorar o seu desempenho de autolimpeza. As descobertas deste estudo podem ter implicações significativas para o desenvolvimento de tecnologias de tratamento de água mais eficientes e sustentáveis.

Conclusão

O tratamento de águas residuais oleosas é um problema desafiador que os métodos convencionais ainda não conseguiram resolver totalmente. No entanto, membranas fotocatalíticas têm mostrado resultados promissores na degradação de poluentes orgânicos na superfície da membrana sob irradiação UV. A incorporação de fotocatalisadores na estrutura da membrana usando modificação assistida por PDA aumentou significativamente a eficiência da membrana e a incorporação de TiO_2 em membranas de PVDF usando PDA produziu membranas fotocatalíticas autolimpantes capazes de serem utilizadas por vários ciclos de permeação. Embora mais pesquisas sejam necessárias para avaliar a sua praticidade e

estabilidade a longo prazo, essas descobertas sugerem que essa abordagem oferece uma solução promissora e eficaz para o tratamento de águas residuais oleosas.

Palavras-chave: Processos com membranas. Modificação de membranas. Dopamina. Titânia. Emulsões oleosas.

ABSTRACT

Contamination of water bodies by oily compounds is an environmental problem that has been gaining ground in scientific research in recent years since these compounds are normally found emulsified in the medium, making their separation difficult. A range of physical and chemical processes can be used to minimize or avoid the adverse effects caused by the presence of oily compounds in wastewater. The work in question seeks to obtain a photocatalytic membrane for treating these compounds, combining the photocatalytic function of a catalyst with the separation obtained with membrane processes and then optimizing the treatment of this type of effluent. This study investigates and demonstrates a practical method of surface modification of poly(vinylidene fluoride) (PVDF) membranes with polydopamine (PDA) and TiO_2 to obtain photocatalytic membranes. For this purpose, a PVDF membrane was initially modified with TiO_2 concentrations ranging from 0.2 to 2.0% by mass. TiO_2 deposition was confirmed by a characteristic TiO_2 peak in X-ray diffraction analysis (XRD). Scanning electron microscopy (SEM) micrographs showed that the PDA modification process caused some pore clogging. However, the membrane modified with 1.0% TiO_2 showed greater water permeance, indicating that this incorporation promoted greater hydrophilicity for the membrane. Subsequently, the effect of different concentrations of PDA and TiO_2 in the solution used in the modification was evaluated in terms of water permeance, TOC rejection, and photocatalytic degradation capacity. The results showed that the incorporation of PDA and TiO_2 conferred antifouling properties to the membrane, with water permeance, TOC rejection, and photocatalytic degradation reaching 781 kg h^{-1} bar^{-1} m^{-2}, 87%, and 97%, respectively, when using a DA concentration of 0.92 g L^{-1}, an amount of TiO_2 of 1.39% and an agitation speed of 106 rpm in the modification. After the photocatalytic self-cleaning process, flux recovery reached 86%, indicating that the presence of TiO_2 improved the antifouling properties of the membrane. These findings suggest that incorporating PDA and TiO_2 can improve the separation of oily compounds, reduce fouling, and promote self-cleaning through surface modification of the membrane. This study provides valuable information for the development of separation processes, in which using PDA and TiO_2 as surface modifiers can be an effective strategy to improve the performance and durability of PVDF membranes in oily wastewater treatment applications.

Keywords: Membrane processes. Membrane modification. Polydopamine. Titania. Oil emulsions.

LIST OF FIGURES

LIST OF TABLES

LIST OF ABREVIATIONS AND SYMBOLS

4-CP	p-chlorophenol
AgCl	Silver chloride
ANOVA	Analysis of variance
AOP	Advanced oxidative processes
ATR	Attenuated total reflection
$Bi_{12}O_{17}Cl_2$	Bismuth oxyhalide
bPEI	Branched poly(ethylenimine)
CAPES	Coordenação de Aperfeiçoamento de Pessoal de Nível Superior
CB	Conduction band
CCRD	Central composite rotational design
CNPq	Conselho Nacional de Desenvolvimento Científico e Tecnológico
COD	Chemical oxygen demand
CR	Congo red
CuO	Copper oxide
CV	Crystal violet
DA	Dopamine
DHI	5,6-dihydroxyindole
FM	Functional materials
FTIR	Fourier transform infrared spectroscopy
g-C_3N_4	Graphitic carbon nitride
GO	Graphene oxide
GSH	Thiolate graphene
LDH	Layers-double of hydroxide composite
L-DOPA	3,4-dihydroxy-L-phenylalanine
MB	Methylene blue
MF	Microfiltration
MO	Methyl orange
MOF	Metal-organic framework
MR	Methyl red
MSP	Membrane separation processes

MXene	Two-dimensional inorganic compound
NF	Nanofiltration
PAA	Poly(acrylic acid)
PAN	Polyacrylonitrile
PANI	Polyaniline
PDA	Polydopamine
PEN	Poly(arylene nitrile ether)
PET	Polyethylene terephthalate
PP	Polypropylene
PVA	Polyvinyl acetate
PVDF	Poly(vinylidene fluoride)
RGO	Reduced graphene oxide
RhB	Rhodamine B
RO	Reverse osmosis
SDS	Sodium dodecyl sulfate
SEM	Scanning electron microscopy
SSM	Stainless-steel mesh
TiO_2	Titanium dioxide
TOC	Total organic carbon
UF	Ultrafiltration
UOCA	Underwater oil contact angle
UV	Ultraviolet
VB	Valence band
WO_3	Tungsten oxide
XRD	X-ray diffraction
ZIF	Zeolitic imidazolate framework
ZnO	Zinc oxide
ZrO2	Zirconium dioxide
β-FeOOH	Beta iron oxyhydroxide nanoparticles (akaganéite)

SUMMARY

THESIS CONCEPTUAL SCHEME

Membrane functionalization with titanium dioxide using polydopamine as binding agent: assessment of the separation of oily compounds and photocatalytic performance

What?
- Investigate the feasibility of obtaining self-cleaning photocatalytic membranes for degradation and separation of oily compounds through surface modification of a commercial poly(vinylidene fluoride) (PVDF) membrane using dopamine and titanium dioxide.

Why?
- Oily compounds are one of the most abundant residues found in water sources.
- There is a need to improve and enhance the use of membrane-based separation processes in the treatment of water/wastewater containing oily compounds.
- A better understanding of the characteristics of polymeric membranes modified by surface deposition of inorganic materials (catalysts such as titanium dioxide and polydopamine) is required, as well as the optimization of the process.

Purpose?
- Obtain a photocatalytic membrane, modified with dopamine and titanium dioxide, for the treatment of effluents rich in oily compounds.
- Increase the separation efficiency of oily compounds through the photocatalytic process.
- Obtain a membrane with a "self-cleaning" capability.

What has already been researched?
- The surface modification of membranes using dopamine has been broadly studied lately.
- There are only a few reports on using dopamine to obtain photocatalytic membranes designed to treat oily wastewater. These studies are presented in Table 2.2 (section 2.3.1).
- There are no works, so far, on the surface modification of PVDF membranes by deposition of dopamine and titanium dioxide in a single step for the treatment of oily compounds; thus, this is an unprecedented work.

Hypothesis
- Surface modification of PVDF membranes using dopamine and titanium dioxide deposition is technically feasible.
- The addition of titanium dioxide on the surface of the membrane leads to an increase in the permeate flux.
- The variation in dopamine and titanium dioxide deposition conditions interferes with the efficiency of separation and degradation of oily compounds.
- The membrane obtained is efficient in separating and degrading oily compounds and has self-cleaning performance.

THESIS STRUCTURE FLOWCHART

CHAPTER 1
Introduction and objectives

CHAPTER 2
Article 1 - Review of PDA-assisted photocatalytic membranes

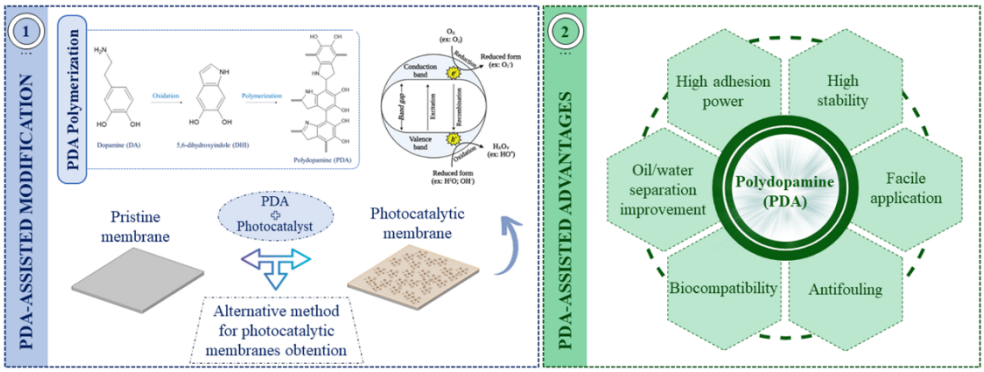

CHAPTER 3
Article 2 - Investigation of the PDA-assisted TiO2 incorporation on the surface of PVDF membrane

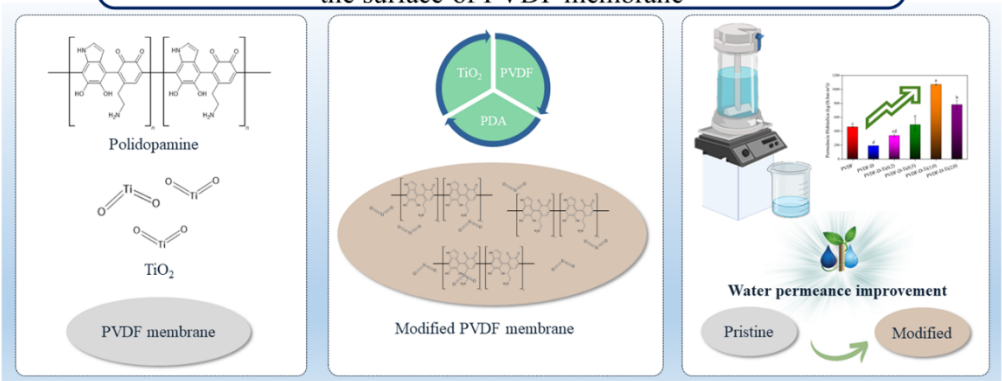

CHAPTER 4
Article 3 - Optimization of modification conditions and investigation of the self-cleaning characteristic

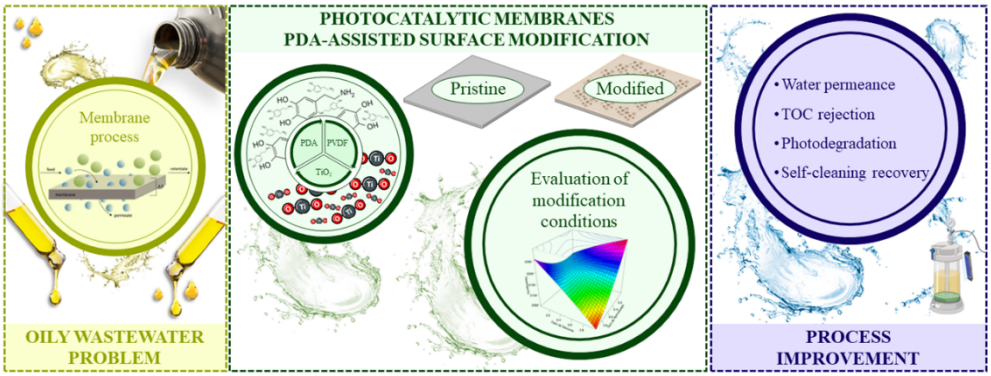

CHAPTER 5
Conclusion and future works

CHAPTER 1

INTRODUCTION AND OBJECTIVES

1 INTRODUCTION

In recent decades, the increasing industrial activity has led to the generation of more waste and pollutants, including oil, which is one of the most significant pollutants in industrial effluents (DONG *et al.*, 2019; GILL *et al.*, 2018). The improper disposal of oil compounds comprising fats, hydrocarbons, and oil fractions can substantially impact the environment and human health (ADETUNJI; OLANIRAN, 2021; GOH *et al.*, 2019; PUTATUNDA *et al.*, 2019). As a result, strict environmental regulations have been put in place to encourage the search for effective processes to treat and reuse water and minimize the scarcity of freshwater resources. Several physical and chemical methods are currently available for removing oil from wastewater, but these methods have some limitations, such as high cost, the use of toxic compounds, and the generation of secondary pollutants (MOKHBI; KORICHI; AKCHICHE, 2019; YU; HAN; HE, 2017).

One of the alternatives that have shown potential in treating oily wastewater is membrane-based processes such as the ultrafiltration (SHALABY; SOŁOWSKI; ABBAS, 2021). However, the polymeric membranes used still face several challenges that need to be addressed, such as improving their separation performance, antifouling properties, and stability (BAIG *et al.*, 2022; HALIM *et al.*, 2021; MULINARI; OLIVEIRA; HOTZA, 2020). To address these issues, simultaneous degradation of pollutants using photocatalysts has been considered a reasonable way to improve membrane processes (KUMARI; BAHADUR; DUMÉE, 2020; SUNDAR; KANMANI, 2020).

Photocatalytic membranes have become a promising alternative, and among the known photocatalysts, titanium dioxide (TiO_2) has been considered a good alternative due to its high photocatalytic activity, versatility, economy, stability, abundance, non-toxicity, and eco-friendliness (GAUR; JAGADEESAN, 2022). While the immobilization of TiO_2 on a membrane surface is crucial, developing new and more efficient catalysts has also been essential (CHEN *et al.*, 2019; KOVÁCS *et al.*, 2018; RIAZ; PARK, 2020; WANG *et al.*, 2022; ZHANG *et al.*, 2018).

Surface modification has also been investigated as one of the viable ways of obtaining photocatalytic membranes, presenting a considerable potential to control membrane fouling by successfully limiting the interactions between the membrane and fouling from the first stage of fouling formation, changing the intrinsic characteristics of the membrane. The use of polydopamine (PDA) as a binding agent between the membrane and specific compounds, not

necessarily catalysts, has gained importance due to its strong interaction with different substrates in humid conditions, becoming a viable alternative (BURZIO; WAITE, 2000; MULINARI *et al.*, 2022; PRONER *et al.*, 2020; ZIN *et al.*, 2019). Despite the significant potential of PDA, there is significant disagreement over its precise synthesis, with only recent studies defining it as a complex mixture of cyclized and non-cyclized polymer conjugates and physical trimers units, combining oxidative polymerization and physical self-assembly.

Overall, the present work aims to contribute to the development of efficient photocatalytic membranes for the treatment of oily wastewater and the reduction of environmental pollution. Specifically, this study aims to evaluate the potential of surface modification with dopamine/polydopamine for immobilizing titanium dioxide onto a commercial PVDF membrane. The resulting photocatalytic membrane are assessed for its oil/water separation performance and its self-cleaning capability to reduce the need for cleaning downtime and the use of chemicals. This investigation aims to advance the current research on developing effective photocatalytic membranes for oily wastewater treatment.

1.1 OBJECTIVES

1.1.1 General Objective

This study evaluates the effectiveness of modifying a commercial polymeric membrane made of poly(vinylidene fluoride) (PVDF) through the use of polydopamine (PDA) and titanium dioxide (TiO_2) for the separation and degradation of oily compounds in water.

1.1.2 Specific Objectives

The specific objectives are presented below, separated by the chapters of the thesis.

Chapter 2

- Present a review and critical discussion on the latest publications on the polydopamine-assisted photocatalytic membranes used for the separation/degradation processes of oily compounds in aqueous media.

Chapter 3

- Investigate the TiO_2 immobilization method on a membrane using PDA as an immobilization agent.

- Evaluate the effect of different catalyst concentrations on the TiO_2 immobilization process on the membrane.
- Assess the influence of TiO_2 incorporation on the membrane's water permeance.
- Characterize the membranes obtained through different techniques, such as SEM, XRD, and FTIR, and correlate the membrane properties with the immobilization process parameters.

Chapter 4

- Optimize the membrane modification process by investigating the effects of DA concentration, TiO_2 concentration, and agitation speed on the immobilization of TiO_2 on the membrane for maximum efficiency.
- Evaluate the performance of the modified membranes in the permeation of oily emulsions and assess the membrane's rejection efficiency, flux, and stability under different operating conditions.
- Evaluate the photocatalytic capacity of the modified membranes by measuring the degradation efficiency of a model organic pollutant and assessing the influence of the immobilized TiO_2 concentration.
- Evaluate the self-cleaning capacity of the modified membranes by analyzing the membrane's fouling behavior and cleaning performance in different permeation cycles.

CHAPTER 2

LITERATURE REVIEW

2 LITERATURE REVIEW

This chapter presents the theoretical background and literature review for the thesis, emphasizing conventional technologies and the use of photocatalytic membranes to treat oily wastewater. The chapter is part of a review article entitled "***Recent advances in surface modification using polydopamine for the development of photocatalytic membranes for oily wastewater treatment***" published in the *Journal of Water Process Engineering* (Impact Factor (2022) – 7.00).[1] According to Elsevier subscription rules, the authors retain the right to include the article in a thesis, provided it is not published commercially.

In addition, a book chapter was published in partnership with fellow group member Jéssica Mulinari entitled *"**Catalytic membranes for the treatment of oily wastewater**"* in the book *Membrane-Based Hybrid Processes for Wastewater Treatment* by Elsevier.[2]

Graphical abstract

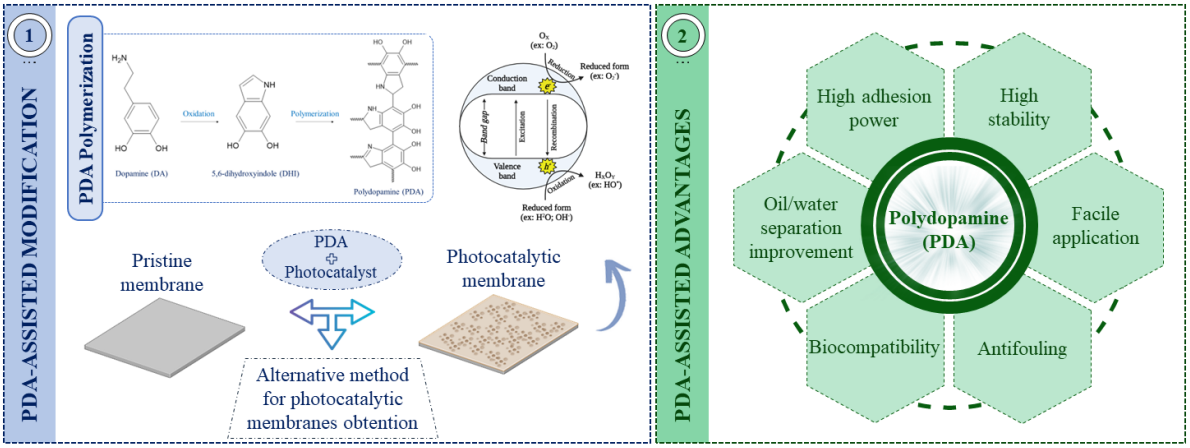

Highlights

- Challenges for photocatalytic membranes in oily wastewater treatment were assessed.
- Using polydopamine to modify photocatalytic membranes was successfully revised.
- Strong adhesive property of polydopamine is essential for catalyst immobilization.

---

[1] DA SILVA, A. F. V.; DA SILVA, J.; VICENTE, R.; AMBROSI, A.; ZIN, G.; DI LUCCIO, M.; DE OLIVEIRA, J. V. Recent advances in surface modification using polydopamine for the development of photocatalytic membranes for oily wastewater treatment. Journal of Water Process Engineering, v. 53, p. 103743, 2023. Disponível em: https://doi.org/10.1016/j.jwpe.2023.103743

[2] MULINARI, J., DA SILVA, A.F.V., VENTURIN, B., et al. Catalytic membranes for the treatment of oily wastewater. In: SHAH, M. P.; RODRIGUEZ-COUTO, S. (org.). Membrane-Based Hybrid Processes for Wastewater Treatment. 1. ed. Cambridge: Elsevier, 2021. p. 73–95. Disponível em: https://doi.org/10.1016/b978-0-12-823804-2.00026-4

• Polydopamine-assisted method is effective for preparing photocatalytic membranes.
• Different photocatalysts have already been efficiently incorporated using this method.

Abstract

The contamination of water sources by oily compounds is a severe environmental problem gaining ground in scientific research in recent years since these compounds are generally emulsified in the medium, making their separation difficult. Using photocatalytic membranes has shown interesting results in treating wastewater containing oily compounds, and research has advanced significantly in developing such membranes. The present work seeks to gather an overview of recent research on developing photocatalytic membranes to treat oil-contaminated water, focusing on membrane preparation from surface modification using polydopamine (PDA). This bio-inspired polymer has strong adhesive properties that have been explored for membrane modification, including the adhesion of catalysts. The combination of the photocatalytic function with the separation property of membrane processes optimizes the treatment of this kind of wastewater. However, developing a simple and viable method for large-scale production of these membranes and its application in industrial wastewater treatment is still challenging. Thus, this review critically discusses the latest related publications on the polydopamine-assisted obtention of photocatalytic membranes used for the separation/degradation processes of oily compounds in aqueous media, presenting the challenges of applying these types of membranes in oily wastewater treatment.
Keywords: membrane process; photocatalysis; wastewater treatment; oily compounds.

2.1 INTRODUCTION

The generation of waste and pollutants has been growing due to industrial activity over these last decades (DONG *et al.*, 2019; GILL *et al.*, 2018). One of the most significant pollutants in industrial effluents is oil from different sources. The oil compounds comprise fats, hydrocarbons, and oil fractions that substantially impact the environment and humans when disposed of incorrectly (ADETUNJI; OLANIRAN, 2021; GOH *et al.*, 2019; PUTATUNDA *et al.*, 2019). Moreover, strict environmental regulations have motivated the search for more effective processes for the treatment and reuse of water, attempting to minimize the scarcity of freshwater resources. In this scenario, adequate technology is dictated by the characteristics of

the compounds in the effluent and the vast degree of dispersion and stability of the oil droplets in the water (ISIAKA; OLANIRAN, 2021; PINTOR *et al.*, 2016).

Membrane processes are an excellent alternative for separating the oily compounds in wastewater and have already been used commercially (polymeric ultrafiltration membranes) (SHALABY; SOŁOWSKI; ABBAS, 2021). Nevertheless, several challenges still need to be solved to improve the membrane's separation performance, antifouling properties, and stability (BAIG *et al.*, 2022; HALIM *et al.*, 2021; MULINARI; OLIVEIRA; HOTZA, 2020). Simultaneously degrading the pollutant using photocatalysts is an excellent and reasonable way to improve the membrane process (MULINARI *et al.*, 2021). Photocatalytic membranes have become a promising alternative for treating oily wastewater (KUMARI; BAHADUR; DUMÉE, 2020; SUNDAR; KANMANI, 2020). Obtaining these membranes and establishing a proper effluent treatment process has been a matter of intense discussion, considering the diversity of membrane materials and catalysts that can be used.

Among the known photocatalysts, titanium dioxide (TiO_2), popularly known as titania, is considered a good alternative for photocatalytic membranes. Its main advantage is its high photocatalytic activity while being a versatile, economical, stable, abundant, non-toxic, and eco-friendly material (GAUR; JAGADEESAN, 2022). Fujishima and Honda (1972) were the first to report using a TiO_2 electrode under ultraviolet (UV) lighting in 1972. Since then, its application has been widely discussed in areas such as the development of sensors (BAI; ZHOU, 2014), hydrogen production (MA *et al.*, 2014; NI *et al.*, 2007), pollutant degradation (HAN *et al.*, 2009; KONSTANTINOU; ALBANIS, 2004), selective organic transformations (SHIRAISHI; HIRAI, 2008; YU; FAN; ZHAO, 2010), and CO_2 reduction for fuel generation (XU *et al.*, 2015; YU *et al.*, 2014). Also, several authors have previously studied its immobilization in different matrices, showing promising results (CHEN *et al.*, 2019; KOVÁCS *et al.*, 2018; RIAZ; PARK, 2020; WANG *et al.*, 2022; ZHANG *et al.*, 2018). However, developing new photocatalysts effective under sunlight has gained much research interest. Examples of sunlight-active photocatalysts are some metal-organic frameworks (MOFs) (WANG *et al.*, 2020d), graphitic carbon nitrides (g-C_3N_4) (ISMAEL, 2020), and bismuth oxyhalides (e.g., $Bi_{12}O_{17}C_{l2}$) (ZHANG *et al.*, 2020).

Although developing new and more efficient catalysts has been essential, fixing them on a surface -the membrane- is also paramount. Surface modification has been widely investigated among the viable ways of obtaining photocatalytic membranes, presenting a considerable potential to control membrane fouling by successfully limiting the interactions

between the membrane and fouling from the first stage of fouling formation, changing the intrinsic characteristics of the membrane.

Given the methods of immobilizing the catalyst on the membrane surface, the use of polydopamine (PDA) as a binding agent between the membrane and specific compounds, not necessarily catalysts, has gained importance due to its strong interaction with different substrates in humid conditions, becoming a viable alternative (BURZIO; WAITE, 2000; MULINARI *et al.*, 2022; PRONER *et al.*, 2020; ZIN *et al.*, 2019). There is significant disagreement over the precise synthesis of PDA. The structure was formerly believed to be based on either a polymeric backbone based on 5,6-dihydroxyindole (DHI) or an open-chain polycatechol model. However, neither of these hypotheses was supported by solid experimental evidence. Only in 2013, PDA was defined as a complex mixture of cyclized and non-cyclized polymer conjugates and physical trimers units, recently described as a combination of oxidative polymerization and physical self-assembly (DELLA VECCHIA *et al.*, 2013; LIU *et al.*, 2016).

Review articles in the literature show alternatives for improving the process of treating oily wastewater using membrane processes (AHMAD; GURIA, 2022; AHMAD; GURIA; MANDAL, 2020). Membrane technology coupled with photocatalysis has emerged as a promising approach for treating oily wastewater, and some published reviews focus on the principles, parameters, and applications (CHEN; HEIJMAN; RIETVELD, 2021; LIANG; ESMAEILI, 2021; SAMUEL *et al.*, 2022). The development of various types of photocatalytic membranes, including TiO_2-based (TETTEH *et al.*, 2021), and other metal-oxide-based membranes (SAWUNYAMA *et al.*, 2023), has been extensively studied. The main advantages of these membranes are their ability to degrade organic pollutants, including oil, and their excellent separation performance. In addition, the effects of various parameters, such as the type and concentration of photocatalyst, light source, and operating conditions, on the performance of photocatalytic membranes have also been investigated (HOMOCIANU; PASCARIU, 2022).

The originality of this work lies in presenting trends and recent developments in the field of PDA-assisted surface modification as an alternative for obtaining photocatalytic membranes. This technique is characterized by its ease of application, high stability, high hydrophilicity, and, most importantly, high binding capacity between materials. The deposition of PDA with different photocatalysts was addressed and discussed. The analysis will provide valuable insights into the innovation capacity of the technology and enable a better understanding of research and endeavors in this field.

This review summarizes the problems caused by the presence of oily compounds in wastewater, the mechanisms of wastewater treatment with membranes, and the advantages of the concomitant use of these processes in photocatalytic membranes, focusing on the methods for obtaining photocatalytic membranes through surface modification with PDA by:

- Presenting a holistic view of the main oily wastewater sources and the traditional treatment processes;
- Assessing the technological innovations promoted so far to develop photocatalytic membranes;
- Demonstrating the relevant contributions of the polydopamine-based membrane modification method for incorporating photocatalysts;
- Indicating promising catalysts for developing photocatalytic membranes designed for oily wastewater treatment.

2.2 OILY WASTEWATER SOURCES AND TRADITIONAL TREATMENT OF OILY WASTEWATER

Oily compounds are often found in wastewater. These compounds, usually consisting of fats and hydrocarbons, are from several industry areas (food, metal and metallurgical, petrochemical, and leather processing) and even domestic sewage (COCA; GUTIÉRREZ; BENITO, 2011; DU *et al.*, 2020).

In food industries, most oily compounds come from processing meat, poultry, seafood, and dairy products. Besides the oil and fat, very high organic carbon content is present in food industry wastewater (JEGANATHAN; BASSI; NAKHLA, 2006). The fish and meat processing industries produce substantial oil and fatty materials during slaughter, cleaning, and by-product processing. This sector disposes of effluents with up to 1000 mg/L of oil and fat (PUTATUNDA *et al.*, 2019).

The cutting oil used in the metal processing industry as a coolant and washing fluid is also a source of contamination. Due to the low oil content (about 1 g L^{-1}), it is unsuitable for incineration, and due to low biodegradability, it may not undergo an efficient biological treatment (TANUDJAJA *et al.*, 2019). Oil emulsions can be used as lubricants or coolants in various processes, among which cutting and machining operations in the metallurgical industries stand out (ALKAYA; DEMIRER, 2013; WU *et al.*, 2017). However, after a certain period of use, the emulsion undergoes chemical and thermal degradation, becomes exhausted,

and must be discarded, thus becoming a process effluent with a high concentration of emulsified oil.

Petrochemical and produced water wastewater are among the most dangerous types of liquid waste when improperly disposed of (MA *et al.*, 2022). They contain high concentrations of dissolved oil, grease, suspended particles, gases, and minerals that can penetrate groundwater or evaporate causing air pollution (GOH *et al.*, 2019; ROBERTSON *et al.*, 2007). Petrochemical wastewater can originate from oilfield production, crude oil refinery plants, olefin process plants, refrigeration, energy unities, and other sporadic wastewater. It is usually composed of several organic and inorganic components that are naturally present or added during oil refining (GHIMIRE; WANG, 2019; WEI *et al.*, 2019).

Produced water is the liquid waste byproduct of oil and gas extraction activities (water naturally formed inside the reservoir, injected for pressure maintenance, or condensed from gas purification). On most offshore platforms, this effluent constitutes the largest waste stream in volume (up to 80% in some cases) (SALEM; THIEMANN, 2022). Produced water contains a mixture of contaminants such as salts, heavy metals, hydrocarbons, and other pollutants, which makes it unsuitable for discharge into the environment without treatment. Without proper treatment, produced water can harm aquatic ecosystems, contaminate soil, and impact on human health. The treatment process typically involves a series of physical, chemical, and biological treatments to remove or reduce the concentration of contaminants in the produced water to acceptable levels. The treated water can then be discharged into the environment, reused in oil and gas operations, or disposed of in underground injection wells (WEI *et al.*, 2019).

The industrial leather process is water-intensive and generates vast amounts of wastewater. In addition to the animal fat that may be present, some organic oils are used during leather tanning, which are not entirely fixed in the leather. Therefore, part of the oil is leached during washing and is released into the wastewater (LEFEBVRE; MOLETTA, 2006; SAWALHA *et al.*, 2019).

Usually, the oil in wastewater is emulsified, making separation a challenge. The degree of dispersion and the stability of the oil droplets are the most critical factors. Droplet diameter characterizes free oil (> 150 μm), dispersed oil (20-150 μm), emulsified oil (< 20 μm), and soluble oil (< 5 μm) (GOODARZI; ZENDEHBOUDI, 2019; PINTOR *et al.*, 2016).

Treatment techniques seek to destabilize the emulsion facilitating the further separation step. The inadequate discharge of oily compounds can harm the environment, a

summary of which is shown in Figure 2.1, as well as the mechanisms of emulsion destabilization. Coalescence occurs when smaller droplets merge to form a larger droplet, resulting from the contact between oil droplets, rupturing the interfacial film between them. Flocculation, in turn, occurs when the emulsion droplets aggregate to form larger units. Creaming occurs due to a density difference where the lighter oil droplets rise to the surface, causing the emulsion to separate. When it occurs in W/O emulsions, it is usually classified as sedimentation. Creaming or settling can be hampered if the viscosity of the continuous phase is high. All these processes can destabilize the emulsion, causing phase separation (emulsion breakage) (SHAH BUDDIN *et al.*, 2022; WANG *et al.*, 2021).

Figure 2.1. Oily wastewater incorrect disposal and representation of the physical mechanisms of emulsion instability.

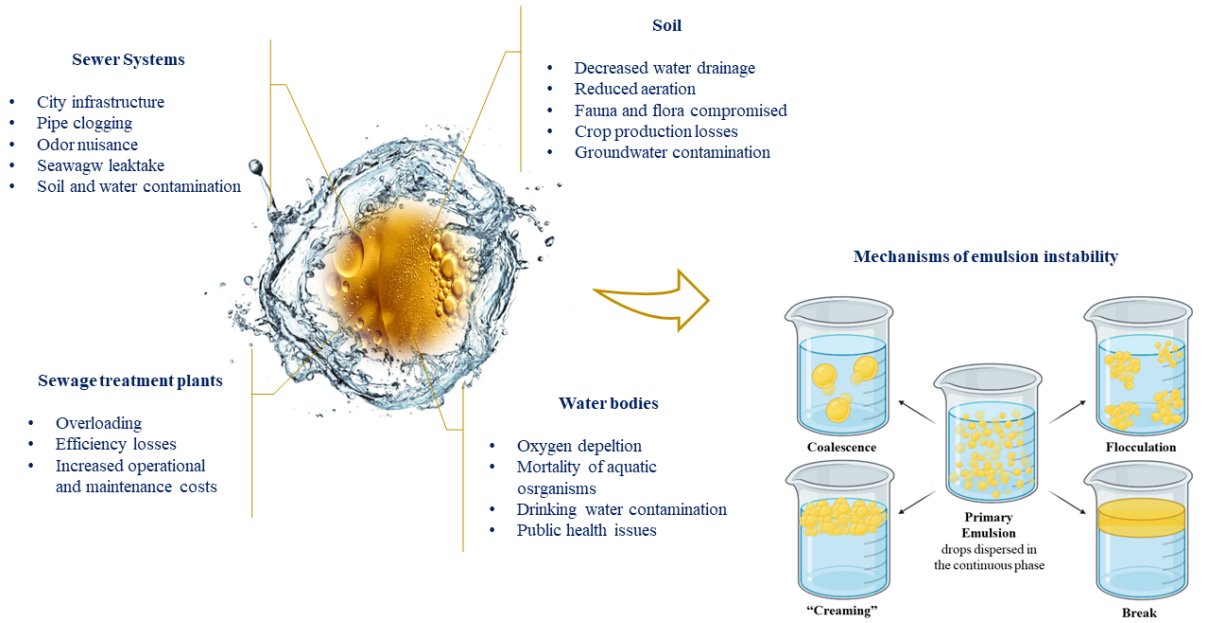

Source: adapted from Hassanshahi et al. (2020).

Several treatment methods to remove oil impurities can minimize or avoid the adverse effects of oily wastewater (JAMALY; GIWA; HASAN, 2015a). Methods for the treatment of oily wastewater include conventional physical and chemical processes. The main physical methods include flotation, adsorption, sand filter, cyclones, and evaporation. The most common chemical methods are flocculation, oxidation, electrochemical, photocatalytic treatment, Fenton, and ozone treatment. These conventional methods have several drawbacks, such as

high cost, use of toxic compounds, large plant footprint, and secondary pollutants generation (YU; HAN; HE, 2017).

Flotation is one of the most common physical treatment processes. The flotation process is based on the preferential adhesion of one of the phases to be separated into gas bubbles that permeate the suspension. The selective adhesion of the bubbles is determined by the behavior of the pollutant toward the water, usually presenting a certain difference in the density between the phases (YU; HAN; HE, 2017). Several flotation units can be used to treat oily water, and these processes differ in how the air is injected. In electroflotation, microbubbles are generated by passing a direct electric current between two electrodes in the medium. In induced air flotation, the bubbles are generated mechanically through an air injection system and a mechanical high-velocity stirrer. In dissolved air flotation, the bubbles are formed from an increase followed by a sudden decrease in water flow pressure. The crucial factors in this separation process are the processing time, droplet diameter, bubble contact, and surfactants (CASQUEIRA; TOREM; KOHLER, 2006; NASCIMBÉN SANTOS *et al.*, 2020).

In the chemical destabilization process, the emulsion is broken through the destabilization of oil droplets by the action of chemical products (coagulants and flocculants) (ABUJAZAR *et al.*, 2022). This way, oil droplets previously separated by electrostatic repulsion tend to contact each other, coalesce, and form large agglomerates easily separated by flotation or sedimentation (EMAMJOMEH; SIVAKUMAR, 2009; KHOUNI *et al.*, 2020; TANSEL; SEVIMOGLU, 2006). The most used coagulants for treating oily wastewater are aluminum sulfate, ferric chloride, and aluminum chloride. Still, developing new, more efficient, low-cost coagulants is also an important field of research (NASCIMBÉN SANTOS *et al.*, 2020). Some authors have reported using natural coagulants to remove oil from aqueous compounds, including chitosan, minerals such as clays, zeolitic materials, and plant extracts (JAGABA *et al.*, 2020; KHADER; MOHAMMED; MIRGHAFFARI, 2018).

The use of microorganisms in oily wastewater treatment has shown promising results in recent years. Isolated microorganisms or a consortium can degrade pollutants in these effluents. The biological treatment of oily wastewater could be a simple and cheap solution. However, many organic substances in these effluents are inhibitory, toxic, or resistant to biological treatment, such as hydrocarbons containing high molecular weight polycyclic aromatics (MAMMA *et al.*, 2004; NASCIMBÉN SANTOS *et al.*, 2020). Thus, biodegradation of oily wastewater is still challenging. Although such an approach still needs to be well developed due to the complexity of microorganisms, some recent research has shown

remarkable oil removal and degradation (COLLINS *et al.*, 2020; LOH *et al.*, 2019; PENG *et al.*, 2023).

Advanced oxidative processes (AOP) are promising methods for the remediation of contaminated sites containing non-biodegradable organic pollutants. The process involves the generation of a reactive hydroxyl radical with a high oxidation potential that attacks organic molecules, which are then transformed into oxidized intermediates, carbon dioxide, and water (CAÑIZARES *et al.*, 2007). AOP are usually categorized as ozone-based, UV-based, electrochemical, catalytic, and physical, depending on the activation methods and modes of oxidant generation. It is worth mentioning that this classification is not rigorous, as many processes involve different technologies and can be assigned to various categories (MIKLOS *et al.*, 2018). The reaction mechanism of a photocatalysis process is presented in Figure 2.2.

Figure 2.2. Mechanisms involved in photocatalysis.

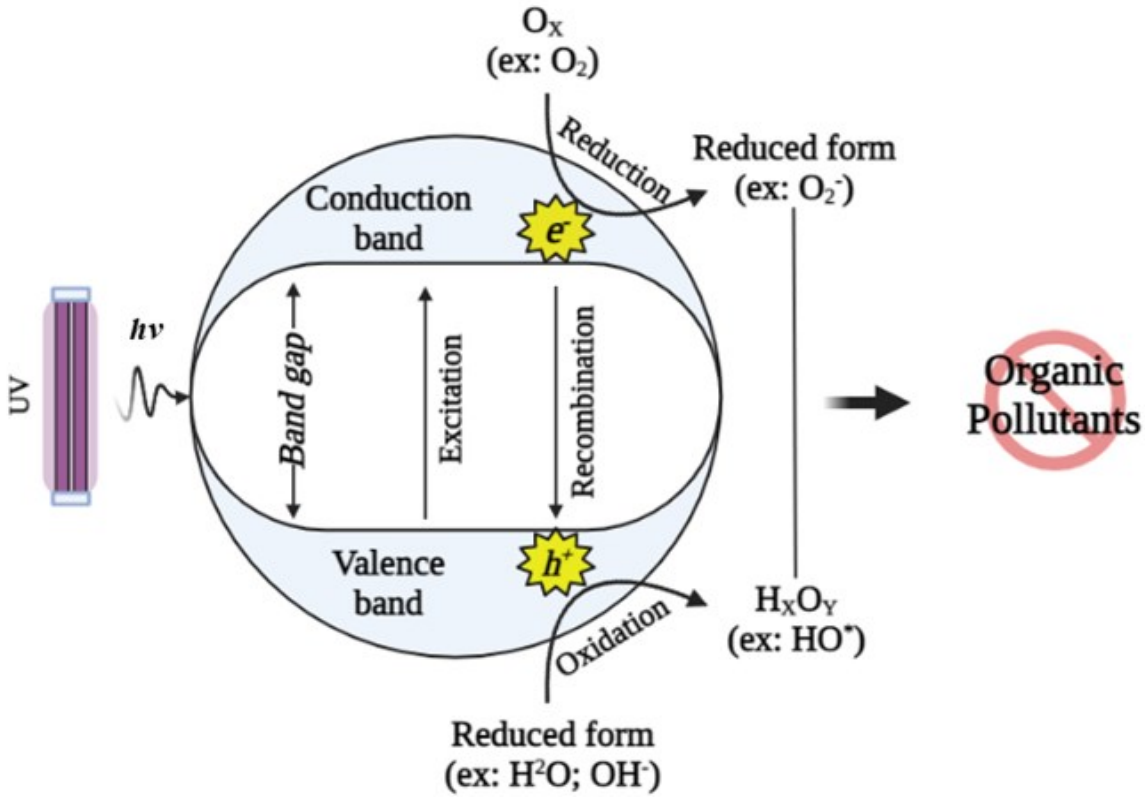

Source: the author (2023).

The photocatalysis principle is based on the catalyst activation under light irradiation. The catalyst is a semiconductor, represented by the presence of a valence band (VB) and a conduction band (CB), separated by a region called the bandgap. When irradiated with photons (*hv*) with energy equal to or greater than its bandgap energy, the catalyst absorbs the photons,

resulting in the excitation of electrons from VB to CB, generating a positive hole (h^+) in VB. The excited electrons react with the oxygen molecules, forming the superoxide anion (O_2^-). Holes can generate hydroxyl radicals ($OH^\bullet$) when interacting with water molecules on the catalyst's surface. These free radicals are potent oxidants capable of attacking organic contaminants in wastewater and performing photodegradation (KAJITVICHYANUKUL *et al.*, 2022; MOZIA *et al.*, 2013). Among the known AOP, photocatalysis has been investigated and suggested as an emerging technology for treating oily wastewater. It is an important technology for treating oily wastewater and can be associated with membrane processes.

Membrane separation processes (MSP) are a highly viable method for oil-water separation. MSPs are mostly based on pressure, concentration, and temperature as driving forces and, in some cases (e.g., pervaporation, gas separation, and reverse osmosis), depend directly on the interaction of the components of the compound to be treated with the membrane surface. Pressure-driven MSP includes microfiltration (MF), ultrafiltration (UF), nanofiltration (NF), and reverse osmosis (RO), which differ in average pore size, thus defining their applications (Figure 2.3) (BAKER, 2012a; COCA; GUTIÉRREZ; BENITO, 2013; HE *et al.*, 2017; HOU, 2012; MALTOS *et al.*, 2018; NASKAR *et al.*, 2018; SHIRAZI; LIN; CHEN, 2010).

Figure 2.3. Main characteristics of membrane separation processes.

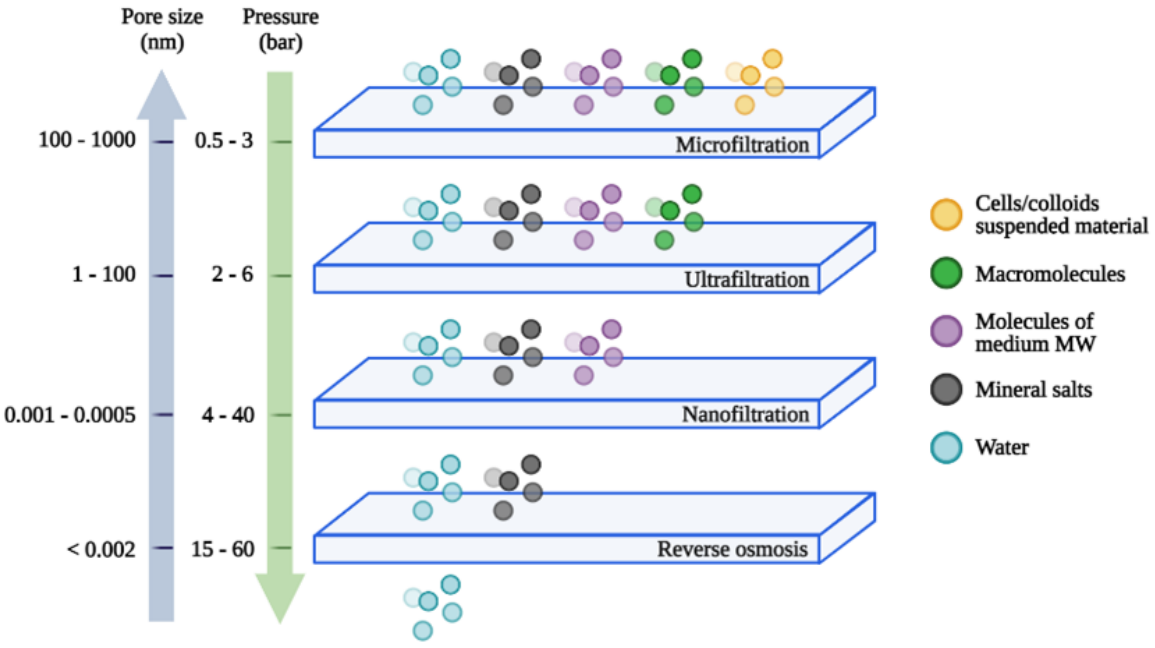

Source: the author (2023).

One of the main issues of membrane-based processes is membrane fouling, which is the deposition and accumulation of material on the membrane surface or inside the pores, leading to loss of performance, the necessity of chemical cleaning, and consequently decreasing membrane life (BAIG; WAHEED, 2023; BAKER, 2012b). The extent of the membrane fouling depends on the feedwater characteristics (concentration and physicochemical properties), membrane properties (roughness, porosity, and hydrophilicity), and operating conditions (flow rate, transmembrane pressure, recovery, and temperature) (NASCIMBÉN SANTOS *et al.*, 2020; TANG; CHONG; FANE, 2011). The fouling mechanisms are related to electrostatic and van der Waals interactions between the membrane surface and colloidal particles and are also influenced by particle-particle interactions. Furthermore, these mechanisms are generally divided into total blocking, partial blocking, cake formation (or gel layer), and internal adsorption (ABDELRASOUL; DOAN; LOHI, 2013; LAI *et al.*, 2015; SINGH; HANKINS, 2016). For oily wastewater, fouling is mainly caused by the presence of oil droplets, primarily causing surface blockage and pore-clogging. The droplet size, ionic strength, temperature, pH, and emulsifier concentration directly affect interactions between the membrane surface and the contaminants (JAFARI; ABBASI; HASHEMIFARD, 2020; LIU *et al.*, 2017; TANUDJAJA; CHEW, 2018).

2.3 EMERGING TECHNOLOGY FOR OILY WASTEWATER TREATMENT

Even though many applications (e.g., water purification, food processing, and radioactive enrichment, among others) are already well developed, several challenges still need to be solved to improve the characteristics of membranes in terms of separation performance, antifouling properties, and stability. The development of hybrid membrane processes has been growing in the last five years (IKHSAN *et al.*, 2018; QADIR; MUKHTAR; KEONG, 2017), especially in gas separation (CARDOSO *et al.*, 2022; SHARMA *et al.*, 2022), nanotechnology (BORJIGIN *et al.*, 2020; SUN *et al.*, 2018), catalysis (LEITE *et al.*, 2022), and photocatalysis (MA *et al.*, 2020c; MEHMOOD *et al.*, 2021). Photocatalytic membranes show promising results, which will be addressed in the following sections.

2.3.1 Preparation of photocatalytic membrane and its application in oily wastewater treatment

Research on catalytic membranes has been growing recently (DANKEAW *et al.*, 2019; ZHANG *et al.*, 2019). This process combines the catalytic function with separation to optimize the industrial process. As a benefit, the synergistic use of these processes can reduce the size of industrial equipment, capital costs, energy consumption, and environmental impact and increase industrial plant efficiency (KIM; VAN DER BRUGGEN, 2010). When combined into a single unit, the photocatalytic membrane generally shows excellent selectivity or recovery. As in non-catalytic processes, the choice of the membrane depends on some parameters, such as productivity, selectivity, service life, mechanical strength, chemical resistance, and cost (ABDALLAH, 2017; GU *et al.*, 2015).

Photocatalytic membranes have gained attention in current research on hybrid processes, especially in photocatalytic membrane reactors (KUMARI; BAHADUR; DUMÉE, 2020; SUNDAR; KANMANI, 2020). However, effective methods for obtaining these membranes and a deeper comprehension of the workings of the wastewater treatment process are still required. The treatment process can occur in two different ways. In the first setup, the catalyst is dispersed in the wastewater, and after the residence time, the stream flows through the membrane (Figure 2.4a) to remove the catalyst. In the second configuration, the catalyst is immobilized on the membrane, and the reaction and separation processes co-occur (Figure 2.4b) (SHAH *et al.*, 2019). The main disadvantage of the dispersed catalyst is the difficulty in its recovery after the operation.

Figure 2.4. Schematic representation of photocatalytic bench-scale membrane modules with the catalyst in (a) suspension and (b) immobilized on the membrane.

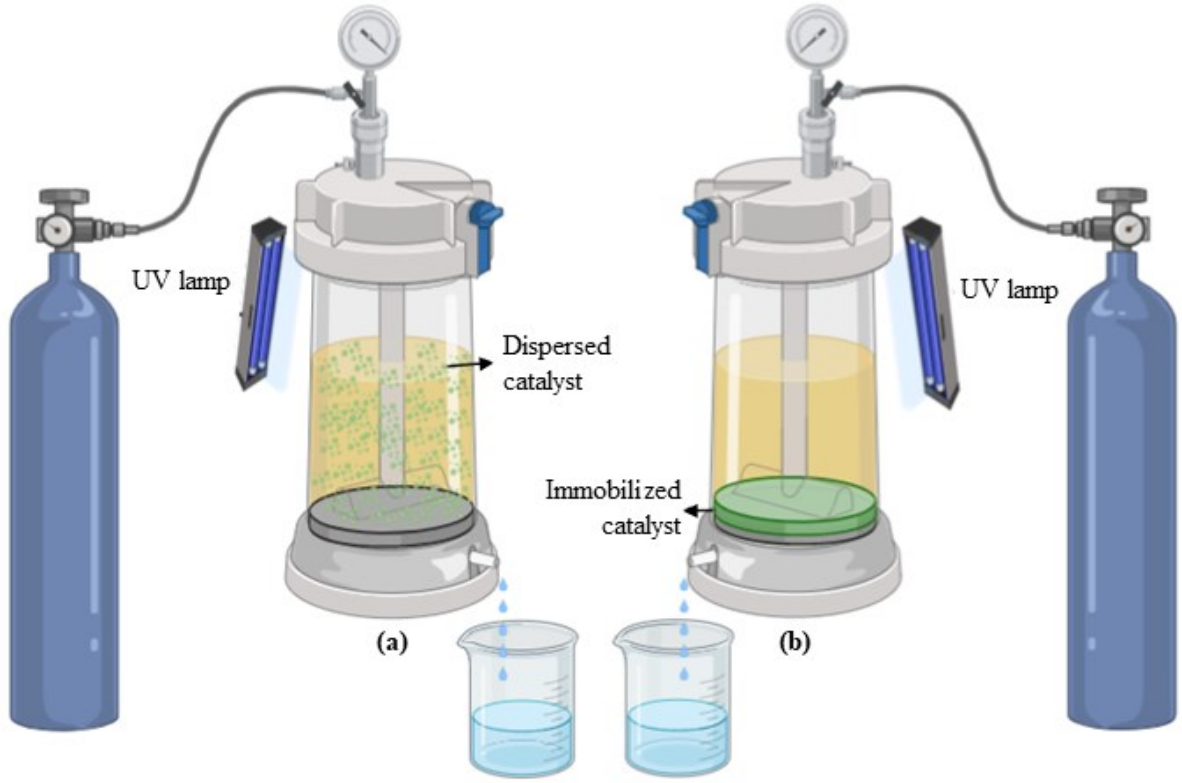

Source: the author (2023).

The photocatalysts in photocatalytic membrane processes absorb visible light irradiation below the donor range. Thus, using lamps capable of inducing the photocatalytic process is essential. The most used light sources are artificial UV lamps, which can be used externally (ESPÍNDOLA *et al.*, 2019) or internally (immersed) (MAGNONE *et al.*, 2022), emitting light in UV-A (λ_{max} = 355–365 nm) or UV-C (germicidal lamps, λ_{max} = 254 nm) range (REHMAN *et al.*, 2009). Artificial sources are used mainly because they generate higher photon fluxes. The reactor design is crucial since it must provide uniform irradiation to the entire membrane surface, achieving the required incident light intensity (MOZIA, 2010).

Photocatalytic membranes have the advantage of the simultaneous process without needing subsequent catalyst recovery. Still, this benefit also generates the inconvenience of a smaller catalyst surface area available for the reaction, thus reducing the photocatalytic efficiency of the process when compared to the dispersed catalyst configuration (KIM; VAN DER BRUGGEN, 2010; RIAZ; PARK, 2020).

Different methods for immobilizing the catalyst on the membrane are extensively reported in the literature (ABDALLAH, 2017; SUNDAR; KANMANI, 2020). The membrane

material plays a relevant role in this process. For polymeric membranes, immobilization can occur in two ways: (i) the catalyst is embedded in the membrane, forming a catalyst/polymer mixture; (ii) the catalyst is incorporated onto the membrane surface either by direct incorporation into the polymer matrix or by precipitation or deposition process (ABDALLAH, 2017; BARRIOS-ESTRADA *et al.*, 2018; VATANPOUR *et al.*, 2012).

In the first case, the catalyst is mixed with the polymer before the preparation of the membrane, usually by phase inversion. In this process, the polymer is solubilized in a solvent and shaped according to the desired membrane geometry. The polymer solution is demixed to yield a polymer-rich and solvent-rich phase. After phase separation, mass transfer between phases occurs, and the polymer-rich phase eventually solidifies, yielding the membrane matrix, while the polymer-lean phase will form the membrane pores. Phase separation can be induced by temperature change, immersion in a non-solvent bath, exposure to non-solvent vapor, or solvent evaporation (VATANPOUR *et al.*, 2012).

In the grafting process, an example of the second case, the effect of the solvent on the mechanism depends on the determination of the solvent ability to transport the monomers. Furthermore, the grafting process cannot occur without an initiator, and the temperature during the grafting step controls the kinetics of graft copolymerization. Generally, grafting yield increases with increasing temperature (BHATTACHARYA; MISRA, 2004; ESTRADA-VILLEGAS; BUCIO, 2013).

The precipitation or deposition process involves polymerizing a mixture of oligomers, forming a coating that adheres to the surface through physical forces or catalyst/membrane interaction. One of the depositions techniques is the dip coating, in which the dry membrane is dipped into a suspension containing photocatalyst particles and subsequently removed. During this process, the porous surface is wetted by the dispersion liquid. The porous surface causes the photocatalyst particles to concentrate at the boundary between the substrate and suspension. A dense, wet cake of defined thickness is formed when the particles fail to enter the pores. The driving force in this process is the membrane's capillary suction pressure (KIM; VAN DER BRUGGEN, 2010; MOZIA *et al.*, 2013).

Given the wide range of techniques and processes for obtaining photocatalytic membranes, several researchers have been developing studies on treating oily wastewater using photocatalytic membranes. To fully understand the current research advances in this area, an overview of the literature over the last ten years was made with related articles. For this purpose, the Web of Science database (www.webofscience.com) was used on September 14, 2022, using

the terms “photocatal*” and “membrane” as keywords, filtering the search for research and review articles; the terms were adjusted for search in title, abstract and keywords. A total of 3566 publications were found from 2012 to 2021. Restricting the search using the terms “oil*,” “wastewater,” “photocatal*” and “membrane” resulted in 134 publications, with 106 research articles and 28 review articles. This good topic has been gaining ground in research and technological development.

Table 2.1 depicts studies of the last three years with significant results in removing and degrading oil and organic compounds using the photocatalytic membrane process. Information regarding the membrane material, catalyst, and form of immobilization is presented, as well as the main results obtained.

Table 2.1. Overview of research on photocatalytic membranes, presenting the membrane material, catalyst, incorporation method, and main results obtained.

Line	Type of material	Membrane material	Pore size (μm)	Catalyst	Catalyst immobilization	Main results	Catalyst limitations	Ref
1	Inorganic	Stainless steel mesh	45	UiO-66 nanoparticles	*in situ* growth	UOCA > 150° and oil rejection > 98% after 20 cleaning cycles and treatment under a wide temperature range (-20-180°C) and high salt concentration (10 wt%)	UiO-66 nanoparticles composite photocatalysts can be expensive to synthesize and may not be a cost-effective option	Zhu et al. (2021)
2	Inorganic	Stainless steel mesh	37 – 74	PANI/TiO_2 nanoclusters	Dip-coating	High fluxes from 46 kL m^{-2} h^{-1} to 176 kL m^{-2} h^{-1}, superhydrophobic with the percentage of oil in the permeate remaining above 99.8% even after 100 separation cycles with 97% MB degradation in visible light	TiO_2 has a relatively wide bandgap, which limits its ability to absorb light in the visible spectrum	Wang et al. (2020a)
3	Inorganic	Stainless steel mesh	37	TiO_2/Co_3O_4/GO	*in situ* growth and vacuum deposition	Oil rejection > 99.5% and photodegradation efficiency 96.5% of CR under simulated solar irradiation and excellent reuse after 10 consecutive cycles	The synthesis of TiO_2/Co_3O_4/GO can be complex and may require specialized equipment	Bao et al. (2020)
4	Inorganic	Diatomite	20	$CoFe_2O_4$ nanoparticles	Deposition/ Coating	Decreased oil concentration from 57 mg L^{-1} to 8 mg L^{-1} RhB from 20 mg L^{-1} to 0 mg L^{-1} and COD from 231 mg L^{-1} to 47 mg L^{-1}	The potential toxicity of $CoFe_2O_4$ nanoparticles is not yet fully understood	Wang, Zhang, and Wang (2020)
5	Inorganic	Ni foam	10	$CoMoO_4$@ Bi_2MoO_6	Two-step hydrothermal process	UOCA of 162.5°, high separation efficiency of 99.67%, and flux of 1449 L m^{-2} h^{-1}. High recyclability for 20 cycles with good maintenance of reject and flow capacity	The synthesis of $CoMoO_4$@Bi_2MoO_6 can be complex and may require specialized equipment, which can limit their availability and accessibility	Li et al. (2021)
6	Inorganic	γ-Al_2O_3	-	TiO_2	*in situ* sol-gel synthesis	Removal efficiencies greater than 90% were achieved under conditions of 1.5 bar and a flow rate of 32 mL min^{-1}	TiO2 has a relatively wide bandgap, which limits its ability to absorb light in the visible spectrum	Golshenas, Sadeghian, and Ashrafizadeh (2020)

Line	Type of material	Membrane material	Pore size (μm)	Catalyst	Catalyst immobilization	Main results	Catalyst limitations	Ref
7	Inorganic	Copper mesh	45	Bi_2WO_6@ CuO nanowires	Hydrothermal synthesis	Copper meshes whit catalyst exhibited superior underwater superoleophobicity and separability with a water flux of 60 kL m^{-2} h^{-1} and oil residue in the filtered water of less than 15 ppm	The potential toxicity of Bi_2WO_6@CuO nanowires is not yet fully understood	Li et al. (2020)
8	Inorganic	Copper mesh	50	$Cu(OH)_2$@ Cu_2O	*in situ* synthesis	WCA < 30° after in situ synthesis with high permeation flux and a high separation efficiency (> 98%) for six different oily compounds with excellent photocatalytic capacity (92% for MB)	$Cu(OH)_2$@Cu_2O may not be selective in degrading oily compounds	Hu et al. (2020)
9	Inorganic	Al_2O_3/YSZ hollow fiber	0.03 - 0.04 [a]	α-Fe_2O_3	Hydrothermal synthesis	Oil rejection > 95%. Under visible light-assisted filtration, oil emulsion flows and rejects increased	α-Fe_2O_3 has a relatively low photocatalytic efficiency compared to other photocatalysts	Paiman et al. (2020)
10	Organic	PVDF	0.2 – 0.6 [a]	β-FeOOH nanorods	*in situ* mineralization	Excellent oil/water separation performance in a crossflow system. Stable permeation flux (~30 L m^{-2} h^{-1}), high separation efficiency (> 97%), and efficient self-cleaning in the presence of UV light and H_2O_2	β-FeOOH has a high rate of electron-hole pair recombination, which reduces its photocatalytic efficiency	Qu et al. (2021)
11	Organic	PVDF	0.22	Porphyrinic Zr-MOF	*in situ* deposition under a vacuum system	Excellent separation efficiency (> 99%) and relatively high flux (829-1542 L m^{-2} h^{-1} bar^{-1}). Good visible-light-driven photocatalytic degradation of organic dyes in static water.	Synthesizing porphyrinic Zr-MOFs with high purity and well-controlled morphology is challenging	Xue et al. (2021)
12	Organic	PVDF	0.033 [a]	G-C_3N_4/RGO-TiO_2	Coating and vacuum filtration	Oil/water removal efficiency above 95.4% for different oils and degradation around 94.2% for MB	G-C_3N_4/RGO-TiO_2 photocatalysts with high purity and well-controlled morphology is challenging	Venkatesh et al. (2020)
13	Organic	PVDF	-	ZIF-8/GO	Layer-by-layer deposition	Flux with UV irradiation 1.5 times higher than membranes without UV irradiation, and separation efficiency greater than 99% of a solution containing toluene as oil contaminant	ZIF-8 has lower photocatalytic activity compared to other photocatalysts	Yue et al. (2020)

Line	Type of material	Membrane material	Pore size (µm)	Catalyst	Catalyst immobilization	Main results	Catalyst limitations	Ref
14	Organic	PVDF hollow fiber	-	ZrO_2 and TiO_2 nanoparticles	Spinning	Improvement in the separation performance of membranes with ZrO_2-TiO_2 nanoparticles by about 5.7% in comparison to the neat membrane	TiO_2 has a relatively wide bandgap, which limits its ability to absorb light in the visible spectrum	Yaacob et al. (2020)
15	Organic	PVDF hollow fiber	0.022 – 0.023 [a]	TiO_2 nanotubes	Spinning	High flux of 40 L m^{-2} h^{-1} and 79.42% MB removal. Recovery of over 95% of performance after four filtration cycles, exhibiting antifouling capability. Membrane usability for more than 20 days	TiO_2 nanotubes may not be selective in degrading oily compounds	Subramaniam et al. (2021)
16	Organic	bPEI e PAA	-	WO_3/PAN	Blow spinning and layer-by-layer	UOCA > 150° and high photocatalytic degradation activity of RB (> 92% in 40 min) under visible light irradiation	WO_3 nanoparticles have been shown to have potential toxicity to human cells, which may limit their application	Ma et al. (2020a)
17	Organic	PI nanofiber	-	ZIF-8@GSH	Electrospinning and *in situ* hydrothermal synthesis	Superhydrophobicity/superoleophilia and high separation efficiency (>99.9%) for a range of oil/water mixtures. In addition, the membrane demonstrated excellent MB photocatalytic degradation	ZIF-8 has lower photocatalytic activity compared to other photocatalysts	Ma et al. (2020b)
18	Organic	Cellulose fiber	-	Ag@AgCl and MOF	Carboxymethylation and *in situ* synthesis	High efficiency of simultaneous removal of dyes (97.3%) and oils (99.64%). Good photocatalytic activity against organic pollutants, resulting in excellent self-cleaning and long-term reusability	The stability of the Ag@AgCl photocatalyst may be limited, and the cost of producing MOF photocatalyst may be higher than other photocatalysts	Lu et al. (2020)
19	Organic	PET	-	β-FeOOH	Sulfonated layer *in situ*	UOCA > 160°, oil rejection > 99% and > 96% MB degradation in 25 min. It provides stable performance even after 100 wash cycles	β-FeOOH has a high rate of electron-hole pair recombination, which reduces its photocatalytic efficiency	Wang et al. (2020b)

* UOCA: underwater oil contact angle; ZIF: zeolitic imidazolate framework; GSH: thiolated graphene; TiO_2: titanium dioxide; g-C_3N_4: graphitic carbon nitride; RGO: reduced graphene oxide; β-FeOOH: beta iron oxyhydroxide nanoparticles (akaganéite); ZrO_2: zirconium dioxide; AgCl: silver chloride; MOF: metal-organic framework; bPEI: branched

poly(ethylenimine); PAA: poly(acrylic acid); PAN: polyacrylonitrile; PET: polyethylene terephthalate; COD: chemical oxygen demand; MB: methylene blue; RhB: rhodamine B; CR: congo red; [a] Experimental pore size by nitrogen adsorption isotherms.

According to the data presented in Table 2.1, several types of membrane materials and catalysts have been investigated. It is interesting to note that stainless steel mesh and PVDF are the primary basis for inorganic and organic photocatalytic membranes, respectively, which may be related to the high stability of these materials for the oil-water separation. Although most of the membranes' (or support) pore sizes are in the range of filters (>10 μm), it can be noticed that some studies have used microfiltration (pore size between 0.1 μm and 10 μm) or ultrafiltration (<0.1 μm) range. This is understandable since the choice of a specific membrane pore size also depends on the type of oil-water system to be separated (as presented in Section 2.2). Different photocatalysts can be used, and a better approach to current trends in this area will be elucidated in section 2.3.3. In addition, several immobilization/deposition methods are used, including the most common as *in-situ* growth, dip-coating, and hydrothermal synthesis, which will be highlighted in this section.

Membrane performance has been evaluated in terms of oil rejection, UOCA, standard contaminant degradation, and reusability. The rejection results presented values above 90%, but can reach up to 99.9%, as in the case presented by Ma et al. (2020b). UOCA values, when presented, were above 150º, indicating a certain oleophobicity of the membrane under water. The most used standard contaminant for photocatalytic degradation was methylene blue (MB), with a degradation capacity greater than 92%. In addition, it was possible to assess that the membranes presented in Table 2.1 indicated a promising reuse capacity, with reuse over 20 cycles without losing the separation capacity.

The methods of immobilization of the catalyst in the membrane, those using an *in-situ* approach, appear in prominence. This approach is based on forming the catalyst directly on the membrane surface. The *in-situ* immobilization strategy better disperses material on the surface and interacts through the mixture at the molecular level between the precursors of the catalyst, membrane material, and solvent in a specific system (LI *et al.*, 2017). Golshenas, Sadeghian and Ashrafizadeh (2020) used this strategy to obtain ceramic membranes coated with γ-Al_2O_3 and modified them with TiO_2. The SEM images (Figure 2.5a and 2.5b) show that after the TiO_2 deposition, the pores became narrower and well-organized densely and homogeneously, probably due to the TiO_2 layer formed. However, that study did not present the average size of the pores nor how much the deposition influenced this parameter.

Figure 2.5. Micrographs of membranes obtained by *in situ* and dip-coating method (a) γ-Al_2O_3, (b) γ-Al_2O_3/TiO_2, (c) pristine stainless-steel mesh (SSM), (d-e) PANI/TiO_2 modified SSM, and (f-g) PANI/TiO_2 modified SSM after 100 cycles of permeation abrasion.

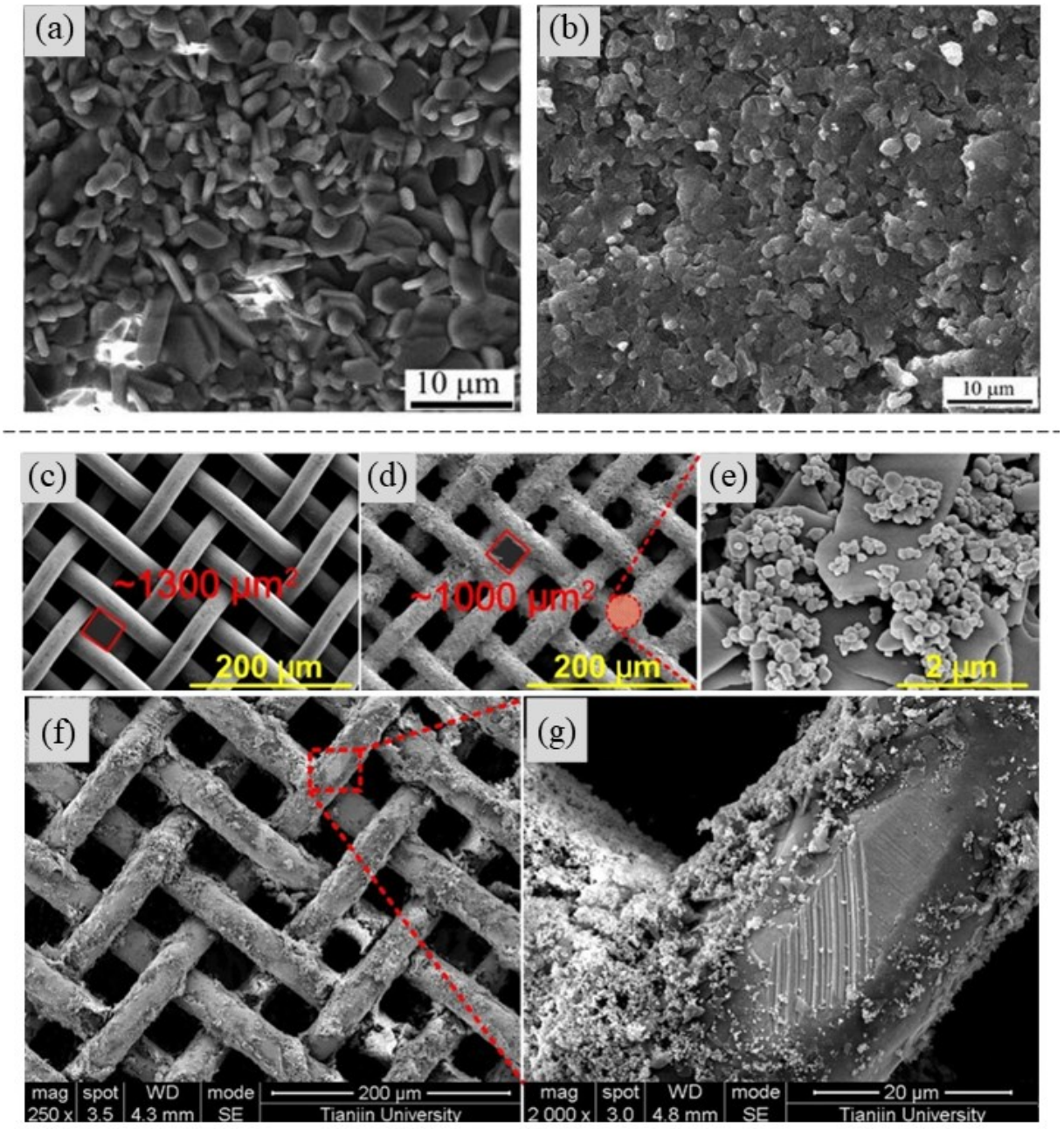

Source: Reprinted (adapted) from Golshenas, Sadeghian and Ashrafizadeh (2020) and Wang et al. (2020a) with permission. Copyright © 2020 Elsevier.

Using dip-coating, Wang et al. (2020a) obtained interesting results when modifying stainless steel meshes (SSM) using PANI nanosheets and TiO_2 nanoparticles. Figure 2.5a, 2.5b and 2.5c show micrographs of pristine SSM and PANI/TiO_2 modified SSM with approximations of 250 and 20,000x, respectively. Pure SSM had a pore area of approximately 1300 μm^2, and after modification, SSM showed a highly rough surface with microstructures of nanoclusters and smaller pores with an approximate area of 1000 μm^2. After the modification, the SSM showed a superhydrophobic character with high values of UOCA (> 150º). Although some surface structures were worn and damaged after 100 cycles of permeation (Figure 2.5d and 2.5e), the modified mesh still showed an oil rejection of 99.3% (hexane/water).

The hydrothermal technique is also a strategy for producing a catalytic membrane. This is a simple and direct method that allows the control of the aggregation of the material formed. The process uses water as a solvent under high pressure and temperature. The increase in pressure causes the water to remain in the liquid state, even at temperatures above the boiling point, making it possible to dissolve the reaction components that would not be dissolved under normal conditions (BYRAPPA; ADSCHIRI, 2007; TAVAKOLI; SOHRABI; KARGARI, 2007). Li et al. (2020) used this technique to modify copper mesh membranes with Bi_2WO_6 and CuO nanowires (Figure 2.6a). The pre-treated copper meshes underwent a process of chemical oxidation and calcination to form the mesh covered by CuO nanowires. The membrane was only incorporated through a hydrothermal reaction, creating the photocatalytic layer. The authors showed effective incorporation through deposition in a hydrothermal reaction, where it is possible to observe that the copper mesh has a relatively smooth surface (Figure 2.6b_1 and 2.6b_2). After CuO nanowires coating, the micrograph shows the membrane has a uniform and rough surface (Figure 2.6c_1 and 2.6c_2). In Figure 2.6d_1 and 2.6d_2, it is possible to observe the presence of Bi_2WO_6 uniformly immobilized on the surface of CuO nanowires.

Figure 2.6. Process and micrographs obtained by the hydrothermal and layer-by-layer methods.

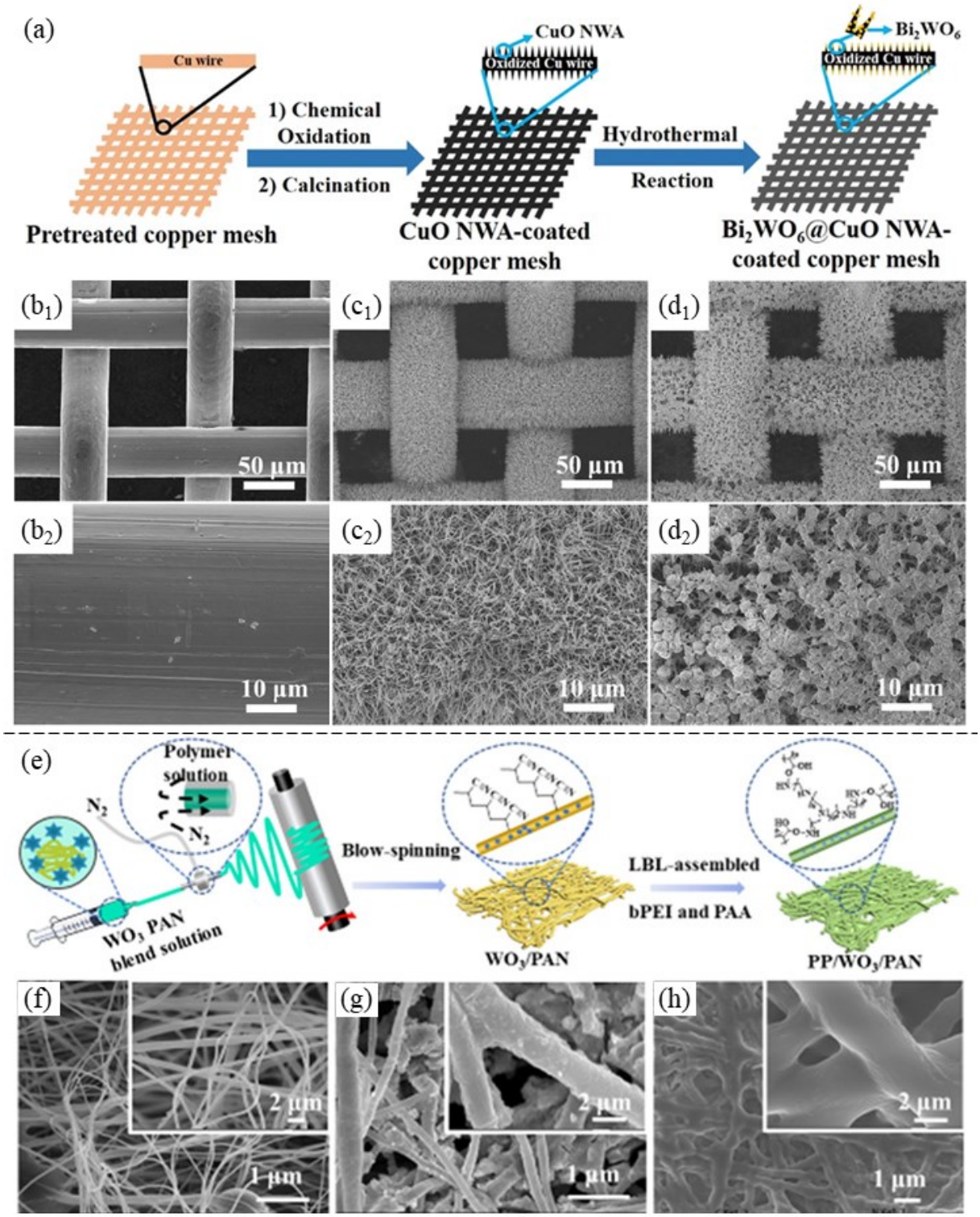

Source: Reprinted (adapted) from Li et al. (2020) and Ma et al. (2020a) with permission.

The layer-by-layer approach is a simpler way to control the composition, thickness, and structure of the membrane at the molecular level. Significant progress has been made, and the modified membrane can hinder the adsorption of foulants on the surface through the photocatalysis process, improving the antifouling capacity and degradation performance (LUO *et al.*, 2020). Ma et al. (2020a) demonstrated the production of polyacrylonitrile (PAN) photocatalytic membranes decorated with WO_3 and poly(ethylenimine)/poly(acrylic acid) (bPEI and PAA) using the combination of blow spinning and layer-by-layer techniques (Figure 2.6e). SEM micrographs show that the pure PAN membrane exhibits porous network structures consisting of smooth fibers (Figure 2.6f). In contrast, the WO_3/PAN membrane showed a rough surface with several protrusions (Figure 2.6g). When treated with bPEI and PAA, the membrane is thicker, with an increase in the average diameter of the fibers from 1.46 to 2.69 μm (Figure 2.6h).

2.3.2 Preparation of DA/PDA surface-modified photocatalytic membrane and its application in oily wastewater treatment

The interest in membrane modification using dopamine (DA) as a precursor of a binding agent between the membrane and the coating compound has been growing. This technique is inspired by mussels' adhesive secretions, which strongly interact with different substrates in humid conditions, allowing these animals to attach to different surfaces (BURZIO; WAITE, 2000). 3,4-dihydroxy-L-phenylalanine (L-DOPA) was identified as a crucial element in conferring the adhesion property of these animals (LYNGE; SCHATTLING; STÄDLER, 2015).

DA is a monomer derived from L-DOPA, which undergoes oxidation and spontaneous polymerization, resulting in the formation of PDA under suitable conditions. PDA is responsible for conferring the ability to adhere to the surfaces of materials (DALSIN *et al.*, 2003; LEE *et al.*, 2007). PDA-based membrane modification is attractive due to advantages such as process simplicity and compatibility with a wide range of membrane materials, including nanoparticles, polymers, or oligomers. Some studies have reported that PDA coverage is not as stable in very alkaline conditions (pH>12), which can be a limitation of this route because it prevents the application of the membrane in high pHs (ZIN *et al.*, 2019). On

the other hand, instability was not observed in very acidic conditions (pH ~2), in which the modified membrane did not show any change (YANG; LIU; CHEN, 2018; ZIN *et al.*, 2019).

2.3.2.1 PDA surface membrane modification

DA is a highly reactive molecule that can oxidize, undergoing the formation of 5,6-dihydroxyindole (DHI). DHI is polymerized forming PDA (Figure 2.7a), which is insoluble in water and organic solvents. The adhesion ability is attributed to the presence of catechol and amine groups in the PDA structure, which can react with hydrophilic molecules containing thiols and amine groups through the Michael addition or Schiff base reactions (GUO *et al.*, 2020a). Thin polymeric films of PDA are generally prepared by auto-polymerizing the DA monomer under weak alkaline conditions (pH = 8.5) to stimulate the oxidation of catechol to quinones and to facilitate the crosslinking reaction (WANG *et al.*, 2018; YAN *et al.*, 2020).

The most widespread DA-based membrane modification methods include one-step modification, two-step modification, metal incorporation, interfacial polymerization, and blending (ABOUNAHIA; QIBLAWEY; ZAIDI, 2022). The one-step modification is based on the simultaneous co-deposition of functional materials (FM) and a DA solution on the membrane surface (Figure 2.7b). In the two-step modification, however, the FM and DA solution deposition on the membrane surface is performed sequentially (Figure 2.7c). The metal incorporation comprehends using the PDA adhesive layer for the *in-situ* growth of metals, being incorporated directly into the PDA-modified surface. Interfacial polymerization is a type of step-growth polymerization in which PDA polymerizes at the interface between two immiscible materials. Blending modification is based on mixing the DA-FM solution with the membrane polymer matrix (membrane background solution), followed by the phase inversion process for membrane formation (ABOUNAHIA; QIBLAWEY; ZAIDI, 2022; WANG *et al.*, 2019; ZENG *et al.*, 2020).

Figure 2.7. Membrane modification using DA and PDA (a) Simplified reaction of PDA formation, (b) one-step PDA membrane modification, and (c) two-step PDA membrane modification. *DA: Dopamine; FM: functional materials; PDA: polydopamine.

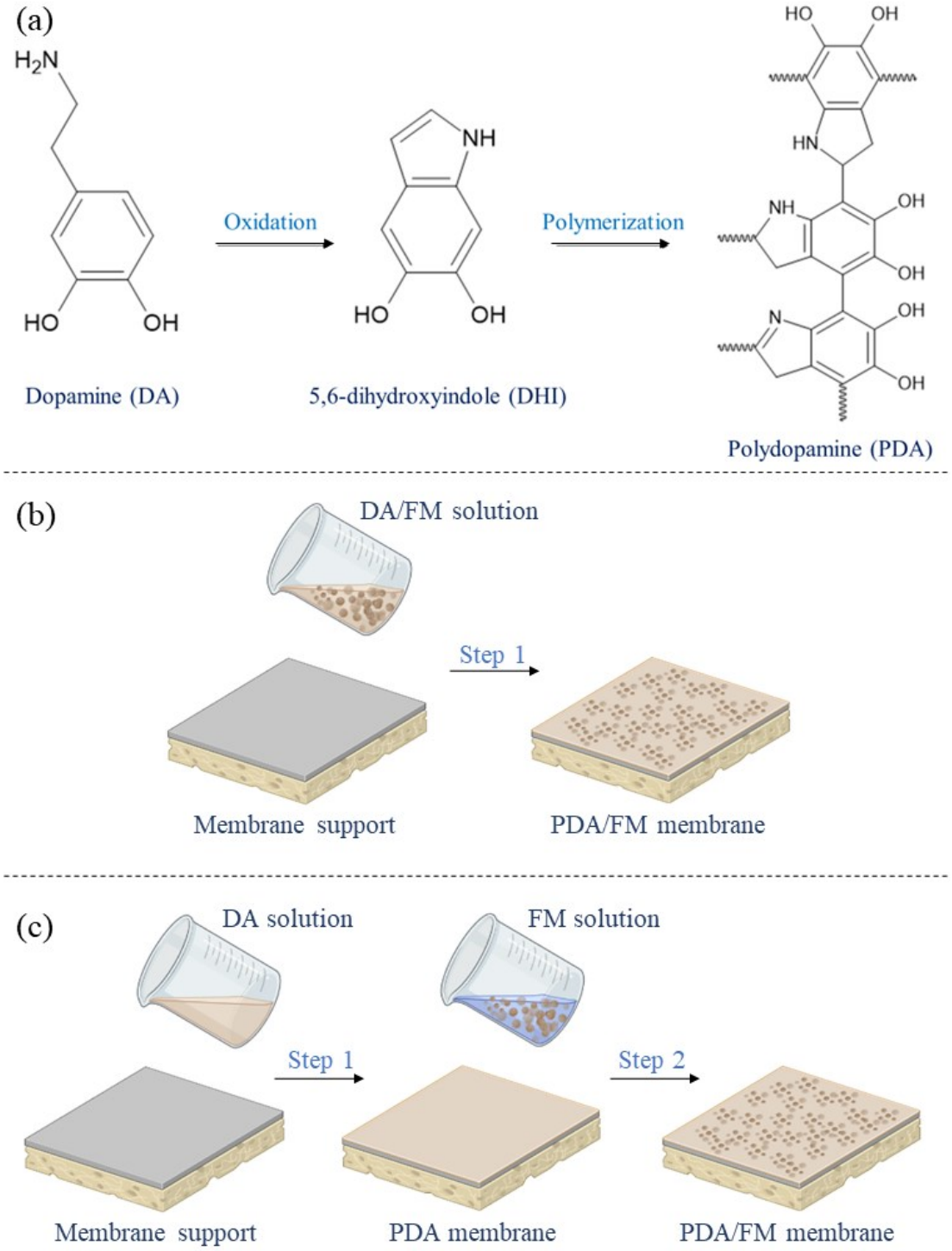

Source: adapted from Abounahia, Qiblawey and Zaidi (2022).

Incorporating the photocatalyst using PDA can cause it to be covered in the polymerization process, losing some of its efficiency. However, some works, such as that from Yang and Guo (2018), have shown that this coating does not significantly interfere with the photocatalytic action. Their results indicated that the degradation rate was initially accelerated after covering TiO_2 nanoparticles with PDA. Only after 30 min was the reaction rate of TiO_2-PDA slower than the uncoated catalyst. The authors attributed this behavior to the improved light absorption by the PDA layer and the induction of the location of the holes on dopamine and the electrons in the lattice of the TiO_2 network.

Meng et al. (2021) proposed a mechanism for the interaction between PDA coating and TiO_2 (the most widespread catalyst) (Figure 2.8). There are numerous unsaturated Ti atoms on the surface of the TiO_2 crystal. During the process, the catechol groups of DA are oxidized to dopamine-quinone at pH ~ 8.5, followed by further oxidation to form 5,6-dihydroxyindole via deprotonation. After that, the PDA cross-linked polymer is formed through intermolecular Michael addition reactions (XIA *et al.*, 2018). Then, the electrons of the oxygen atoms in the hydroxyl group of the PDA access the unoccupied orbitals of Ti atoms, forming chemical bonds between the TiO_2 and the PDA, strongly binding the materials.

Figure 2.8. Proposed mechanism for the interaction between PDA and TiO_2.

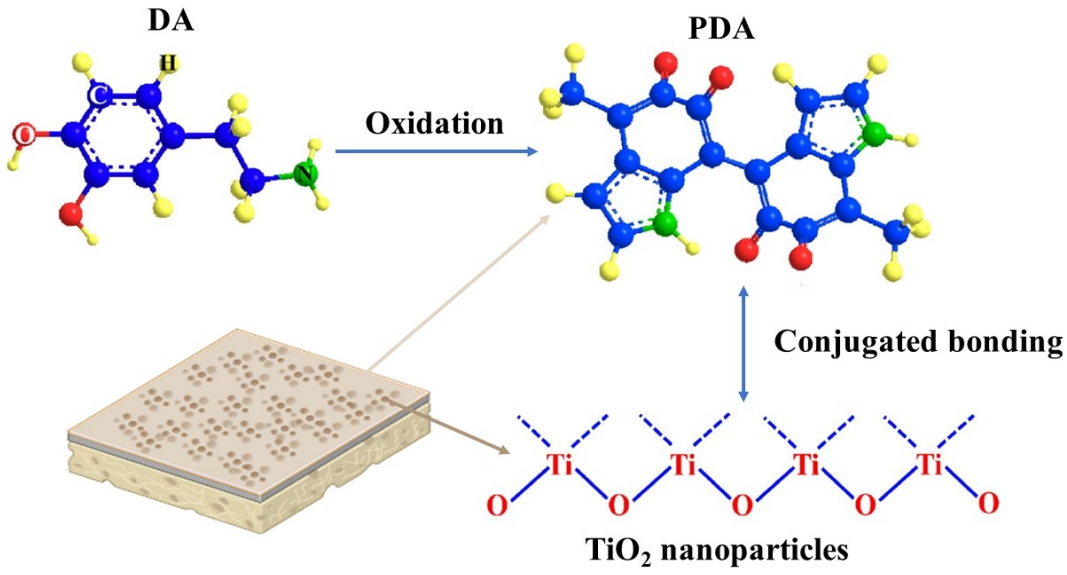

Source: Adapted from Meng et al. (2021). Copyright © 2021 Elsevier.

2.3.2.2 Photocatalytic membranes by PDA surface modification

Considering the methods of immobilizing the catalyst in the membrane previously discussed, the use of PDA has been gaining much space in literature, becoming a viable alternative for incorporating catalysts in the membrane. The terms dopamine OR polydopamine were added to the search to increase the specificity of the analysis. The number of articles decreased to 13 (after reading and selection), all published after 2019. Table 2.2 summarizes these studies, indicating the membrane material, the immobilized catalyst, PDA concentration in modification, the oily contaminant tested, and a brief description of the results.

Table 2.2. Summary of studies carried out to obtain photocatalytic membranes using the surface modification method with DA/PDA with different membrane materials and catalysts.

Line	Membrane material	Pore size (µm)	Catalyst	[PDA] ($g \cdot L^{-1}$)	Oil contaminant tested	Operation mode	UOCA (º)	Oil removal (%)	Photocatalytic capacity and results	PDA novelty	Catalyst limitations	Ref.
1	PVDF	0.2 to 0.6	β-FeOOH	2.0	Soybean oil	Crossflow	-	97.0	Excellent self-cleaning function and high rejection with crude oil testing	Strong binding between catechol group and Fe^{3+} of PDA and β-FeOOH, respectively	β-FeOOH has a high rate of electron-hole pair recombination, which reduces its photocatalytic efficiency	Qu et al. (2021)
2	PVDF	-	TiO_2	2.0	Kerosene	Dead-end	152	98.2	RhB removal > 98% and good degradation capacity after five filtration cycles with a high flux of 1389 ± 67 L m^{-2} h^{-1}	Superoleophobic PVDF/TiO_2 membrane inspired by lotus leaf	TiO_2 has a relatively wide bandgap, which limits its ability to absorb light in the visible spectrum	Sun et al. (2021a)
3	PVDF	0.22	NiAlFe LDH	2.0	Petroleum ether Hexadecane Heptane Soybean oil Kerosene	Dead-end	150	99.0	Tetracycline degradation close to 100% in 20 min of reaction and high flux permeation (925-1913 L m^{-2} h^{-1} bar^{-1})	PDA increased adhesion in *in situ* growth of LDH on modified PVDF-PDA membrane	Synthesize NiAlFe LDH can be costly and time-consuming, which may limit its practical application	Zomg et al. (2021)
4	PVDF	0.15	LDH@g-C_3N_4	1.0	Gasoline Diesel Petroleum ether	Dead-end	-	92.3	MB and RhB removal > 96% and high stability and efficiency even after ten cycles	PDA increased light absorption capacity and increased membrane hydrophilicity	Synthesizing LDH@g-C3N4 photocatalyst with high purity and well-controlled morphology is challenging	Liu et al. (2021)

Line	Membrane material	Pore size (µm)	Catalyst	[PDA] ($g \cdot L^{-1}$)	Oil contaminant tested	Operation mode	UOCA (º)	Oil removal (%)	Photocatalytic capacity and results	PDA novelty	Catalyst limitations	Ref.
5	PVDF	0.58 to 0.72	ZnO	2.0	Petroleum ether Toluene Hexane Dichloroethane Hexadecane	Dead-end	153	99.1	MB removal of 97.4%	PDA incorporated with ZnO showed robust service life due to its good oxidation resistance capability	ZnO is not stable under acidic conditions, which limits its use in acidic environments	Wang et al. (2020c)
6	PP	0.22	ZIF-67	0.2	-	Crossflow	-	-	MB removal > 92% and 2.5x increase in membrane permeability	PDA presence increased the contact between PP and ZIF-67 (catalyst with large specific surface area, high catalytic activity, and strong chemical stability)	ZIF-67 has lower photocatalytic activity compared to other photocatalysts	Li et al. (2019)
7	PVA	-	Pd nanoparticles	2.0	Kerosene Hexane Petroleum ether Chloroform Toluene	Dead-end	150	99.9	MB and CR removal > 99%	PDA enables an active interface inducing mild secondary reactions to create a variety of layers, making possible in-situ reducing of Pd nanoparticles in a favorable green way	Pd nanoparticles themselves can be toxic to the environment and human health if not properly handled or disposed	Yin et al. (2020)
8	Cotton cloth	-	β-FeOOH	2.0	Hexane Kerosene Toluene Chloroform Dichloroethane	Dead-end	-	98.0	MB removal > 90% after 5 cycles and durability up to 50 cycles	PDA served as the basis for in situ hydrothermal growth of β-FeOOH nanorods on patterned cotton fabrics	β-FeOOH has a high rate of electron-hole pair recombination, which reduces its photocatalytic efficiency	Cheng et al. (2020)
9	PAN	0.62 to 0.85	TiO_2	2.0	Kerosene	Dead-end	138	99.0	MB degradation of 98% and high flux permeation (15427 L m^{-2} h^{-1} bar^{-1})	PDA was used adhere TiO_2 to the multi-scale hierarchical membrane to improve the hydrophilicity and underwater oleophobicity	TiO_2 has a relatively wide bandgap, which limits its ability to absorb light in the visible spectrum	Sun et al. (2021b)

Line	Membrane material	Pore size (µm)	Catalyst	[PDA] ($g \cdot L^{-1}$)	Oil contaminant tested	Operation mode	UOCA (°)	Oil removal (%)	Photocatalytic capacity and results	PDA novelty	Catalyst limitations	Ref.
10	Paper fiber	193.6 to 200.4	TiO_2 nanowires	2.0	Dichloroethane Petroleum ether Toluene Soybean oil Diesel Hexane	Dead-end	156	99.0	Flux recovered after a self-cleaning process with UV and UV-induced antifouling performance for 80 cycles	PDA was used to coat TiO_2 and ensure better particle adhesion to the paper fiber membrane via vacuum filtration	TiO_2 nanowires may not be selective in degrading oily compounds	Chen et al. (2019)
11	Cellulose acetate	0.22	$Bi_{12}O_{17}Cl_2$	0.33	Diesel Gasoline Dichloroethane	Dead-end	135	95.0	98% MB removal efficiency in 100 minutes, 96% 4-CP removal efficiency in 160 minutes, and recyclability of at least ten cycles	PDA has improved the adherence between $Bi_{12}O_{17}Cl_2$ with graphene matrix and made the RGO/PDA/$Bi_{12}O_{17}Cl_2$ more stable and strongly linked with the cellulose acetate membrane	$Bi_{12}O_{17}Cl_2$ photocatalyst can degrade over time and lose its catalytic activity, which can limit its effectiveness in the long term	Yu et al. (2019)
12	Cellulose acetate	0.016	TiO_2/LDH	1.0	-	Dead-end	-	-	MB rejection > 99% with higher flux to membranes with higher catalyst concentration	PDA was used to coat the GO which was used as a cross-linking agent in the co-intercalation process of TiO_2 and LDH	Synthesizing TiO_2/LDH photocatalysts with high purity and well-controlled morphology is challenging	Wang et al. (2022)
13	PEN	-	MXene @TiO_2	2.0	Isooctane Hexane Petroleum ether Heptane Trimethyl benzene	Dead-end	155	99.0	MB, CV, CR, and MO degradation > 92.3%	The intercalation of TiO_2 nanoparticles optimally regulated the interlayer spacing and PDA-triggered crosslinking	There is limited research on the photocatalytic properties and applications of MXene@TiO_2 compared to other photocatalysts	Feng et al. (2022)

* UOCA: underwater oil contact angle; MB: methylene blue; RhB: rhodamine B; MR: methyl red, CR: Congo red; CV: Crystal violet; MO: Methyl orange; 4-CP: p-chlorophenol; PVDF: poly(vinylidene fluoride); PAN: polyacrylonitrile; PP: polypropylene; PVA: polyvinyl acetate; PEN: poly(arylene nitrile ether); TiO_2: titanium dioxide;

$Bi_{12}O_{17}C_{l2}$: bismuth oxyhalide; LDH: layers-double of hydroxide composite; β-FeOOH: beta iron oxyhydroxide nanoparticles (akaganéite); ZIF: zeolitic imidazolate framework; g-C_3N_4: graphitic carbon nitride; MXene: two-dimensional inorganic compound.

The studies in Table 2.2 show that, besides the expected adhesion and interaction between the photocatalyst and the membrane material, the PDA plays different roles when used in membrane modification. Considering the oil separation from water, it is worth highlighting, as reported by Liu et al. (2021), that using PDA to immobilize the photocatalyst can be advantageous due to the increase in hydrophilicity, the improvement of light absorption after coating with PDA, and the generation of holes and electrons in the PDA and photocatalyst layer, respectively. Some of these studies on membrane modification with PDA and the respective results are highlighted hereafter.

Chen et al. (2019) prepared membranes of paper fiber and TiO_2 nanowires using DA as a binding agent in a simple vacuum filtration process. The TiO_2 particles were dispersed in water and sonicated; then, a solution containing the paper fiber was added and stirred, followed by the addition of DA and tris(hydroxymethyl)aminomethane to make the environment conducive to the polymerization process of DA in PDA. The solution was left under stirring for 6h. Then vacuum filtration and drying were carried out to obtain the membrane (Figure 2.9a). The membrane obtained by this method has excellent stability and regenerative capacity. In addition, it retains its UV-triggered self-cleaning property after multiple permeation cycles with organic solvents.

Cheng et al. (2020) used a cotton fabric membrane and β-FeOOH nanorods as catalysts. With a sequential approach, the DA deposition process on the membrane was first carried out by the traditional PDA polymerization process. After this process, the membrane was treated with hydrochloric acid and ferric chloride solution for the in situ hydrothermal cultivation of β-FeOOH nanorods (Figure 2.9b). In this case, it is reported that β-FeOOH nanoparticles have excellent, effective photocatalytic performance triggered by visible light, which gives the reported coating mechanism potential for real applications. It has been reported that the catalyst embedding process has been improved due to PDA embedding.

Wang et al. (2020c) used the hydrothermal reactor to synthesize ZnO nanoparticles directly on the PDA-modified PVDF membrane. In this case, the deposition of dopamine was initially performed on the membrane previously obtained by phase inversion. The nanoparticles were sequentially synthesized on the membrane, using anhydrous zinc acetate as a synthesis precursor (Figure 2.9c). This membrane has a high separation efficiency and can successfully separate different emulsions. The PVDF@PDA@ZnO composite membrane exhibits results

with promising long-time prospects for the purification of oily wastewater in terms of self-cleaning ability.

Figure 2.9. Processes for obtaining different photocatalytic membranes using PDA.

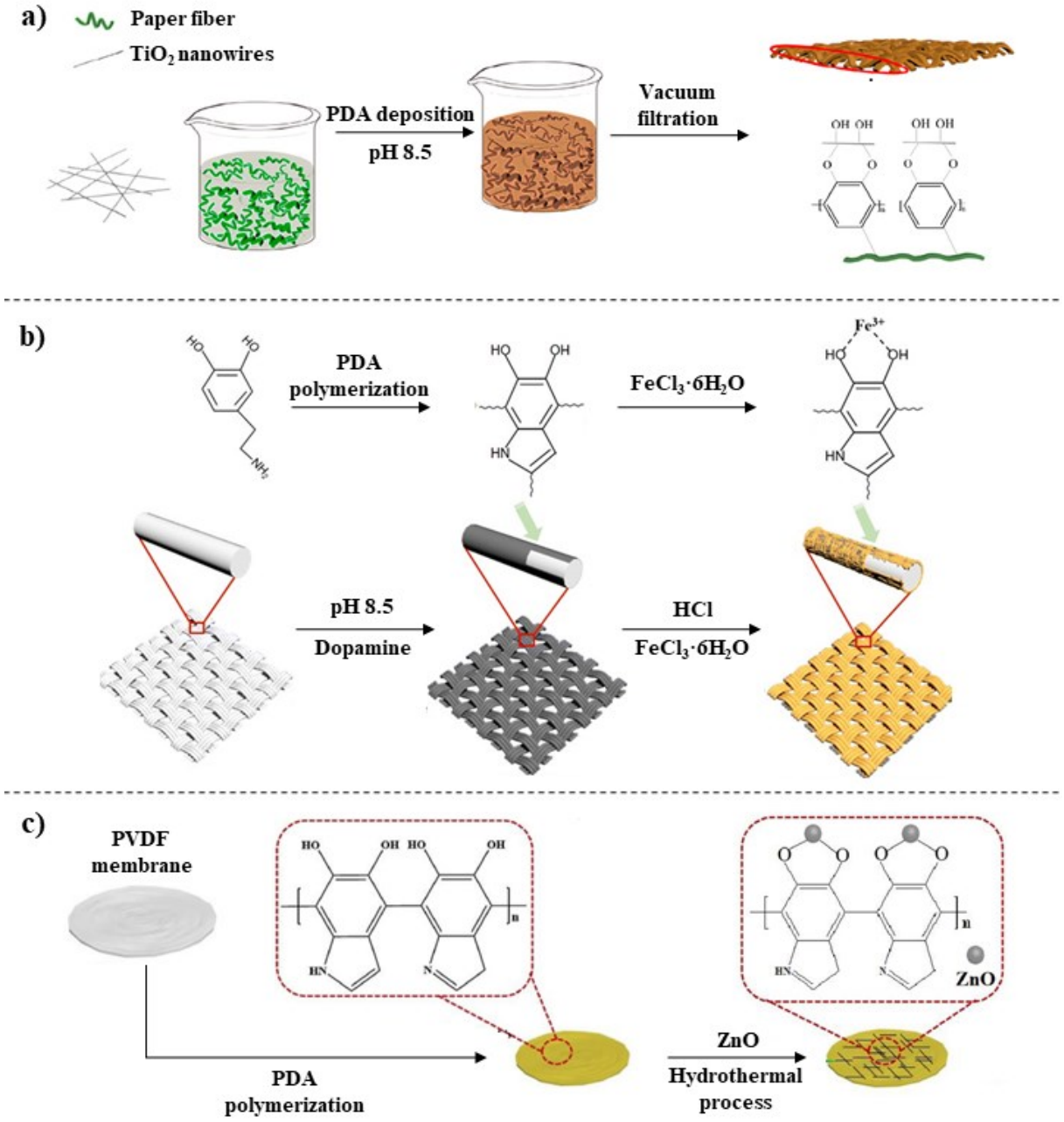

Source: adapted from Chen et al. (2019), Cheng et al. (2020), and Wang et al. (2020c).

Sun et al. (2021a) worked with PVDF membrane with TiO_2 to obtain the photocatalytic membrane using DA. Titania was incorporated by electrospraying TiO_2 on electrospun-PVDF

support. The polymerization of PDA in the membrane was only carried out to get an oleophobic and hydrophilic effect when submerged. The synthesis scheme of this membrane is shown in Figure 2.10.

Figure 2.10. Process for obtaining PVDF/TiO_2 photocatalytic membrane from the electrospinning process.

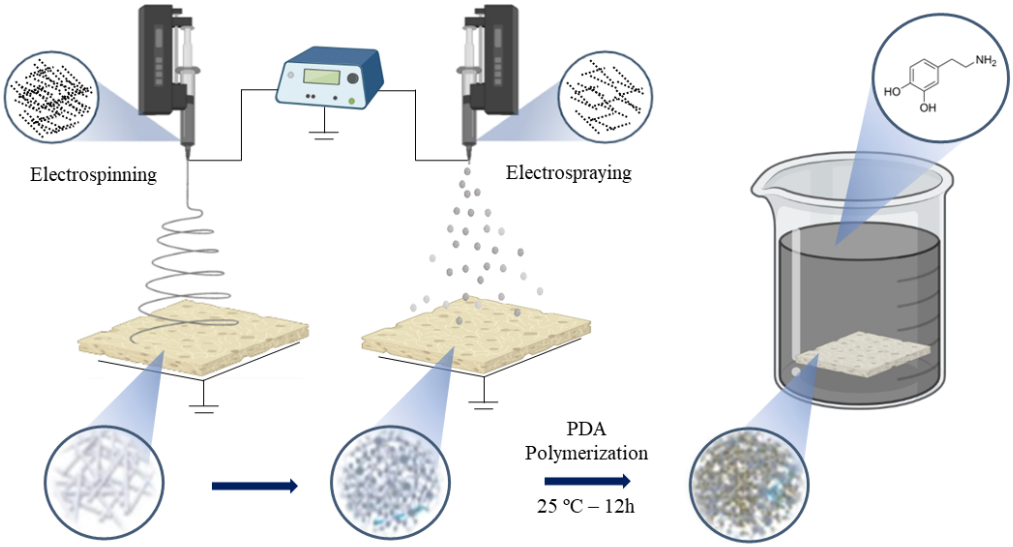

Source: adapted from Sun et al. (2021a).

All the studies in Table 2 used polymeric membranes, especially PVDF membranes. This polymer has high mechanical resistance, good chemical and thermal stability, and excellent resistance to aging (PRAMODA *et al.*, 2005; VO; GIANNELIS, 2007). PVDF can crystallize in at least three well-known crystalline phases. The α-phase is nonpolar and generated in the melting process from crystallization at any temperature and is the most common and thermodynamically stable form. The β-phase has a zigzag conformation with polar characteristics and is an oriented phase resulting from extensive mechanical deformation studied for its potential piezoelectric applications. The γ-phase is also a polar conformation with a polarity lower than the β that develops under specific conditions generated by crystallization at temperatures close to the melting point of the α-phase (GIANNETTI, 2001; RAMASUNDARAM *et al.*, 2008). Manufacturing conditions (such as dissolving temperature, precipitation temperature, coagulation medium, and coagulation temperature) impact the degree of crystallization and the crystalline phase during membrane formation. As a result,

crystallization affects PVDF membranes' final shape, chemical stability, thermal conductivity, and mechanical strength. Given PVDF characteristics, more research is still required to understand how crystallization (liquid-solid phase separation) affects the creation of the membrane structure (LIU *et al.*, 2011).

The DA concentration ranged from 0.2 to 2.0 g L^{-1} (Table 2). Previous studies show that this compound's concentration can influence the hydrophilicity result. However, the material that will be incorporated also affects the interaction with the membrane. This result is reported by Zin et al. (2019) when investigating the modification of PVDF membranes using DA/PEI (0.3 – 4.0 g L^{-1}/ 0.15 – 8.0 g L^{-1}) to increase their hydrophilic capacity. The authors observed that water uptake was only increased when using concentrations up to 0.5 g L^{-1} of DA solution. The use of higher or lower concentrations of DA did not positively interfere with the hydrophilicity of the membrane in this study.

A trend between the underwater oil contact angle (UOCA) and the oil removal percentage can be seen in Figure 2.11a, indicating that membranes with contact angles higher than 135° were responsible for oil removal greater than 98%. The lowest oil removal obtained was 95%, by Yu et al. (2019), who used the lowest PDA concentration to prepare the membrane. We noticed that most of the papers that investigated the use of PDA at concentrations lower than 2.0 g L^{-1} did not present results regarding UOCA and oil removal (Figure 2.11b). In this case, Liu et al. (2021) when using 1.0 g L^{-1} of PDA obtained a removal close to 92%, indicating that the concentration of 2.0 g L^{-1} is the one that has shown the best results in oil separation in the evaluated studies.

Figure 2.11. Effect of the membrane Underwater Oil Contact Angle (UOCA) (a) and the PDA concentration (b) used in the membrane preparation step on the oil removal from wastewater.

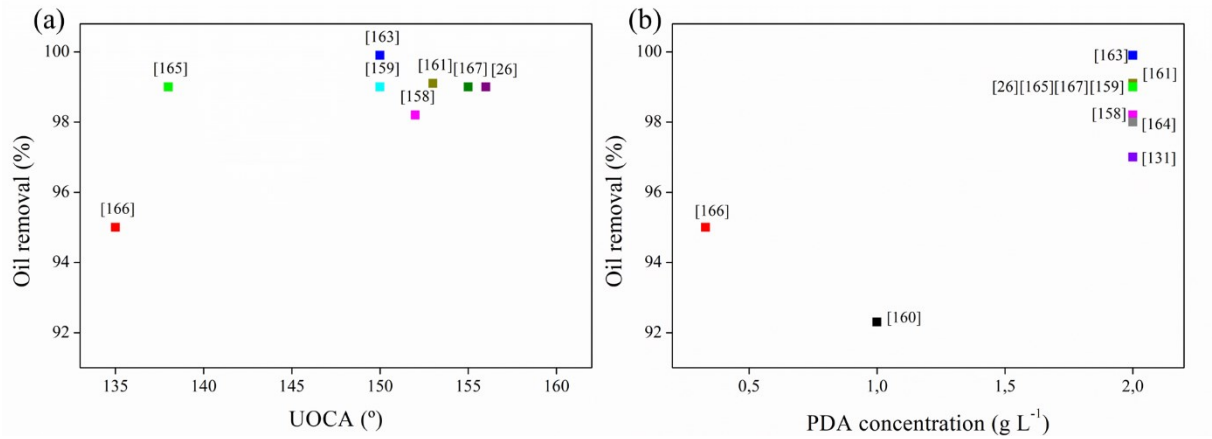

Source: the author (2023).

It is possible to observe in Table 2.2 that the photocatalytic capacity obtained with the use of PDA as a binding agent between the membrane materials and the catalyst was not compromised when compared with the results obtained without using PDA. All studies showed contaminant degradation greater than 90%. Emphasis can be given to the work of Zong et al. (2021), who demonstrated the degradation of tetracycline close to 100% by a PVDF membrane modified with LDH. The work of Feng et al. (2022) should also be highlighted. They presented the degradation efficiency (>92%) of contaminants (methylene blue, methyl blue, crystal violet, congo red, methyl orange) by a PEN membrane modified with MXene@TiO_2.

Analyzing the action of the PDA in the modification process and what function and improvement it brought to these membranes (see PDA novelty in Table 2), some points can be highlighted: strong connection and power of adhesion between the membrane polymer and the catalyst, reported by 7 of the 13 evaluated works (CHEN *et al.*, 2019; LI *et al.*, 2019; QU *et al.*, 2021; SUN *et al.*, 2021b; WANG *et al.*, 2022; YU *et al.*, 2019; ZONG *et al.*, 2021), increased chemical stability (LI *et al.*, 2019; WANG *et al.*, 2020c; YU *et al.*, 2019), increased the hydrophilicity (LIU *et al.*, 2021; SUN *et al.*, 2021b), and increased light absorption (LIU *et al.*, 2021).

In summary, modifying photocatalytic membranes with PDA can improve their performance in treating oily wastewater in several ways. Here are some potential benefits:

- Enhancing photocatalytic activity: PDA can act as a bridge between the photocatalyst and the membrane substrate, improving the photocatalytic activity of the membrane,

and resulting in faster and more effective removal of oil and other pollutants from wastewater;

- Improving membrane stability: PDA can form a robust and stable coating on the membrane surface, protecting it from degradation caused by harsh environmental conditions, such as high temperature and chemical exposure;
- Enhancing hydrophilicity: PDA can increase the hydrophilicity of the membrane surface, which can reduce fouling and improve the antifouling properties of the membrane. This feature can increase the durability and lifespan of the membrane, as well as reduce the need for cleaning and maintenance.

2.4 CATALYSTS USED IN PHOTOCATALYTIC MEMBRANES

TiO_2 is one of the most prevalent photocatalytic membranes and it is used in three of the 13 studies presented, proving to be a good catalyst option, and showing promising results. Some studies use TiO_2 as a catalyst with interesting degradation and oil retention results, even not using the surface modification method with dopamine. For example, Ong et al. (2014) evaluated the performance of a membrane photocatalytic reactor for treating synthetic cutting oil wastewater. They compared a PVDF hollow fiber ultrafiltration membrane with PVDF membranes with different concentrations of TiO_2 synthesized by the dry jet spinning method. The manufactured membrane can reach 80% of TOC degradation. Li et al. (2015) showed the oil-water separation capacity of a membrane made from the growth of hierarchical TiO_2 nanotubes anodized on a porous titanium surface. The membrane exhibited superoleophobic capacity and could degrade methylene blue organic molecules during permeation.

Recently, a study by our research group evaluated the incorporation of TiO_2 using PDA in a PVDF membrane. The incorporation of TiO_2 was effective and increased the water permeance of the membrane by 2.3-fold. This result is significant for oily wastewater treatment since it indicates that the membrane's hydrophilic character has improved (DA SILVA *et al.*, 2022).

Chen et al. (2020b) prepared a flower-shaped visible light-activated antifouling membrane from TiO_2 and Bi_2MoO_6 supported on carbon fabric by the hydrothermal method. It separated oil/water mixtures with up to 99% rejection. In addition, the membrane exhibited superior antifouling and regeneration properties when subjected to visible light, showing

stability after 140 separation cycles. They obtained almost complete methylene blue degradation efficiency (model pollutant) in 14 min.

TiO_2 is widely used due to some properties considered superior to other metallic oxides, such as excellent optical and electronic properties, high photocatalytic activity, high chemical stability, low cost, non-toxicity, and being environmentally friendly (KANAN *et al.*, 2020). Several studies were reported comparing TiO_2 with other semiconductors, such as the study by Wu (2004), who reported a higher photodegradation rate of Procion Red MX-5B using TiO_2 (0.34 h^{-1}) versus ZnO (0.25 h^{-1}) at pH 7.

TiO_2 has some limitations, including poor performance under visible light, a poor affinity for organic pollutants (especially hydrophobic ones, whose low adsorption on the TiO_2 surface leads to poor photocatalytic degradation rates), and aggregation because of the instability of the nanoparticle (hindering the incidence of light on the active sites, thus reducing degradation) (DONG *et al.*, 2015). In addition, one of the main practical challenges to be overcome is the recovery of nanometric TiO_2 particles from treated water for economic and biosafety concerns. Incorporating this photocatalyst in membranes is a great alternative to solve this drawback (MALLAKPOUR; NIKKHOO, 2014).

Some other catalysts have been developed and were addressed in research for incorporation into photocatalytic membranes for oily wastewater treatment. Among them, the metal-organic framework (MOF) constitutes a large family of micro or mesoporous crystalline materials that can present extensive surface areas; within the MOF catalysts, the zeolitic imidazolium frameworks (ZIF) stand out for their catalytic and adsorption capacity (WANG *et al.*, 2020d). Among carbon nitrides, the graphitic carbon nitride (g-C_3N_4) consists of units that can be described as three fused triazine rings, forming a layered structure with semiconducting properties (ISMAEL, 2020). Graphene and its oxide form (GO) comprise a single carbon layer with an allotropic network. It has generated a revolution in material science due to its properties with potential application in several areas (PADMANABHAN *et al.*, 2021). Bismuth oxyhalides (e.g., $Bi_{12}O_{17}C_{l2}$) have been gaining ground also due to the unique layered structure and internal static electric fields perpendicular to each layer, achieving improved photocatalytic performance (ZHANG *et al.*, 2020).

Using free photocatalysts in a process has several drawbacks, such as difficult separation from the mixture, surface contamination, photocorrosion, restricted stability, and aggregation. These issues can result in the gradual deactivation of the photocatalyst over time,

leading to low durability. Incorporating the photocatalyst on a membrane can prevent its aggregation and protect it from photocorrosion and surface contamination, improving stability and prolonging its lifetime. In summary, incorporating photocatalysts into membranes can surpass some major disadvantages of photocatalysis, and PDA-assisted modification is a promising route. This approach can improve the efficiency and effectiveness of photocatalytic processes and enable the practical development of this technology.

2.5 FUTURE PERSPECTIVES ON PDA-ASSISTED PHOTOCATALYTIC MEMBRANES

Several studies have reported using PDA-assisted membrane modification to improve the adhesion capacity between different materials, such as polymers, enzymes, hydrophilic and hydrophobic agents, and catalysts. The deposition of photocatalysts onto membranes using PDA as a binding agent has been indicated as a promising strategy for producing stable photocatalytic membranes designed to treat oily wastewater. However, several issues must be addressed to promote the sustainable industrial use of polydopamine as a binding agent and the use of photocatalysts. The future perspectives in the development of these PDA-photocatalytic membranes include:

- Optimization of polydopamine and photocatalyst coating - investigate the thickness and uniformity of the layer by modifying the concentration and number of deposition steps and the deposition strategy. Moreover, detailed studies of the attachment between the different catalysts, membrane materials, or membrane morphology are still needed.
- Integration with other technologies - assess using photocatalytic membranes with advanced treatment technologies such as electrocoagulation, ultrasound, and adsorption to enhance the overall treatment efficiency.
- Scale-up and commercialization - investigate the sustainability of incorporating the PDA and photocatalysts onto membranes regarding economics and environmental points of view to optimize production and reduce associated costs.
- Application to other types of wastewaters - in-depth study of application on different kinds of municipal and industrial wastewater to remove various pollutants, mainly emerging contaminants, such as residues from pharmaceutical industries.

- Environmental sustainability - future research may focus on the environmental impact of these membranes and their potential for reuse and recycling, evaluating the durability of the PDA coating.

Most published studies are still at the laboratory level, and the validation of the performance of photocatalytic membranes on oil removal in surface water, sewage, and wastewater treatment still needs to be explored. Developing simple and fast modification methods to accelerate the process is essential for producing effective photocatalytic membranes, but the large-scale application is still a challenge. Process upscaling is complex due to the challenge of designing a photocatalytic membrane module that optimizes light incidence on the membrane. Finally, future research should be directed toward optimizing membrane synthesis, module design, and system performance assessment in wastewater treatment. The development of PDA-assisted photocatalytic membrane modification can be promising to improve oily wastewater treatment, favoring industrial activity's economic, social, and environmental aspects.

2.6 CONCLUSIONS

The treatment of oily wastewater is still a problem that requires research and development of new strategies or even technologies. Conventionally, coagulation, adsorption, and chemical oxidation have been employed to treat oily wastewater, but with limitations regarding efficiency, cost-effectiveness, and environmental impact. On the other hand, emerging technologies such as photocatalytic membranes, which combine the advantages of membrane filtration and photocatalysis were identified as promising for oily wastewater treatment. Recently published research demonstrated that photocatalytic membranes could provide high removal efficiency and effectively treat recalcitrant organic compounds.

Developing photocatalytic membranes is a challenging task due to the difficulty of incorporating photocatalysts into the membrane structure without compromising its mechanical strength and stability. Achieving a uniform distribution of the photocatalyst is crucial for optimal membrane performance. Fortunately, recent advancements in PDA-assisted membrane modification have allowed the incorporation of photocatalysts into the membranes while improving their stability. This method presents new opportunities for enhancing the efficiency of treatment processes. Further research and development in this field, through optimization of

the coating process, investigation of the adhesion of new catalysts, scale-up, and detailed evaluation of membrane reuse, as well as their application in other areas, can significantly improve the efficiency of wastewater treatment, promoting a more sustainable future for industries and the environment.

2.7 ACKNOWLEDGMENTS

The authors acknowledge the Conselho Nacional de Desenvolvimento Científico e Tecnológico (CNPq) and Coordenação de Aperfeiçoamento de Pessoal de Nível Superior (CAPES) for financial support and scholarships.

CHAPTER 3

INCORPORATION OF TITANIUN DIOXIDE INTO PVDF MEMBRANE BY SURFACE MODIFICATION USING POLYDOPAMINE: MEMBRANE CHARACTERIZATION AND PERFORMANCE ASSESSMENT

3 Incorporation of titanium dioxide into PVDF membrane by surface modification using polydopamine: membrane characterization and performance assessment

This chapter presents the preliminary results obtained in this thesis. Once promising results concerning the water permeance of the commercial PFDV membranes were obtained through the PDA modification, the study was published as a short communication research article entitled "***An expedite facile method for modification of PVDF membranes with polydopamine and TiO_2 to improve water permeation***" in the journal *Materials Letters* (Impact Factor (2022) - 3.00).[3] According to Elsevier subscription rules, the authors retain the right to include the article in a thesis, provided it is not published commercially.

Graphical abstract

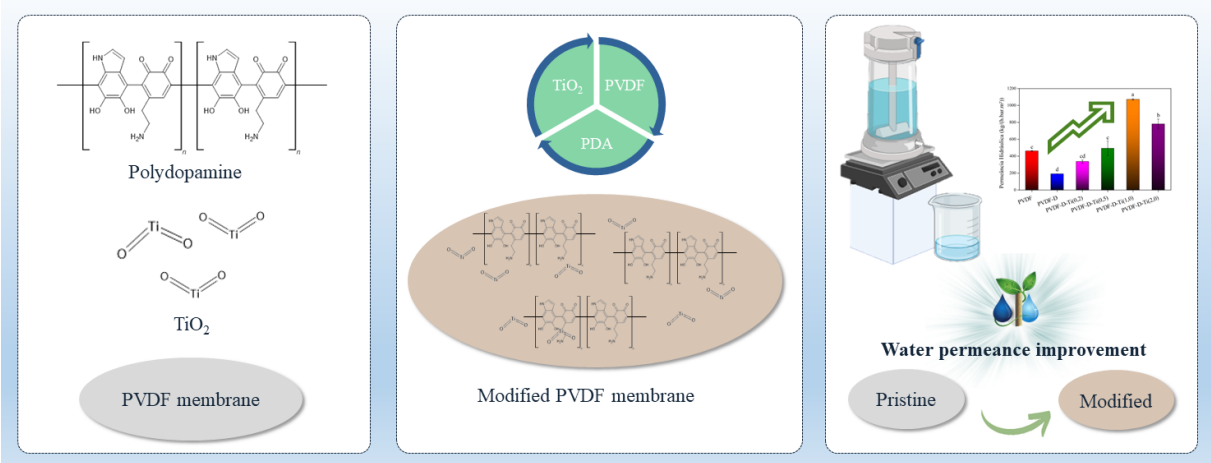

Highlights

• The use of PDA and TiO_2 to modify a commercial PVDF membrane was successful.

• For TiO_2-modified membranes, a small peak could be attributed to TiO_2 presence.

• A 2.3-fold increase in water flux was obtained at the 1.0% of TiO_2 incorporation.

[3] DA SILVA, A. F. V.; CESCA, K.; AMBROSI, A.; ZIN, G.; DI LUCCIO, M.; OLIVEIRA, J. V. An expedite facile method for modification of PVDF membranes with polydopamine and TiO2 to improve water permeation. Materials Letters, p. 132611, 2022. Disponível em: https://doi.org/10.1016/J.MATLET.2022.132611

Abstract

This study demonstrates a facile method of poly(vinylidene fluoride) (PVDF) membrane surface modification with polydopamine and TiO_2 to increase water permeation. For this purpose, a PVDF membrane was modified with TiO_2 concentrations ranging from 0.2 to 2.0 wt%. Deposition of TiO_2 was confirmed by a characteristic peak of TiO_2 from X-ray diffraction (XRD). Scanning Electron Microscopy (SEM) micrographs showed that the modification process with polydopamine caused some obstruction of the pores. Nevertheless, the membrane modified with 1.0% TiO_2 showed greater water permeance, indicating that this incorporation promoted higher membrane hydrophilicity.

Keywords: membrane process; polydopamine; hydrophilicity; titania.

3.1 INTRODUCTION

Membrane processes are an excellent and promising alternative to conventional thermal methods for separating different compounds present in industrial wastewaters. Even though many applications are already well developed, several challenges still need to be solved to improve the characteristics of membranes in terms of separation performance, antifouling properties, and stability (BAIG *et al.*, 2022; MULINARI; OLIVEIRA; HOTZA, 2020).

Surface modification has been studied among the viable ways of improving membrane selectivity. The use of dopamine (DA) as a binding agent between membrane and modification material has gained appreciable importance in recent years (PRONER *et al.*, 2020; ZIN *et al.*, 2019). This technique is inspired by the adhesive secretions of mussels, which form a strong interaction with different substrates in humid conditions and can be used with many materials (BURZIO; WAITE, 2000). Dopamine is a monomer derived from 3,4-dihydroxy-L-phenylalanine (L-DOPA), which undergoes oxidation and goes through a spontaneous polymerization process resulting in the formation of polydopamine (PDA), a polymer responsible for the ability to adhere to different surfaces (LEE *et al.*, 2007). The thermodynamic compatibility of PVDF and PDA with TiO_2 in terms of interaction parameters also needs to be studied based on similar reports (RANA *et al.*, 2000; RANA; MANDAL; BHATTACHARYYA, 1996).

The hydrophilic nature of TiO_2 makes it great for membrane modifications used for water separation. Furthermore, TiO_2 is widely described in the literature as a versatile,

inexpensive, stable, abundant, and ecological compound (SINGH GAUR; JAGADEESAN, 2021). This study aims to present an alternative method of membrane modification using PDA and TiO_2 to improve membrane hydrophilicity. To the best of our knowledge, the investigation of PVDF membrane modification using PDA and TiO_2 in a single and simple step has not been previously reported.

3.2 MATERIALS AND METHODS

3.2.1 Materials

Poly(vinylidene fluoride) (PVDF) microfiltration membranes with a pore size of 0.2 µm were obtained from MICRODYN-NADIR® (NADIR® MV020, USA). Dopamine hydrochloride (DA) (98%, Sigma-Aldrich, USA), tris(hydroxymethyl) aminomethane (99.5%, Neon, Brazil), titanium dioxide (TiO_2) (99%, Neon, Brazil), hydrochloric acid (37%, Neon, Brazil), sodium dodecyl sulfate (SDS) (90%, Synth, Brazil), and ethanol (99.8%, Neon, Brazil) were used during the experiments as purchased. Refined soybean oil (Coamo®) was purchased from a local market.

3.2.2 Membrane modification

Initially, 25 mL of dopamine hydrochloride solution (2 g L^{-1}) were prepared in Tris-HCl solution (pH 8.5, 50 mM), then TiO_2 (0.2; 0.5, 1.0 and 2.0% w/v) was added to this solution and homogenized. The PVDF membrane (0.2 µm, NADIR® MV020, USA) samples were cut into discs (5 cm), immersed in the solution, and shaken (Solab, SL-223, Brazil) for 24 h at 160 rpm and 25 °C. The membrane was then washed with ultrapure water, dried at 65 °C for 24 h, and stored (Figure 3.1). Membranes were identified as PVDF-D-Ti(C), where C is the concentration of TiO_2.

Figure 3.1. Schematic diagram of membrane modification steps.

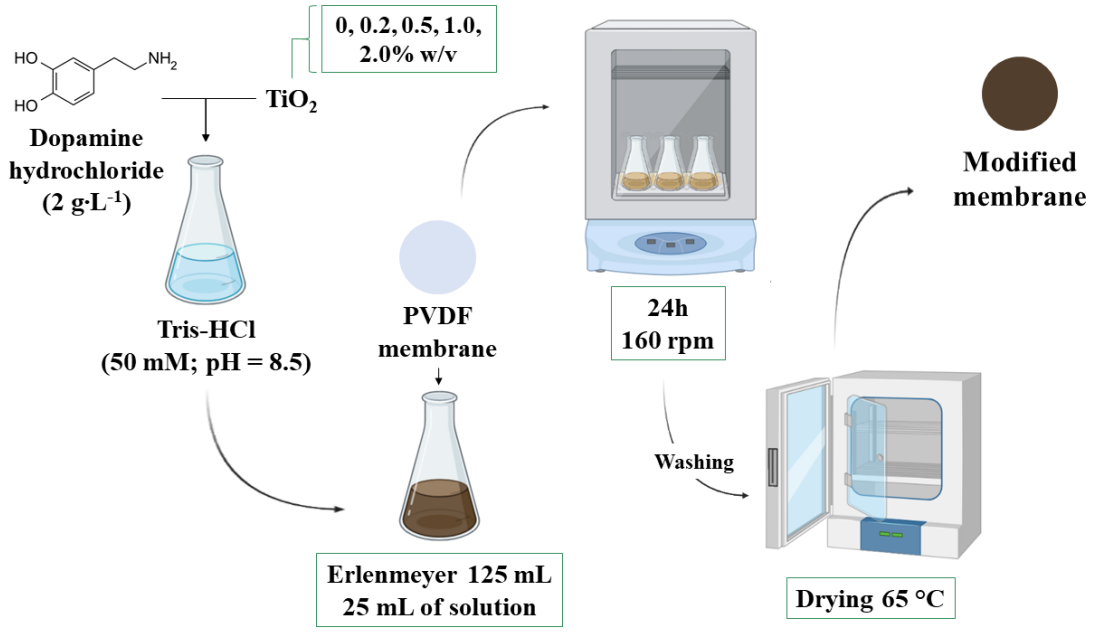

Source: the author (2023).

3.2.3 Membrane characterization

Fourier transform infrared spectroscopy (FTIR), X-ray diffractometry (XRD), scanning electron microscopy (SEM), and wettability were applied to study de functional groups, TiO_2 immobilization, surface morphology, and hydrophilicity of the samples, respectively.

3.2.3.1 Surface chemical composition

Analyzes were performed using a Fourier transform infrared spectrometer (Agilent Technologies, Cary 600, Australia). The TiO_2 samples (powder) were analyzed in the range from 4000 to 400 cm^{-1} and prepared using the KBr pellet technique, while the membrane samples were analyzed in the range from 4000 to 600 cm^{-1} using the Attenuated Total Reflection (ATR) technique.

3.2.3.2 Crystalline phases identification

The X-ray diffractograms were obtained in a diffractometer (Rikagu, MiniFlex600, Germany), using the copper Kα line (0.1542 nm) obtained in the 2θ range from 10 to 80° in steps of 0.02º with a velocity of acquisition of 10º min^{-1}. The diffractograms were analyzed using the X'pert Highscore Plus® software to identify the crystalline phase and to obtain average sizes of TiO_2 crystallite based on the highest intensity peak of the referred diffractograms using the Scherrer equation (Eq. 3.1).

$$D = \frac{K\lambda}{\beta \cos\theta} \tag{3.1}$$

where D is the average diameter of the crystallites (nm), K the constant that depends on the shape of the particles (equal to 0.9 for spherical particles), λ the wavelength of electromagnetic radiation (Cu = 0.15405 nm), θ the diffraction angle and β the width at half the height of the diffraction peak.

3.2.3.3 Surface morphology

Scanning electron microscopy images were performed using a scanning microscope (JEOL, JSM 6390LV, Japan), approximation 25x to 10,000x and acceleration voltage of 10 kV. The samples were prepared in stubs and coated with a gold layer (LEICA EM, SCD500, Germany).

3.2.3.4 Hydrophilicity

The membranes will be characterized in relation to the mass gain in water (wettability) was carried out using samples of membranes cut into 5 cm diameter discs, for this the membranes were dried in an oven for 2 h at 65 °C and after that immersed in 99% PA ethyl alcohol for 2 h, washed with ultrapure water and then immersed in ultrapure water for 12 h. Pre-treatment with alcohol aimed to ensure full wettability of the membrane pores. This test will be performed in duplicate and the mass gain in water (M_a) was calculated by Eq. 3.2.

$$M_a = \frac{M_m - M_s}{M_s} \quad (3.2)$$

where M_a is the membrane water mass gain (g water/g dry membrane), M_m the wet membrane mass (g) and M_s the dry membrane mass (g).

3.2.4 Membrane performance

Experimental assays were carried out in a dead-end cell with a filtration area of 14.5 cm^2. The system was pressurized to 2.0 bar until the complete membrane compaction. The water flux and permeance were then determined. For water permeance, the membrane system was coupled to an 8 L tank filled with ultrapure water. The system was then pressurized at 2.0 bar, and samples were taken every 10 minutes, collecting the permeate for a period of 30 seconds, and measuring the mass of water that was permeated. This process was repeated until the mass difference was less than 10%, where total membrane compaction was considered. The permeate flux (J) is calculated based on Eq. 3.3.

$$J = \frac{V_p}{t \cdot A} \quad (3.3)$$

where V_p is the permeate volume (L), A is the membrane filtering area (m^2), and t is the sample collection time (h).

Water permeance was obtained from the angular coefficient of the plot of the permeate flux versus pressure. The permeate volume was collected for 30 seconds, varying the pressure from 2 to 0.5 bar in intervals of 0.5 bar every 15 minutes in triplicate (Figure A1, Appendix A).

For oil rejection tests (emulsion permeation), the cell was filled with 150 mL of an oil emulsion that was prepared with 1 g L^{-1} of soybean oil in water containing 2 mmol L^{-1} of sodium dodecyl sulfate and stirred in a magnetic stirrer at 800 rpm for 10 min, and subsequently sonicated in an ultrasonic sonicator (Ultronique, Q 550W, Brazil) at 250 W. The permeation of the emulsions was carried out under stirring at 300 rpm (magnetic stirrer with 2.0 cm suspended around 0.5 cm over the membrane) and the constant pressure of 0.25 bar. Aliquots of the first

2 mL of permeate were collected with aliquots of the feed and analyzed concerning total organic carbon (TOC) content, performed in a total organic carbon analyzer (Shimadzu, TOC-Vcph, Japan). The TOC retention of the membrane, R(%), was calculated according to Eq. 3.4.

$$R(\%) = \left(1 - \frac{P}{A}\right) \cdot 100 \quad (3.4)$$

where P is the TOC content in permeate (g L^{-1}), and A is the TOC content in feed (g L^{-1}).

3.2.5 Statistical analysis

The evaluation of the responses and the difference between them was evaluated using analysis of variance (ANOVA) and a comparison test between means (Tukey) at a significance level of 5% ($p<0.05$) using the *Statistica 12.0*® software.

3.3 RESULTS AND DISCUSSION

The FTIR spectra of modified and pristine membranes are shown in Figure 3.2a. For the TiO_2 spectrum, intense bands at 688 and 523 cm^{-1} are attributed to the stretching of the vibrations of the Ti-O-Ti bond. These bands have also been attributed to the anatase phase of titania (PRAVEEN *et al.*, 2014). Pristine PVDF membrane and TiO_2 particles show a large band between 3700 and 3000 cm^{-1} (dashed area), attributed to the stretching of the OH group, probably resulting from the presence of water (MINELLA *et al.*, 2010).

Figure 3.2. FTIR spectra of modified and pristine membranes (a) complete spectra (b) detailed low wavenumber region.

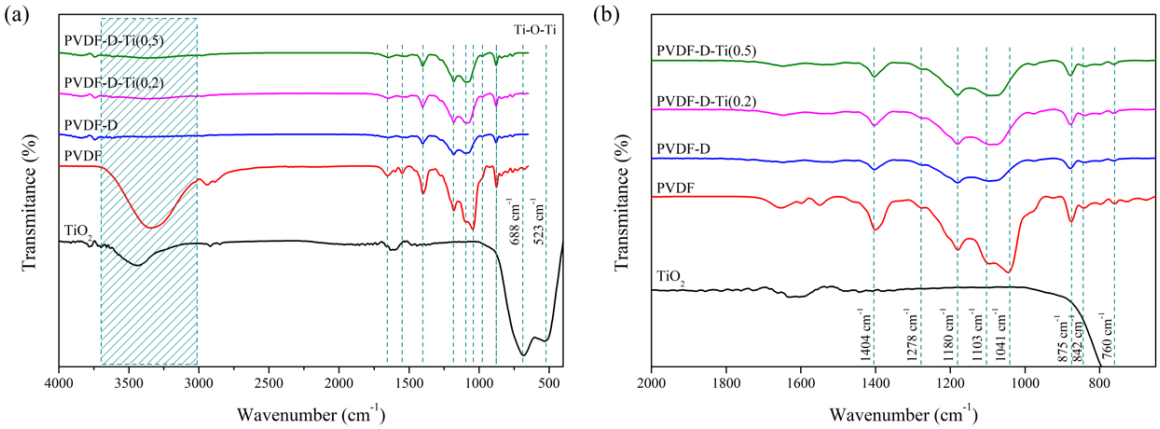

Source: the author (2023).

In the PVDF spectrum (Figure 3.2b), the band at 760 cm^{-1} is related to in-plane bending or α phase swing vibration, and the band at 842 cm^{-1} was associated with β or γ-phase stretching (BENZ; EULER; GREGORY, 2002). The bands at 1041 and 1103 cm^{-1} were attributed to the β-phase of PVDF (YU *et al.*, 2009). The bands at 1180 cm^{-1} and 1278 cm^{-1} are associated with the symmetrical elongation of the C–F bond of the CF_2 group and with the γ-phase, respectively. The absorption at 1404 cm^{-1} is assigned to the in-plane bending of the C–H bond of the CH_2 group (YU *et al.*, 2009). After the modification, we can observe the attenuation of the PVDF-specific bands, probably due to the DA coating. However, no characteristic absorption band of TiO_2 could be detected.

The XRD pattern for TiO_2 particles (Figure 3.3a) confirmed the titania anatase crystalline phase (ICDD 00-004-0477), with an average crystallite size of 42.9 nm. The characteristic peaks are highlighted in the image. Figure 3.3b shows the diffractogram for the PVDF and PVDF-D membranes. The coating with polydopamine did not cause any change in the diffractogram. The peaks at 2θ = 17.3, 19.8, and 25.5° refer to the characteristic planes of the α-phase of PVDF. The highest intensity peak found at 2θ = 22.3° was reported as characteristic of the β-phase (RAWINDRAN *et al.*, 2019). For PVDF-D-Ti membranes (Figure 3.3c), a small peak that could be attributed to TiO_2 was observed at 2θ = 25.09°. The appearance of characteristic TiO_2 peaks has been previously reported by Sun et al. (2021b) after modifying polyacrylonitrile membranes with TiO_2 and PDA.

Figure 3.3. XRD of (a) TiO_2, (b) PVDF and PVDF-D, and (c) PVDF-D-Ti membranes.

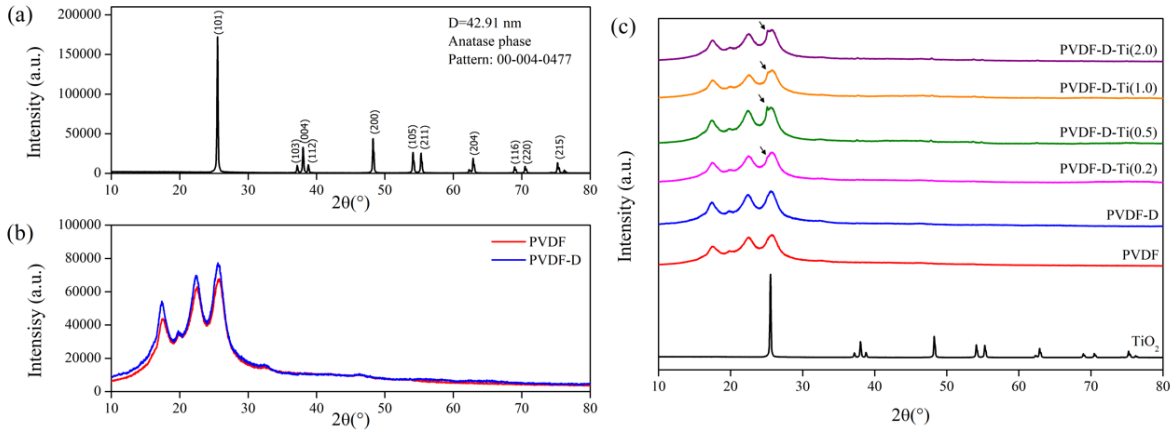

Source: the author (2023).

Figures 3.4a, 3.4b, and 3.4c show the SEM micrographs for the PVDF, PVDF-D, and PVDF-D-Ti(1.0), respectively. Pristine PVDF membrane shows well-defined pores on its surface. The coating with polydopamine caused the decrease in the surface porosity, as observed in Figure 3.4b and 3.4c, probably due to the obstruction arising from the deposition of polydopamine. On the other hand, the co-deposition of TiO_2 with PDA decreased the pore blockage (Figure 3.4c), suggesting that TiO_2 interfered in PDA coating, minimizing the obstruction of the porous surface.

Permeation tests were carried out to check whether the membrane modification influenced the membrane flux and water permeance. Figure 3.4d shows the evolution of the normalized flux with time for the membranes in the compaction period. The higher flux decrease was noted for PVDF-D, while the membrane modified with PVDF-D-Ti(1.0) showed minor flux decay.

Figure 3.4. SEM micrographs of membrane top surfaces (a) PVDF, (b) PVDF-D and (c) PVDF-D-Ti(1.0). Temporal evolution of normalized flux (d) and water permeance (e) for pristine and modified membranes.

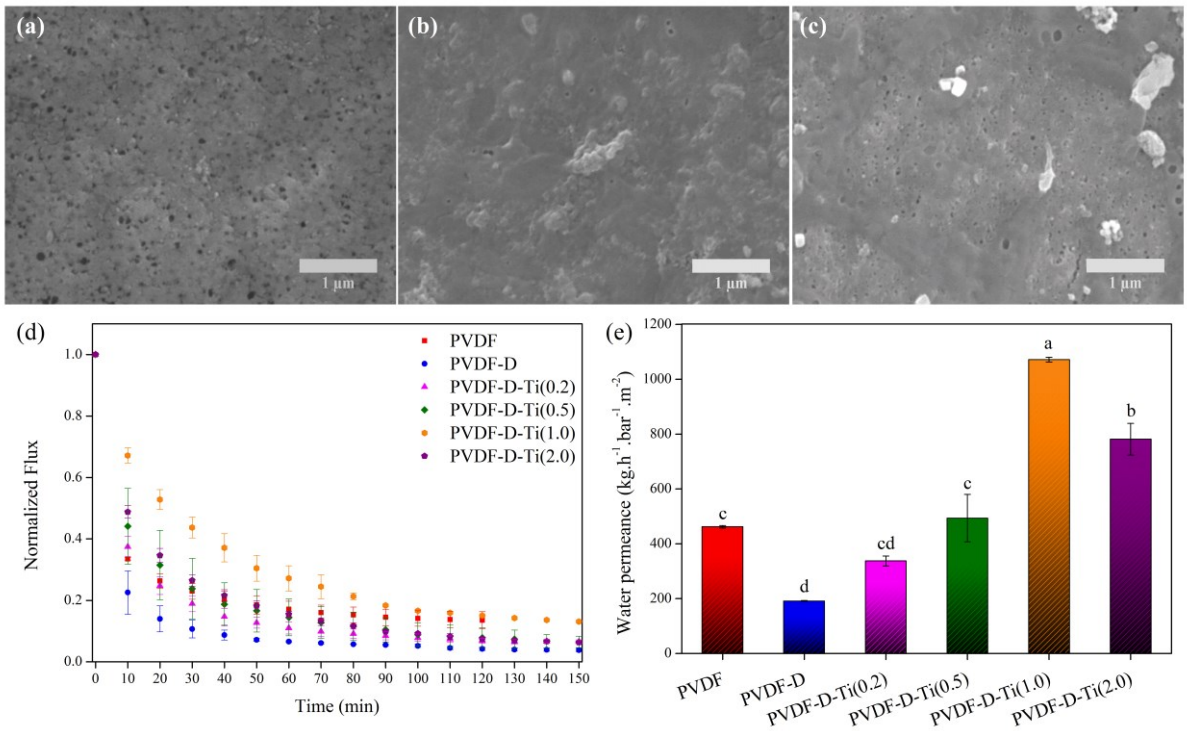

Source: the author (2023).

This behavior can be better observed in Figure 3.4e, which presents the water permeance of these membranes. We can see that the deposition of PDA caused a decrease in PVDF membrane flux from 462 to 191 kg h^{-1} bar^{-1} m^{-2}, probably due to partial pore obstruction, as observed in SEM images (Figure 3.4b). Adding up to 1 % TiO_2 to the coating solution caused a continuous increase in permeance. A 2.3-fold increase in water flux was obtained at the latter TiO_2 concentration. Further increase in the TiO_2 concentration to 2.0% caused a reduction in permeance to 781 kg h^{-1} bar^{-1} m^{-2}, indicating that a higher titania concentration was ineffective and contributed to pore blockage. Thus, it is possible to infer that the incorporation of TiO_2 in the coating solution has a positive response on the surface hydrophilicity since even with the pore obstruction shown in SEM images (Figure 3.4c), the PVDF-D-Ti(1.0) membrane showed improved water permeance. Decreased permeability with the polydopamine deposition process has been previously reported (MULINARI *et al.*, 2022; PRONER *et al.*, 2020). Therefore,

strategies that seek to recover this characteristic are of paramount importance. The application of TiO_2 has shown promising results, indicating the effective incorporation into the membrane.

Figure 3.5. (a) Wettability, and (b) TOC removal for pristine and modified membranes.

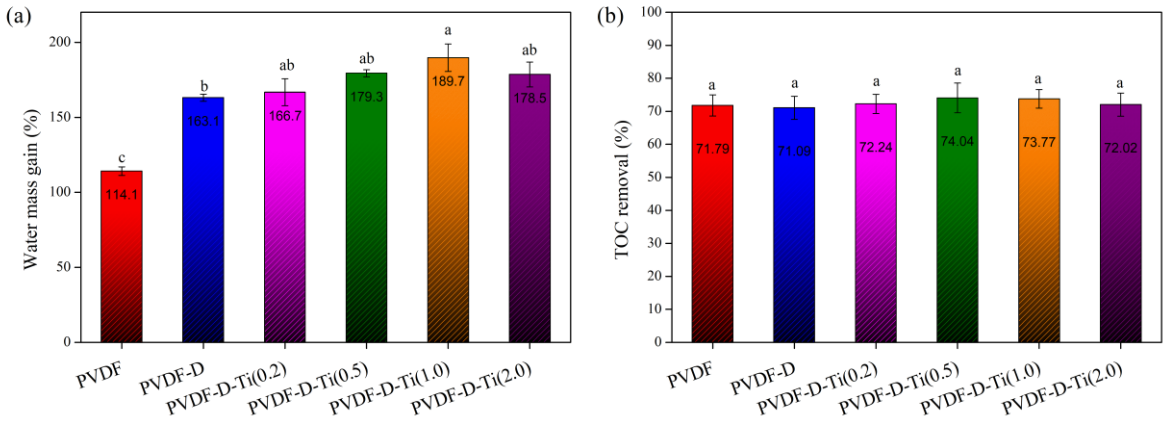

Source: the author (2023).

Regarding wettability (Figure 3.5a), the modified membranes showed a higher value than the pristine PVDF membrane. When modified with dopamine, only the membrane with 1.0% TiO_2 showed a significant difference in relation to the control (PVDF-D). This result corroborates with the indication that the PVDF-D-Ti(1.0) membrane presented the best permeance result. Regarding TOC rejection (Figure 3.5b), no significant difference was observed between the evaluated membranes, indicating that the modification did not impair the oil removal from the process. Even though there was no difference in rejection, the membrane with greater hydrophilicity generated a greater flow of process permeate, indicating the effectiveness of modifying the membrane. It is worth noting that the values presented are relative to the TOC reduction of the permeate over the feed, and this value refers to the TOC of the oil and surfactant (SDS) used in the emulsion, with the presence of SDS representing about 24.7% of the total TOC of the emulsion.

3.4 CONCLUSION

The use of PDA and TiO_2 to modify the surface of a commercial PVDF membrane was successful. According to XRD analysis, TiO_2 was incorporated into the membrane, presenting the characteristic TiO_2 peak. The modified membrane with 1.0 percent of TiO_2

(PVDF-D -Ti(1.0)) showed the best results for water permeance, 2.3x higher than the pristine membrane, even with partial clogging of the pores. The results indicate that the incorporation of TiO_2 brought a more hydrophilic character to the membrane surface, and did not interfere with the oil rejection, presenting improved characteristics for its application in oil wastewater treatment.

3.5 ACKNOWLEDGEMENTS

The authors acknowledge the support from the Conselho Nacional de Desenvolvimento Científico e Tecnológico (CNPq), Coordenação de Aperfeiçoamento de Pessoal de Nível Superior (CAPES), Central Laboratory of Electron Microscopy (LCME), and Interdisciplinary Laboratory for the Development of Nanostructures (LINDEN).

CHAPTER 4

OPTIMIZATION OF PDA-ASSISTED TiO_2 INCORPORATION ON A PVDF MEMBRANE AND INVESTIGATION OF SELF-CLEANING CHARACTERISTIC

4 Optimization of PDA-assisted TiO2 incorporation on a PVDF membrane and investigation of self-cleaning characteristic

This chapter presents the study regarding the optimization of the PDA-assisted incorporation of the TiO_2 on the PVDF membrane, as well the evaluation of the membrane's self-cleaning characteristic and stability over a few permeation cycles. The study is part of a research article entitled "***Enhanced Photocatalytic Activity and Self-cleaning Property of Membrane for Oil/Water Separation via Surface Functionalization with Polydopamine and Titanium Dioxide***" submitted to a high impact factor journal.[4]

Graphical abstract

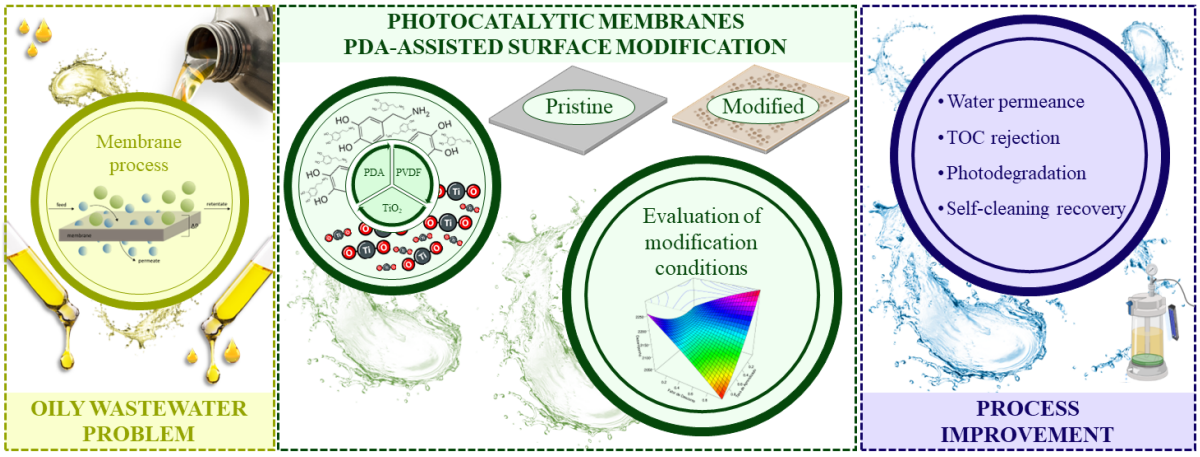

Highlights

• PVDF membranes modified with PDA and TiO_2 have improved antifouling properties.

• Water permeance reached 781 kg h^{-1} bar^{-1} m^{-2} and TOC rejection reached 87%.

• Photocatalytic degradation capacity reaches 97% for Methylene Blue.

• PDA-assisted modification improves self-cleaning with increased flux recovery by 86%.

Abstract

This study investigates the surface modification of poly(vinylidene fluoride) (PVDF) membranes using polydopamine (PDA) and titanium dioxide (TiO2) for effective separation of

[4] Article to be submitted: DA SILVA, A. F. V., ROCCA, D. G. D., MOREIRA, R. F. P. M., OLIVEIRA, J. V., DI LUCCIO, M., AMBROSI, A. **Enhanced Photocatalytic Activity and Self-cleaning Property of Membrane for Oil/Water Separation via Surface Functionalization with Polydopamine and Titanium Dioxide.**

oily compounds and self-cleaning photocatalytic behavior. The aim was to improve the antifouling properties of the membrane, which was modified by varied PDA and TiO_2 concentrations and evaluated regarding the water permeance, total organic carbon (TOC) rejection, and photocatalytic degradation activity. The results demonstrated considerable improvements in the membrane's antifouling properties, achieving a water permeance of 781 kg h^{-1} bar^{-1} m^{-2}, TOC rejection of 87%, and methylene blue photocatalytic degradation of 97%, using DA and TiO_2 concentration of 0.92 g L^{-1} and 1.4% (w/w), respectively, and a solution agitation speed of 106 rpm. Additionally, flux recovery reached 86% after the photocatalytic self-cleaning process, indicating that TiO2 improved the membrane's antifouling properties. These findings highlight the potential of PDA and TiO_2 as effective surface modifiers for enhancing oil/water separation, reducing fouling, and promoting self-cleaning effect in photocatalytic PVDF membranes. This study's outcomes provide valuable insights for developing efficient and sustainable membrane-based separation processes for oily wastewater treatment applications.
Keywords: Antifouling; Photocatalysis; Membrane process; Oily wastewater.

4.1 INTRODUCTION

The global significance of preserving natural resources, mainly water resources, is growing daily (YANG; YANG; XIA, 2021). The availability of clean water is extremely important for human development, and the improper disposal of wastewater can lead to serious environmental and public health problems (FARHAN HANAFI; SAPAWE, 2020). As the quantity and chemical complexity of industrial effluents generation increase, conventional water and sewage treatment techniques face limitations in their effectiveness. Thus, the development of new techniques or hybrid treatment systems play a vital role in addressing current techniques' limitations for the treatment of wastewater and removing pollutants (NASROLLAHI *et al.*, 2021). One significant challenge in wastewater discharge from several industries is the presence of oily compounds, which can include fats, hydrocarbons, and petroleum fractions (JAMALY; GIWA; HASAN, 2015b). Industries such as petrochemical, metallurgy, food, leather, and metal finishing produce a huge amount of oily wastewater (YU; HAN; HE, 2017). The disposal of such wastewater significantly impacts the environment and human health due to the presence of hazardous compounds (GOH; ONG; NG, 2019).

Membrane processes are a great and promising alternative to traditional methods for treating oily wastewater (TANUDJAJA *et al.*, 2019). While many applications of membrane processes are well established, there remain several unresolved issues related to improving the separation efficiency, antifouling performance, and membranes stability (HUANG; RAS; TIAN, 2018). Recently, photocatalytic techniques have been used as an alternative to address some of these limitations. This process involves using an appropriate light source to activate a photocatalyst that is deposited on the membrane surface to produce highly reactive radicals. These radicals aid in removing toxic and fouling compounds deposited on the membrane surface (MOKHBI; KORICHI; AKCHICHE, 2019; ZIOUI *et al.*, 2019). The most popular photocatalyst is the titanium dioxide (TiO_2), specifically the anatase phase. TiO_2 is excellent for modifying membranes used for water separation due to its hydrophilic nature. Additionally, TiO_2 is frequently referred to in the literature as a versatile, affordable, stable, abundant, and environmentally friendly substance (CHEN *et al.*, 2020a).

Surface modification to enhance membrane selectivity has been a subject of investigations, with recent years witnessing a notable increase in the utilization of polydopamine (PDA) as a binding agent between membrane and modification materials (MULINARI *et al.*, 2022, 2023; PRONER *et al.*, 2020; ZIN *et al.*, 2019). Inspired by the adhesive secretions of mussels, PDA demonstrates a strong interaction with various substrates in humid settings and can be employed with different materials. Dopamine, a monomer derived from 3,4-dihydroxy-L-phenylalanine (L-DOPA), undergoes oxidation and spontaneous polymerization to form PDA, which grants surfaces the ability to adhere (LEE *et al.*, 2007). Recently, Mulinari et al. (2023) used PDA to incorporate lipases on ceramic membranes and compared a one-step with a two-step modification strategy. They found that the lipases incorporated to the membrane presented good hydrolytic activity to control fouling in oily wastewater treatment, and that the simpler approach (one-step) resulted in similar results to the usual two-steps. This indicates that this technique has great application capacity for incorporating catalysts into membranes. In a previous study of our group (DA SILVA *et al.*, 2022), we observed that the incorporation of TiO_2 improved the water permeance of a PVDF membrane, but we needed to go further and investigate the photocatalytic activity and optimize the modification process. The optimization of parameters in membrane modification is an essential and critical step to ensure the effectiveness and efficiency of the application. Design of experiments (DoE) is an important tool to determine improved process conditions in the most

diverse fields, such as biotechnology (SILVA *et al.*, 2022), simulation (LIRA *et al.*, 2020), materials (DA SILVA *et al.*, 2019), and membrane processes (VALE DE MACEDO *et al.*, 2022).

This study aims to investigate the synergy between the presence of PDA and TiO_2, as well as the mass transfer promoted by stirring the modifying solution on the performance of the membrane. Thus, a design of experiments was used to optimize the modification process to obtain membranes with enhanced separation and photocatalytic capacity. A novel single-simple step strategy was used to incorporate the photocatalyst onto the membrane, offering a simplified and efficient approach.

4.2 MATERIALS AND METHODS

4.2.1 Materials

Poly(vinylidene fluoride) (PVDF) microfiltration membranes with a pore size of 0.2 µm were obtained from MICRODYN-NADIR® (NADIR® MV020, USA). Dopamine hydrochloride (DA) (98%, Sigma-Aldrich, USA), tris(hydroxymethyl) aminomethane (99.5%, Neon, Brazil), titanium dioxide (TiO_2) (99%, Neon, Brazil), hydrochloric acid (37%, Neon, Brazil), sodium dodecyl sulfate (SDS) (90%, Synth, Brazil), and ethanol (99.8%, Neon, Brazil) were used during the experiments as purchased. Refined soybean oil (Coamo®) was purchased from a local market.

4.2.2 Membrane modification process

Dopamine hydrochloride solution (0.7 – 2.3 g L^{-1}) was prepared in Tris-HCl solution (pH 8.5, 50 mM), then TiO_2 (0.7 – 2.3%) was added to 25 mL of this solution and homogenized. The PVDF membrane samples were cut into discs (5 cm), immersed in the solution, and shaken (Solab, SL-223, Brazil) for 24 h at 25 °C, with fixed agitation speed according to the experimental condition (106 – 174 rpm). The membrane was then washed with ultrapure water, dried at 65 °C for 24 h, and stored (Figure 4.1).

Figure 4.1. Schematic diagram of membrane modification steps. Created with BioRender.com.

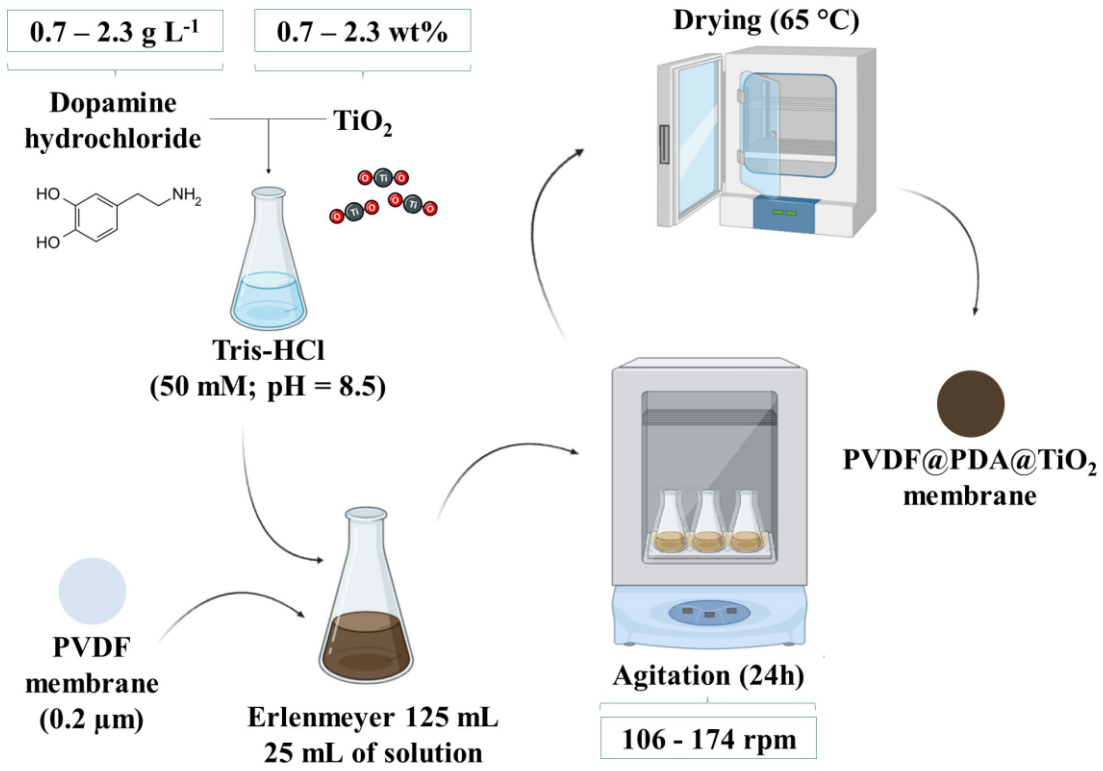

Source: the authors (2023).

A 2^3 central composite rotational design (CCRD) with DA concentration, TiO_2 amount, and agitation speed was used to assess the effects of these variables on the membrane modification and optimize the process. A triplicate at the central point was used to assess the error, resulting in 17 assays. The different factors and their respective levels are shown in Table 4.1.

Table 4.1. Factors and their respective levels of the CCRD used to perform the membrane modification assays.

Factors	Levels				
	-1.68	-1	0	+1	+1.68
X_1 - DA concentration (g L^{-1})	0.7	1.0	1.5	2.0	2.3
X_2 - TiO_2 amount (%)	0.7	1.0	1.5	2.0	2.3
X_3 – Agitation speed (rpm)	106	120	140	160	174

The experimental conditions and the levels of factors used were selected from preliminary tests (DA SILVA *et al.*, 2022). The water permeance, the oil rejection, and the degradation of a standard contaminant (methylene blue - MB) were the response variables, evaluated for each membrane sample of each modification condition. The data obtained were statistically analyzed by analysis of variance (ANOVA), Pareto diagram, and response surfaces at a significance level of 5% ($p < 0.05$) using Statistica 13.5® software. A regression model was proposed, and the response variables were related to the independent variables by a second-order quadratic polynomial equation (Eq. 4.1). Furthermore, the desirability function (DF) was used to identify the best membrane modification condition. Based on the simultaneous detection of multiple responses, this methodology is utilized to improve the conditions of the variables under study. This approach, which seeks to maximize the values of the independent variables while simultaneously identifying the optimum conditions, is expressed as a function on a desirability scale.

$$y = \beta_0 + \beta_1 X_1 + \beta_2 X_2 + \beta_3 X_3 + \beta_{11} X_1^2 + \beta_{22} X_2^2 + \beta_{33} X_3^2 + \beta_{12} X_1 X_2 + \beta_{13} X_1 X_3 + \beta_{23} X_2 X_3 \quad (4.1)$$

where y represents the answer (dependent variable), X_1, X_2 and X_3 represent the explanatory variable (independent variable), β_1, β_2 and β_3 are the linear parameters of the model, β_{11}, β_{22} and β_{33} are the quadratic parameters of the model, β_0 is the interception term and β_{12}, β_{13} and β_{23} is the interaction terms.

4.2.3 Membrane performance

Water flux and permeance were determined in a dead-end permeation module with a filtration area of 14.5 cm^2. The membrane module was coupled to an 8 L tank filled with ultrapure water for water permeance. Initially, the membrane was compacted by pressurizing the system to 2.0 bar and collecting the permeate for 30 seconds every 10 minutes. When the difference in mass was less than 10%, the membrane was considered compacted. Water permeance was obtained from the angular coefficient of the plot of the permeate flux vs. pressure. The permeate volume was collected for 30 seconds, varying the pressure from 2.0 to 0.5 bar in intervals of 0.5 bar every 15 minutes in triplicate. The permeate flux, J (L m^{-2} h^{-1}), was calculated based on Eq. 4.2.

$$J = \frac{V_p}{t \cdot A} \tag{4.2}$$

where Vp is the permeate volume (L), A is the membrane filtering area (m^2), and t is the sample collection time (h).

For oil rejection tests, the dead-end permeation module was filled with 150 mL of a 1 g L^{-1} soybean oil emulsion in an aqueous solution of the emulsifier sodium dodecyl sulfate (SDS) (2 mmol L^{-1}), stirred in a magnetic stirrer at 800 rpm for 10 min and subsequently sonicated in an ultrasonic sonicator (Ultronique, Q 550W, Brazil) at 250 W for 5 min, according to Zin et al. (2019), with modifications. The droplet size of the obtained emulsion was determined using a dispersion analyzer (LUM corporation, LUMiSizer®, USA). The resulting mean droplet size was approximately 84 ± 2 nm (Figure B1, Appendix B). The permeation of emulsions was carried out under magnetic stirring at 300 rpm and the constant pressure of 0.25 bar until obtaining a concentration factor equal to 3. The permeate was collected at different times (1, 2.5, 5, 7.5, 10, 15, and 20 min, after that at 10 min intervals). Aliquots of the first 2 mL of permeate and feed were collected and analyzed for total organic carbon (TOC) content, performed in a total organic carbon analyzer (Shimadzu, TOC-Vcph, Japan). TOC rejection of the membrane, R (%), was calculated according to Eq. 4.3.

$$R(\%) = \left(1 - \frac{P}{F}\right) \cdot 100 \quad (4.3)$$

where P is the TOC content in permeate (g L^{-1}), and F is the TOC content in feed (g L^{-1}).

The photocatalytic activity was evaluated using photocatalytic discoloration of methylene blue (MB) under ultraviolet (UV) irradiation. Membrane samples (1.5 x 1.5 cm) were placed in a beaker containing 10 mL of an MB solution (3.2 mg L^{-1}) in water and kept in the dark for 12 h to ensure adsorption equilibrium. Then, the membranes were transferred to a new MB solution (3.2 mg L^{-1}) and exposed to UV light (365 nm, 20 W) for 24 h, with a distance of 10 cm between the lamp and the membrane. The resulting MB discoloration was analyzed using a UV-Vis spectrophotometer (Quimis, Q898U2M5, Brazil) through absorbance decay measurements at a wavelength of 665 nm (COELHO *et al.*, 2022). A control assay without the membrane (photolysis) was also carried out. The MB removal, D (%), was calculated according to 4.4.

$$D(\%) = \left(1 - \frac{C}{C_0}\right) \cdot 100 \quad (4.4)$$

where C_0 and C are the initial and final concentration of MB (mg L^{-1}) in the solution, respectively.

4.2.4 Membrane characterization

Fourier transform infrared spectroscopy (FTIR), X-ray diffractometry (XRD), scanning electron microscopy (SEM), and wettability were applied to study the functional groups, TiO_2 immobilization, surface morphology, and hydrophilicity of the samples, respectively. FTIR analyses were performed using a Fourier transform infrared spectrometer (Agilent Technologies, Cary 600, Australia). The TiO_2 samples (powder) were prepared using the KBr pellet technique and analyzed in the 4000 - 400 cm^{-1} range, while the membrane samples were analyzed using the Attenuated Total Reflection (ATR) method in 4000 - 600 cm^{-1} range. XRD diffractograms were acquired in a diffractometer (Rikagu, MiniFlex600, Germany), using the copper Kα line (0.1542 nm) obtained in the 2θ range from 10 to 80° in

steps of 0.02º with a velocity of acquisition of 10º min^{-1}. The diffractograms were analyzed using the X'pert Highscore Plus® software to identify the crystalline phase. SEM images were performed using a scanning electron microscope (JEOL, JSM 6390LV, Japan), at an acceleration voltage of 10 kV. The samples were prepared in stubs and coated with a gold layer (LEICA EM, SCD500, Germany).

The amount of TiO_2 incorporated to the membrane was determined from the difference in mass between the membrane modified with PDA and TiO_2 and only with PDA after the sample calcination in a furnace (triplicate analysis).

Membrane wettability was investigated using water and n-heptane vapor adsorption measurements that were performed by placing Eppendorf's with approximately 0.1 g of membrane samples (~0.56 cm^2) inside closed Erlenmeyer flasks containing water or n- heptane at 23 °C. The samples were weighed at the beginning of the test and after 24 h to determine the vapor adsorption, expressed in mmol g^{-1} and the water/n-heptane ratio (MULINARI *et al.*, 2022).

In addition, the stability of the membranes was evaluated by subjecting the membranes to extreme conditions of acidity (pH 2) and alkalinity (pH 12), and the leached solutions were analyzed in a UV-Vis spectrophotometer.

4.2.5 Photocatalytic self-cleaning performance

Membranes self-cleaning performance was evaluated using a membrane sample prepared with the optimized conditions from the experimental design and the same permeation module mentioned in item 2.3. The following procedure was performed:

1. Evaluation of the membrane water permeance
2. Model emulsion filtration
3. Treatment of the membrane with UV (self-cleaning)
4. Evaluation of the membrane water permeance after self-cleaning
5. Repeating steps 2, 3 and 4 two times (three cycles of emulsion filtration)

The self-cleaning tests were carried out in a dark chamber, with a UV lamp turned on for 12 h with water, using the same apparatus used in the MB degradation tests.

4.3 RESULTS AND DISCUSSION

4.3.1 Optimization of functionalization conditions

The modified membranes were evaluated for water permeation, TOC rejection, and photocatalytic degradation of a standard contaminant. The results obtained for each condition of the experimental design are presented in Table B1 (Appendix B), while Figure 4.2 clearly indicates that the modified membranes presented better responses than the pristine membrane. The water permeance of the experimental condition PM08 (X_1 - 2.0 g L^{-1}, X_2 - 2.0%, X_3 - 160 rpm), for example, was 2.4x higher than that of the pristine membrane. The difference was smaller for TOC rejection, which in the best case (PM12, X_1 - 1.5 g L^{-1}, X_2 - 2.3%, X_3 - 140 rpm), was 1.2x greater than the pristine. It is worth mentioning that the TOC refers to the organic carbon from both oil and surfactant (SDS) used to prepare the emulsion. The permeate collected in the experiments did not present any characteristic of oil presence. When evaluating a solution with only the surfactant, it was observed that it showed a TOC of 27.86%, indicating that the modified membranes, in addition to removing the oil, also removed part of the surfactant during the separation process, since all modified membranes showed TOC rejection greater than 72.14%.

Evaluating the photocatalytic degradation activity, the pure membrane showed a slightly higher response than the degradation generated from the photolysis process, with a value of 22.07% color removal, an expected result since this membrane does not have the presence of a photocatalyst. The higher degradation result of the pristine membrane than the photolysis value can be attributed to some residual adsorption process. The responses of photocatalytic membranes were quite diverse, but notably, some of the modified membranes promoted a degradation higher than 95%, proving that the proposed modification is effective for obtaining photocatalytic membranes. A discussion regarding the interaction of process conditions for each of the response variables of the CCRD is presented in the following sections.

Figure 4.2. CCRD responses for the variables evaluated concerning (a) water permeance, (b) TOC rejection, and (c) photocatalytic degradation.

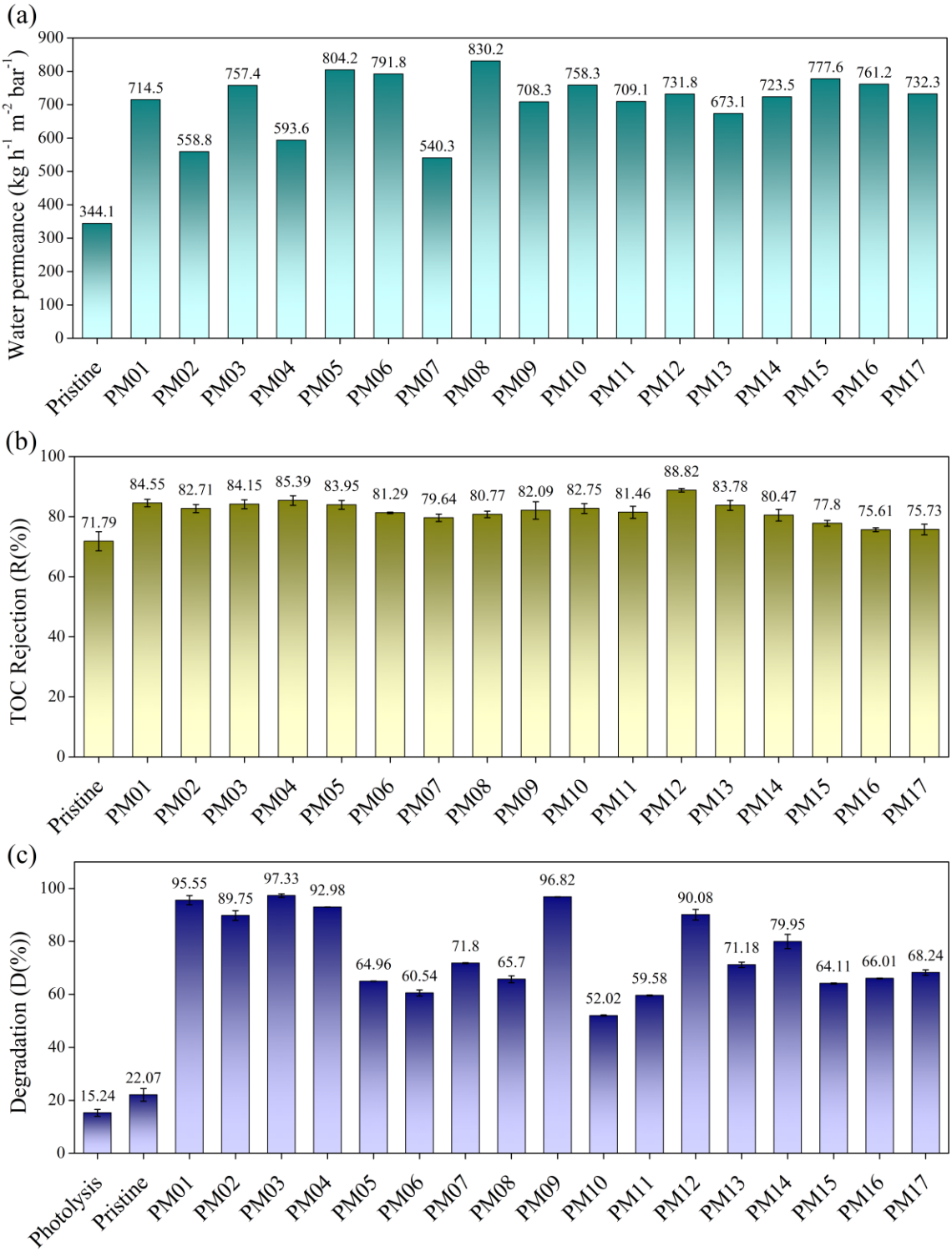

* Photolysis: solution subjected to light. Pristine: membrane without any modification. PM01 to PM17: modified membranes from the experimental design. Source: the authors (2023).

4.3.1.1 Water permeance

From the Pareto chart (Figure 4.3a), it is possible to note that the first-order DA concentration and the first-order linear interactions are the parameters with significant effect ($p < 0.05$) on the water permeance. The analysis of variance (ANOVA, Table B2) of the results indicates, after removing the non-significant parameters, that the proposed regression model (Eq. 4.5) shows about 82% of the variability in the responses ($R^2 = 0.82$). A non-significant lack of fit (p-value of 0.13) validates the model.

$$Water\ permeance = 758.06 + 31.22\ X_1 - 37.89\ X_1 X_2 + 74.63\ X_1 X_3 + 36.78\ X_2 X_3 \quad (4.5)$$

The DA concentration has a positive linear effect, which indicates that using a high DA concentration in the membrane modification benefits the water permeance (within the range studied). To elucidate the effects of the variables' interaction, response surfaces were plotted fixing one of the variables at the middle level.

Since the interaction between the DA concentration and the TiO_2 amount has a negative effect, i.e., the parameters are at opposite levels, the water permeance increases when using high DA concentration and low TiO_2 amount or vice-versa (Figure 4.3b). Moreover, the positive effect between the DA concentration and agitation speed (Figure 4.3c) indicates that the water permeance of the membrane is improved when these factors are at the same level of interaction (both positive or both negative). In this case, it should also be considered the positive effect of the DA concentration, because if the TiO_2 amount is fixed in the middle level, the best response is at the highest DA concentration and greater agitation speed. A similar behavior is found when evaluating the interaction between the TiO_2 amount and agitation speed (Figure 4.3d), in which the permeance is benefited when both factor levels are positive or negative. In this case, as neither the TiO_2 amount nor the agitation had a significant effect individually, it is not possible to observe much difference when the two factors were changed equally from negative to positive.

Figure 4.3. (a) Pareto chart and response surface plots for the interaction between (b) DA concentration *vs.* TiO_2 amount, (c) DA concentration *vs.* agitation, and (d) TiO_2 amount *vs.* agitation for water permeance.

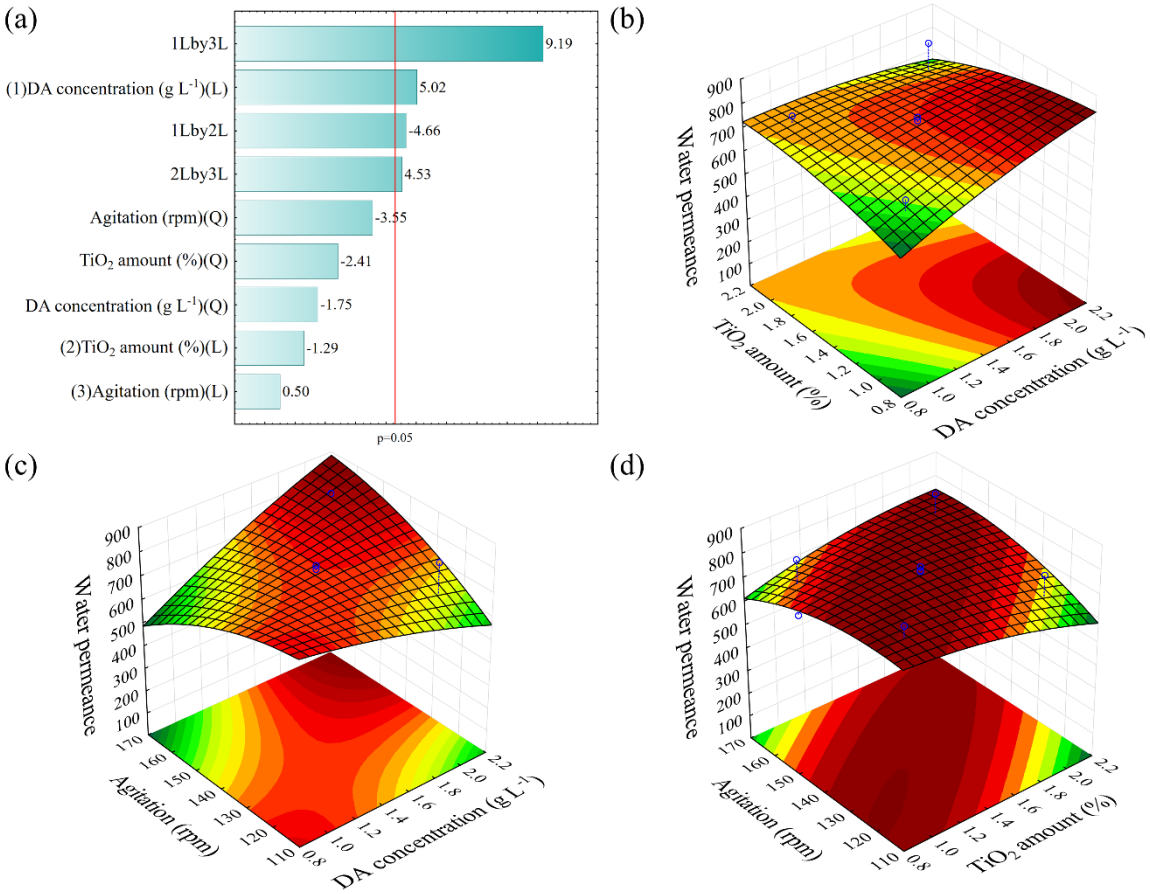

Source: the authors (2023).

4.3.1.2 TOC rejection

For TOC rejection, in the Pareto chart (Figure 4.4a), it is observed that all first-order quadratic factors proved to be positively significant in the process, meaning that the concavity of the parabola formed by the model is upwards, that is, TOC rejection benefits at more positive or more negative levels of the factors. The analysis of variance (Table B2) indicated that the proposed regression model (Eq. 4.6) did not show lack of fit, with an explained variation of about 80% ($R^2 = 0.80$), thus the response surfaces (Figure 4.4b, 4.4c, and 4.4d) show that the greatest TOC rejections occur in the upper or lower limits of the factors (in the vertices of the surfaces). As the effect promoted by the amount of TiO_2 was slightly greater than the other

factors, it is possible to observe that in Figure 4.4b and 4.4d, the tips in which the TiO_2 amount is higher have a higher value.

$$TOC\ rejection = 76.44 + 1.95\,X_1^2 + 2.91\,X_2^2 + 1.84\,X_3^2 \quad (4.6)$$

Figure 4.4. (a) Pareto chart and response surface for the interaction between (b) DA concentration *vs.* TiO_2 amount, (c) DA concentration *vs.* agitation, and (d) TiO_2 amount *vs.* agitation for TOC rejection.

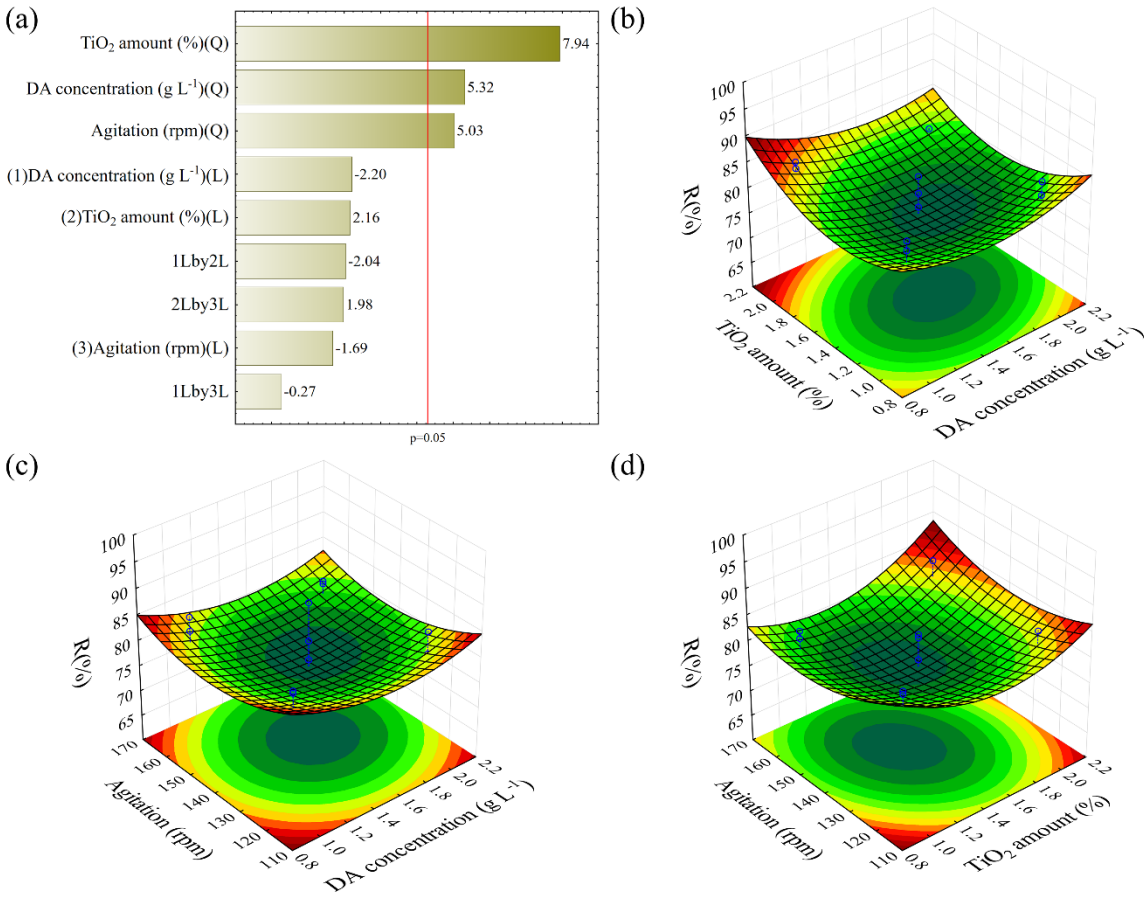

Source: the authors (2023).

4.3.1.3 Photocatalytic degradation

Analyzing the Pareto chart (Figure 4.5a), it is possible to observe that the linear effects of DA concentration and TiO_2 amount were significant in the process, presenting negative and positive values, respectively, implying that a lower DA concentration and a higher TiO_2 amount

benefit the modification process regarding photocatalytic degradation. However, all first-order quadratic factors also proved to be significative and with positive values, suggesting that the formed parabola is concave upwards, and the degradation is more efficient at the high or low level of the factors.

The regression model proposed (Eq. 4.7) for photocatalytic degradation did not show a lack of fit, with an explained variation of 91% ($R^2 = 0.91$), according to the analysis of variance (ANOVA) (Table B2).

$$Degradation = 65.81 - 13.76\,X_1 + 5.00\,X_2 + 3.91\,X_1^2 + 4.06\,X_2^2 + 4.32\,X_3^2 \quad (4.7)$$

Analyzing the response surface formed between the concentration of dopamine and the TiO_2 amount (Figure 4.5b), it is possible to observe that the best response is exactly when these factors present lower and higher values, respectively. As the linear effect of agitation was not significative, in Figure 4.5c and 4.5d, it is possible to observe that the responses are better in the low level of DA and the high level of TiO_2, respectively.

Figure 4.5. (a) Pareto chart and response surface for the interaction between (b) DA concentration *vs.* TiO_2 amount, (c) DA concentration *vs.* agitation, and (d) TiO_2 amount *vs.* agitation for photocatalytic degradation.

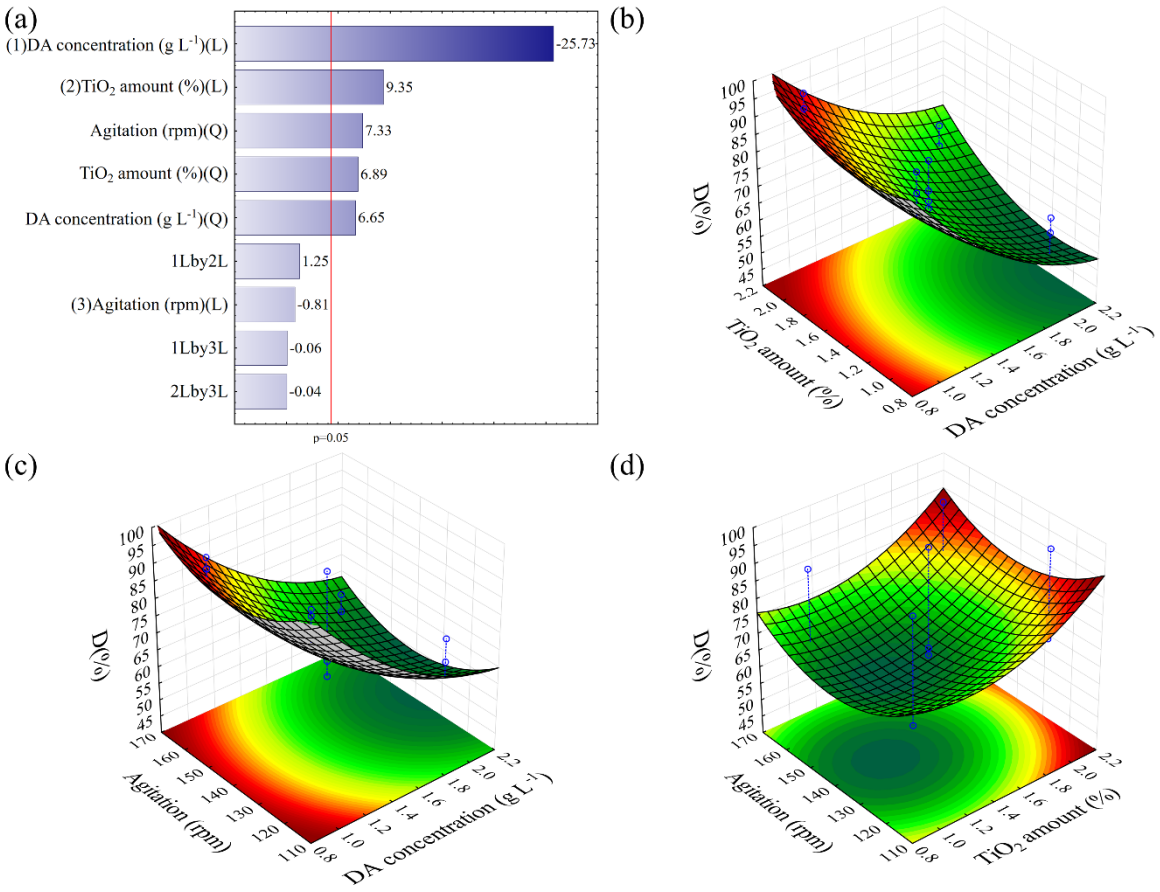

Source: the authors (2023).

4.3.1.4 Optimization of the modification conditions

The desirability function was used in the optimization process to find a modification condition that benefited all the responses simultaneously. A global function is generated from the three regression models and is maximized using a scale from 0 (undesirable) to 1 (very desirable) for each factor. Figure 4.6 shows the desirability profile obtained. It is possible to observe that the responses had a variability between 540.30 - 830.22, 75.61 - 88.82, and 52.02 - 97.33 for water permeance, TOC rejection, and photocatalytic degradation, respectively.

Figure 4.6. Profiles of predicted values from the desirability function concerning the water permeance, TOC rejection, and photocatalytic degradation for the modifier membranes.

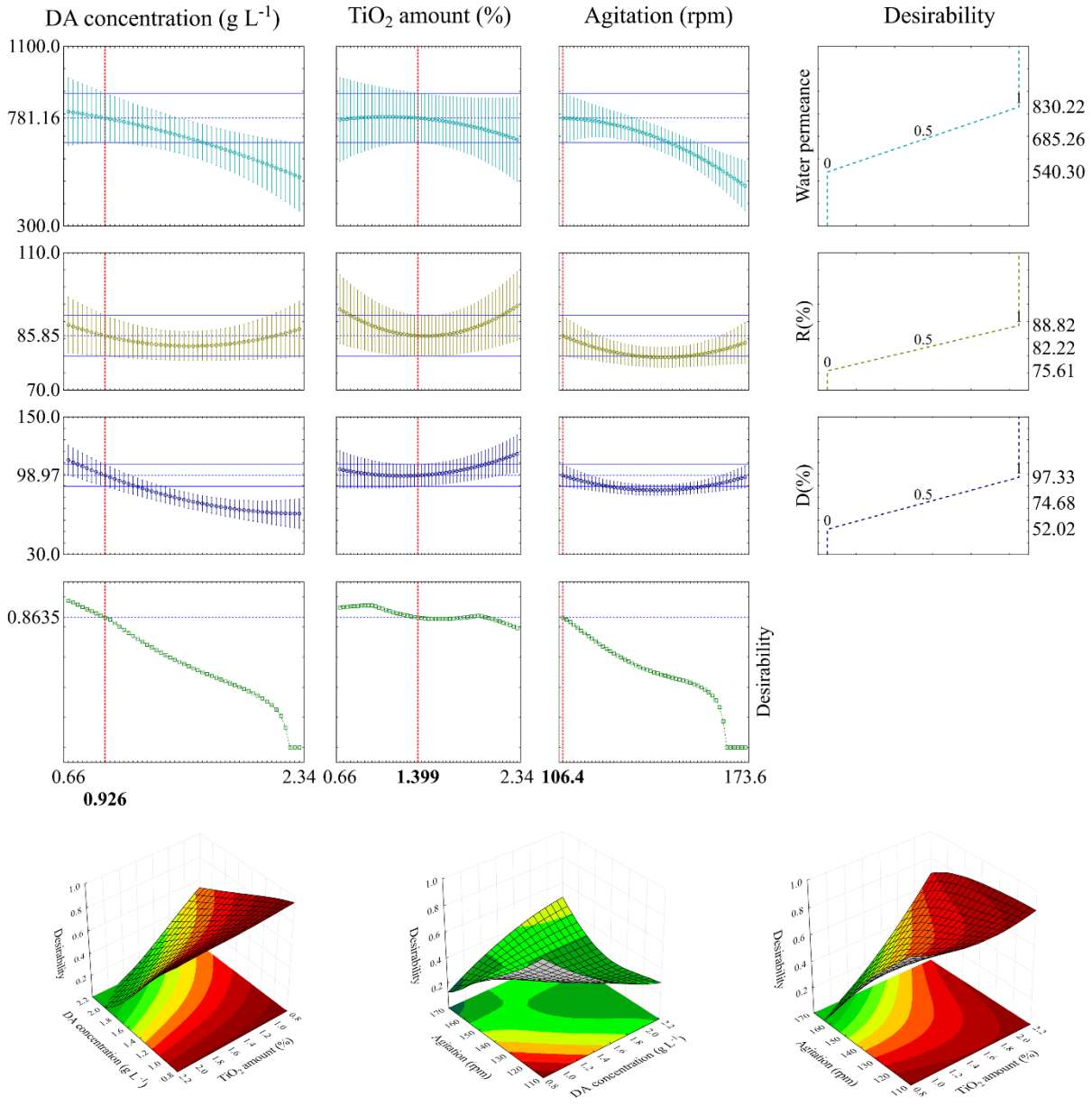

Source: the authors (2023).

Obtained results using the desirability function show that the best (desirability value of 0.8635) water permeance, rejection and MB degradation can be obtained using DA concentration, TiO_2 amount, and agitation at 0.92 g L^{-1}, 1.4%, and 106 rpm, respectively.

Using the optimized modification conditions, a new set of experiments was performed, and the results obtained (EV) were compared with the predicted values (PV) for each response (Table 4.2). As observed, a strong agreement with relative error (E%) with less than 2% proves that the predictive model found is applicable to describe the performance of the membrane modification in relation to the responses evaluated.

Table 4.2. Validation of the condition obtained from the desirability function comparing predicted and experimental values for the different responses.

Response variable	Desirability conditions			PV	EV	E%
	X_1 (g L^{-1})	X_2 (%)	X_3 (rpm)			
Water permeance, kg h^{-1} bar^{-1} m^{-2}	0.92	1.4	106	781.16	785.81	0.59
TOC rejection, %				85.85	87.21	1.58
Degradation, %				98.97	97.42	1.57

*X_1: DA concentration; X_2: TiO_2 amount; X_3: agitation; PV: predict value; EV: experimental value; E%: relative error (%).

The optimized modification condition was then used to continue the work, evaluating the characteristics of the obtained membrane and performance in the self-cleaning process.

4.3.2 Membrane performance and characterization

For comparison purposes, the analyzes were performed with the membrane obtained in the best modification condition (PVDF-PDA-Ti), a membrane modified only with PDA (PVDF-PDA) at the optimum concentration, and the pristine membrane (PVDF). Figure 4.7a shows that the PVDF-PDA membrane has a 23% lower water permeance in comparison with the pristine membrane. Previous studies have observed similar behavior, and it has been reported that PDA coating can clog membrane pores (OYMACI; NIJMEIJER; BORNEMAN, 2020; PRONER *et al.*, 2020). On the other hand, the PVDF-PDA-Ti membrane presented 2.3x higher permeance than PVDF, indicating that the presence of TiO_2 positively affected the membrane water flux, even with the same PDA concentration as the PVDF-PVA membrane. This is probably due to the hydrophilic character of TiO_2 (RIAZ; PARK, 2020).

Figure 4.7. Comparison of the optimal condition (PVDF-PDA-Ti), only PDA-modified (0.92 g L^{-1}) (PVDF-PDA) and pristine membrane (PVDF), regarding (a) water permeance, (b) permeate flux of emulsion (1 g L^{-1}), (c) TOC rejection, and (d) methylene blue photocatalytic degradation.

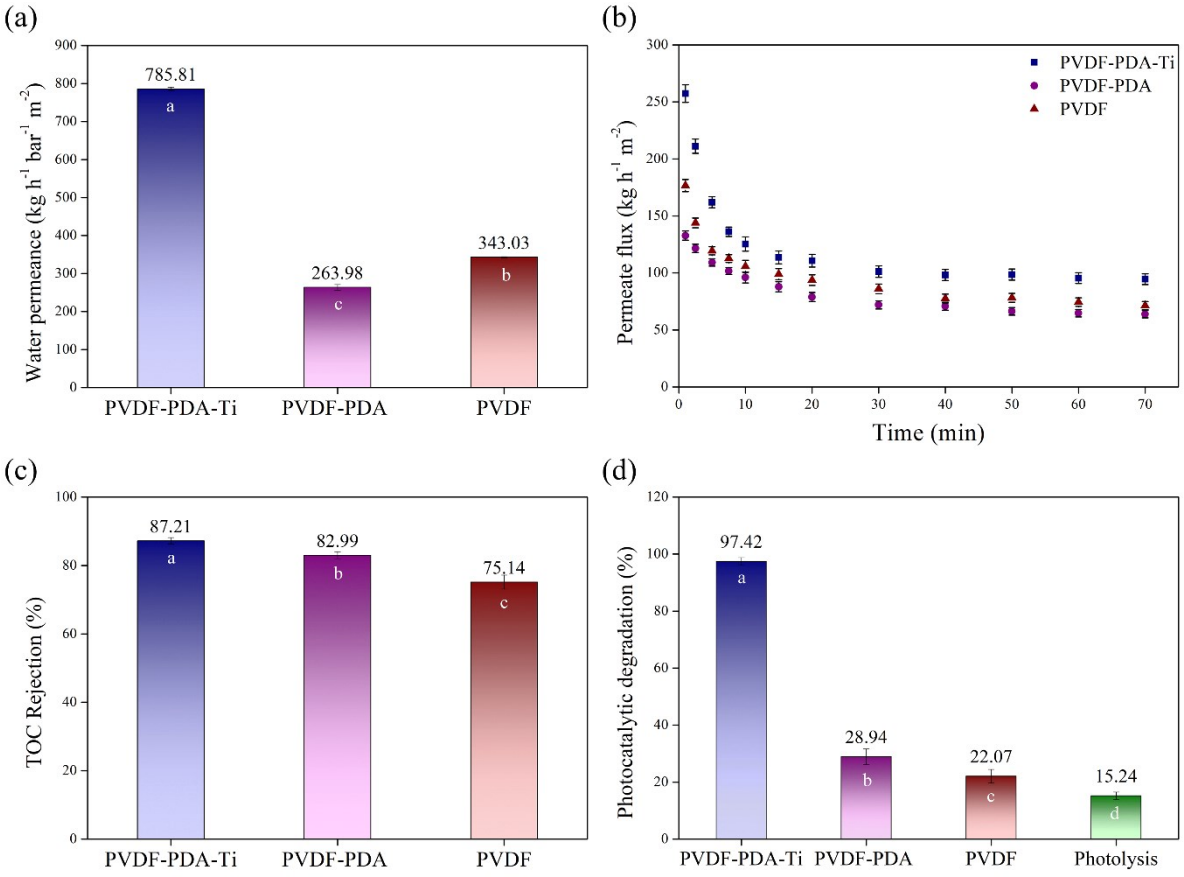

Source: the authors (2023).

The modified PVDF-PDA-Ti membrane was effective when permeating a standard oil/water emulsion (1 g L^{-1}), presenting higher flux (Figure 4.7b) and TOC rejection (Figure 4.7c) in comparison to the PVDF and PVDF-PDA membranes. Moreover, the membrane containing TiO_2 presented a much higher photocatalytic degradation (Figure 4.7d) of the methylene blue (effectiveness of about 97%), indicating excellent photocatalytic performance.

Figure 4.8 shows the infrared spectrum (FTIR) for TiO_2 photocatalyst and PVDF, PVDF-PDA, and PVDF-PDA-Ti membranes. It is possible to observe that the TiO_2 spectrum presents intense bands at 688 and 523 cm^{-1} that can be attributed to the elongation of the

vibrations of the Ti-O-Ti bond, previously reported (DJAOUED *et al.*, 2002; OSEGHE; NDUNGU; JONNALAGADDA, 2015; VASCONCELOS *et al.*, 2011); these bands have also been attributed to the presence of the anatase phase of titania, which presents high photocatalytic activity (YU *et al.*, 2014). In the PVDF membrane spectrum, Lanceros-Méndez et al. (2001) indicated that the band at 762 cm^{-1} results from the in-plane bending or rocking vibration of the PVDF α phase, while the band at 876 cm^{-1} is related to the stretching of β or γ phase the polymer (BENZ; EULER; GREGORY, 2002). The bands at 1040 cm^{-1} are associated with the β phase (YU *et al.*, 2009), while the band at 1188 cm^{-1} is associated with the symmetrical elongation of the C–F bond of the CF_2 group. Finally, Theophanides (2012) associated the band in 1278 cm^{-1} to the γ phase, and that at 1404 cm^{-1} from bending in the plane of the C–H bond in the CH_2 group.

After the modification process (PVDF-PDA and PVDF-PDA-Ti), it is possible to observe an attenuation in the size of the PVDF characteristic bands, probably due to the PDA coating. In addition, it is not possible to identify any changes that can be attributed to the presence of TiO_2, so it is necessary to identify the presence of this material using other techniques. Similar results have already been observed in previous work, in which the coating was performed with PDA and TiO_2 under higher concentration conditions (DA SILVA *et al.*, 2022).

Figure 4.8. FTIR spectra for TiO_2 and PVDF, PVDF-PDA and PVDF-PDA-Ti membranes.

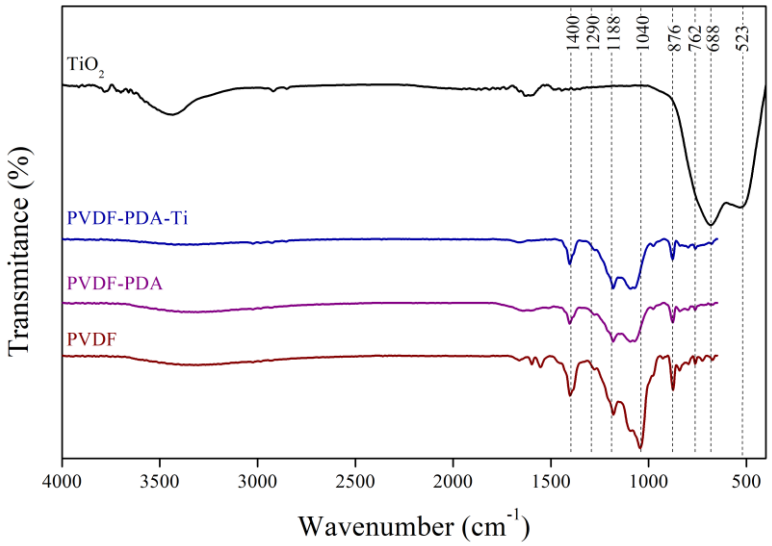

Source: the authors (2023).

X-ray diffractograms are shown in Figure 4.9. The TiO_2 sample was classified as the titania anatase crystalline phase (pattern 00-004-0477) with characteristic peaks at 25.5 (101), 37.2 (103), 37.8 (004), 38, 8 (112), 48.2 (200), 54.0 (105), 55.4 (211), 62.9 (204), 68.9 (116), 70.5 (220) and 75.4 ° (215) (SHARON; MODI; SHARON, 2016). For the membranes, the behavior obtained is very similar to that obtained by other authors (RAWINDRAN *et al.*, 2019; YANG *et al.*, 2020); the peaks present at 17.7, 19.9, and 25.9° refer to characteristic peaks of the PVDF α phase, whereas the peak found at 22.6° was reported as being characteristic of the β phase. This result corroborates the result found from the FTIR analysis, demonstrating that the commercial membrane surface presents a mixture of PVDF phases.

Figure 4.9. XRD diffractograms for TiO_2 and PVDF, PVDF-PDA and PVDF-PDA-Ti membranes.

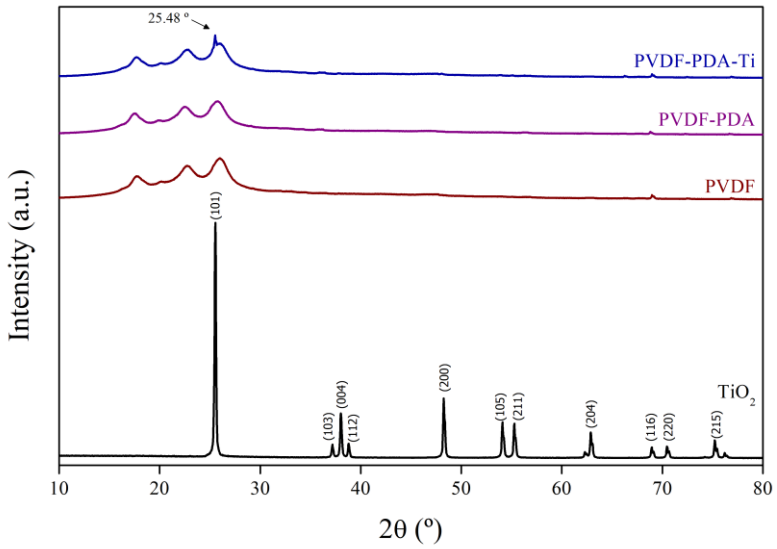

Source: the authors (2023).

Comparing the PVDF and PVDF-PDA, it is not possible to identify any difference in the diffractogram related to the deposition of PDA on the membrane surface. However, the PVDF-PDA-Ti, has the presence of a small peak close to 25.48°, very close to the highest intensity peak in TiO_2 (25.55°) diffractogram. The presence of this peak is related to the incorporation of TiO_2 in the PVDF-PDA-Ti membrane. The appearance of characteristic peaks in modified membranes has already been reported previously. Sun et al. (2021a) observed the

presence of titania peaks at 25.3 and 48.0° in their polyacrylonitrile (PAN) membranes modified using PDA and TiO_2. A similar case was shown in another study by the same research group, in which Sun et al. (2021b), this time modifying PVDF membranes, observed the appearance of the peak at 25° in the modified membranes.

The results of the EDS and SEM analysis comparing the modified PVDF-PDA and PVDF-PDA-Ti membranes are shown in Figure 4.10. The membrane modified with PDA (Figure 4.10a) showed pore obstruction, indicating that the modification process had effect on the membrane structure. On the other hand, the membrane modified with both PDA and TiO_2 (Figure 4.10b) showed pore obstruction as well, but there were also lighter points present, which could be attributed to the presence of TiO_2. The EDS analysis confirmed the presence of TiO_2 in the PVDF-PDA-Ti membrane, showing peaks of the titanium element when analyzing the white points shown in the micrographs (Figure 4.10b), not being present in PVDF-PDA (Figure 4.10a). Still, by decomposing the membrane in the furnace, an inorganic remaining material was detected, which represents 5.75 ± 0.64 % of the total PVDF-PDA-Ti membrane mass, associated to the TiO_2 incorporation.

Figure 4.10. Energy Dispersive Spectroscopy (EDS) and Scanning electron microscopy (MEV) of membranes (a) PVDF-PDA, and (b) PVDF-PDA-Ti.

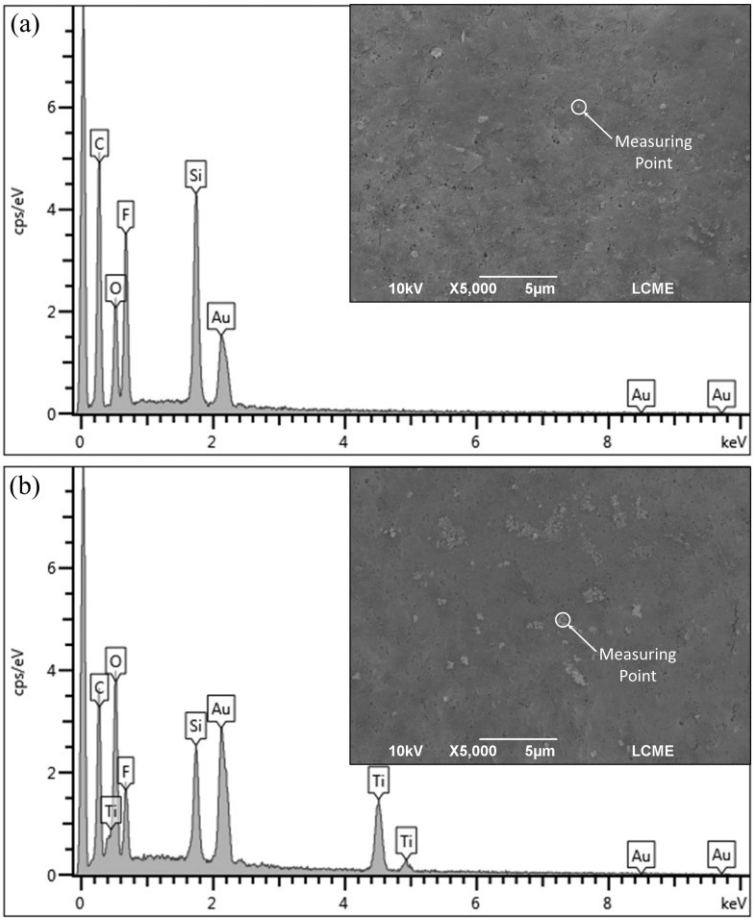

Source: the authors (2023).

The pore obstruction observed in both modified membranes could be due to PDA and TiO_2 particle deposition on the membrane surface. This PDA deposition may cause the formation of a layer that partially blocks the pores, leading to a reduction in permeance, as already noted by Proner et al. (2020), and Shah, Prasetya and Li (2021). On the other hand, the presence of TiO_2 particles on the membrane surface (points with lighter color in the image) may be contributing to the increase in permeance because of the rougher surface and higher hydrophilic character (to be shown in Figure 4.11), which can facilitate the transport of water molecules through the membrane (KAMEYA; YABE, 2019; KOPPÁNY *et al.*, 2023). This observation is consistent with previous studies with the presence of TiO_2 particles on the surface of modified membranes using similar modification techniques (DA SILVA *et al.*, 2022).

Figure 4.11 shows the adsorption ratio of water vapor and n-heptane. The water molecules will initially adsorb onto the surface of the membrane due to their polar nature and affinity for the hydrophilic surface. On the other hand, n-heptane molecules are non-polar and have a greater affinity for the hydrophobic regions of the membrane (VATANPARAST *et al.*, 2019). The PVDF membrane showed better adsorption of n-heptane vapor than water vapor, owing to its polymer non-polar α phase nature, reported by XRD (GUO *et al.*, 2020b). The expectation was that the membrane modified with PDA, would exhibit good water adsorption due to the hydrophilic character of polydopamine reported earlier (MULINARI *et al.*, 2023). However, SEM analysis revealed pore obstruction, probably hindering water adsorption.

Figure 4.11. Water and n-heptane vapor adsorption at 23 °C (left axis) and the ratio of water and n-heptane adsorption (right axis) for the PVDF, PVDF-PDA, and PVDF-PDA-Ti membranes.

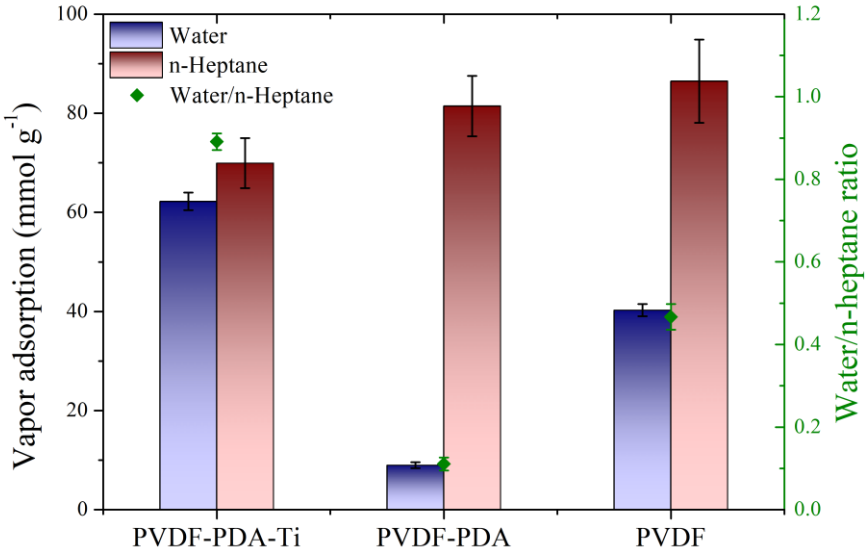

Source: the authors (2023).

The incorporation of TiO_2 effectively enhanced the hydrophilicity of the material, leading to an increase in water vapor adsorption. Simultaneously, the presence of TiO_2 reduced the adsorption of n-heptane while increasing water adsorption, resulting in an elevated water/n-heptane ratio and an enhanced hydrophilic nature following the modification. These outcomes

provide evidence in favor of the PVDF-PDA-Ti membrane exhibiting superior water permeance.

Investigating the stability of the modified membrane to extreme pH conditions (pH 2 and pH 12) (results presented in the Figure B2 of Appendix B), we observed that part of the PDA was released from the membranes exposed to alkaline condition since the aqueous solutions presented a brown color. Moreover, the UV-Vis analysis of the aqueous solutions confirms the hypothesis. Further studies still need to be performed regarding the long-term alkaline and acid stability of PDA incorporation into surfaces.

4.3.3 Membrane self-cleaning

The PVDF-PDA-Ti and the PVDF membranes were subjected to three cycles of emulsion permeation (~ 70 min), self-cleaning (UV irradiation for about 12 hours), and water permeance and rejection determination. Figure 4.12 shows the evolution of the emulsion permeation flux in the evaluated period for both membranes. It is possible to note that the flux recovery in the second and third cycles was higher for the modified membrane (around 87 and 85%, respectively). This result indicates that the membrane with TiO_2 incorporation has a good flux recovery, and that the self-cleaning process is effective for membrane reuse.

Figure 4.12. Comparison of the permeate flux during oil emulsion filtration for the PVDF, and PVDF-PDA-Ti membranes.

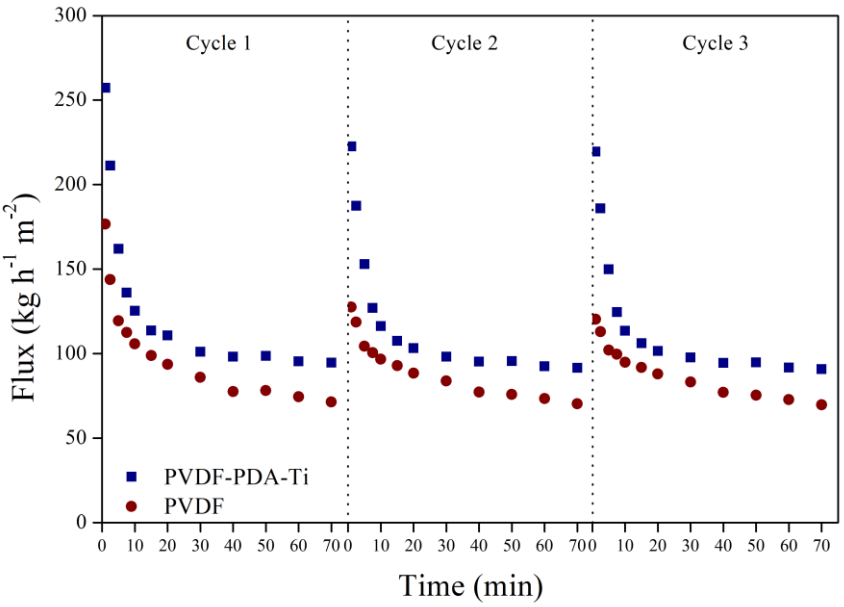

Source: the authors (2023).

Table 4.3 shows the water permeance and TOC rejection results for PVDF and PVDF-PDA-Ti after each permeation cycle. It is possible to observe that for the third cycle, the water permeance of the modified membrane presented a value about 2.1x greater than the pure membrane. In addition, the TOC rejection was also greater, remaining stable throughout the cycles, with an approximate variation of only 2%.

Table 4.3. Water permeance and TOC rejection in each cycle performed for PVDF and PVDF-PDA-Ti membranes.

Cycle	Water permeance, kg h^{-1} bar^{-1} m^{-2}		TOC rejection, %	
	PVDF	PVDF-PDA-Ti	PVDF	PVDF-PDA-Ti
1	344.1	789.0	75.14	87.20
2	272.4	617.9	73.82	86.06
3	268.8	606.0	73.06	85.01

Experimental results suggest that incorporating TiO_2 using PDA increases the hydrophilicity of the membrane and improves its water permeability. Furthermore, the

incorporation of TiO_2 also leads to the formation of reactive oxygen species, which, under UV irradiation, can effectively degrade the organic compounds that are encrusted on the membrane surface and improve the self-cleaning performance of the membranes. The findings of this study could have significant implications for the development of more efficient and sustainable water treatment technologies. Further studies are still needed to assess the long-term stability and practical application of the membranes reported here.

4.4 CONCLUSION

This study successfully demonstrated the effectiveness of incorporating TiO_2 into PVDF membranes using PDA to produce self-cleaning photocatalytic membranes. The design of experiments helped to understand that most responses do not show linear behavior, and the synergy between the evaluated factors proved to be significant when evaluating the responses. Morover, the optimal conditions for modifying the membrane and obtain the highest self-cleaning performance are a DA concentration of 0.92 g L^{-1}, 1.4% of TiO_2 and agitation of 106 rpm. Experimental results demonstrated strong agreement between predicted and actual values, validating the accuracy of the predictive model. Furthermore, the PVDF-PDA-Ti membrane showed a water permeance 2 times higher than the pure PVDF membrane after three cycles of emulsion filtration, along with stable TOC rejection with a minimum variation of approximately 2%. These findings highlight the promising and effective nature of incorporating TiO_2 into PVDF using PDA to produce high-performance photocatalytic membranes for water treatment applications. However, more research is needed to fully evaluate these membranes long-term stability under industrial conditions.

4.5 ACKNOWLEDGEMENTS

The authors acknowledge the Conselho Nacional de Desenvolvimento Científico e Tecnológico (CNPq), Coordenação de Aperfeiçoamento de Pessoal de Nível Superior (CAPES), Central Laboratory of Electron Microscopy (LCME), Laboratory of Energy and Environment (LEMA), Interdisciplinary Laboratory for the Development of Nanostructures (LINDEN), and Analysis Center of the Department of Chemical Engineering and Food Engineering (CA-EQA).

CHAPTER 5

FINAL CONSIDERATIONS AND PERSPECTIVES

5 FINAL CONSIDERATIONS AND PERSPECTIVES

5.1 CONCLUSION

The treatment of oily wastewater remains a challenging problem that conventional methods have not been able to fully address. However, emerging technologies such as photocatalytic membranes, which combine membrane filtration and photocatalysis, have shown promising results in effectively treating oily wastewater. Recent research has demonstrated that the incorporation of photocatalysts into the membrane structure using PDA-assisted modification can significantly enhance the membrane's efficiency. Furthermore, incorporation of TiO_2 in PVDF membranes using PDA has shown to be a successful approach to produce self-cleaning photocatalytic membranes for water treatment applications. The optimized photocatalytic membranes have shown excellent self-cleaning efficiency in degrading organic pollutants on the membrane surface under UV irradiation. Although further research is necessary to evaluate their feasibility and long-term stability, findings from the present work suggest that the approach adopted may offer a promising and effective solution for oily wastewater treatment.

5.2 SUGGESTIONS FOR FUTURE WORK

While this process has shown promising results, there are still gaps for improvement and further development. Therefore, in this section, we suggest several potential areas for future work to enhance the performance of the photocatalytic permeation process.

- Investigating the permeation process in crossflow mode of operation: this could help to better understand the process and optimize its performance.
- Investigate the membrane's stability: understanding the membrane's behavior in extreme pH conditions is a key point to be studied.
- Development of a photocatalytic permeation module: for integrating the photocatalysis process into the permeation process: this could help to enhance the efficiency and effectiveness of the overall process.
- Process conditions evaluation of the photocatalytic permeation module: once the photocatalytic permeation module is developed, it will be important to evaluate the

process conditions to optimize its performance. This could include variables such as the flow rate, temperature, and concentration of the solution being treated.

- Degradation of emerging contaminants, such as drug and hormone residues: this could help to broaden the applications of the photocatalytic permeation process.
- Incorporation of other photocatalysts: it may be beneficial to investigate the incorporation of different photocatalysts through the PDA-assisted process. This could help to enhance the effectiveness of the photocatalytic permeation process and further expand its capabilities.

REFERENCES

ABDALLAH, H. A review on catalytic membranes production and applications. **Bulletin of Chemical Reaction Engineering & Catalysis**, v. 12, n. 2, p. 136–156, 2017. Disponível em: https://doi.org/10.9767/bcrec.12.2.462.136-156

ABDELRASOUL, A.; DOAN, H.; LOHI, A. Fouling in Membrane Filtration and Remediation Methods. *In*: NAKAJIMA, H. (org.). **Mass Transfer - Advances in Sustainable Energy and Environment Oriented Numerical Modeling**. Rijeka: InTech, 2013. *E-book*. Disponível em: https://doi.org/10.5772/52370

ABOUNAHIA, N.; QIBLAWEY, H.; ZAIDI, S. J. Progress for Co-Incorporation of Polydopamine and Nanoparticles for Improving Membranes Performance. **Membranes**, v. 12, n. 7, 2022. Disponível em: https://doi.org/10.3390/membranes12070675

ABUJAZAR, M. S. S.; KARAAĞAÇ, S. U.; ABU AMR, S. S.; ALAZAIZA, M. Y. D.; BASHIR, M. J. Recent advancement in the application of hybrid coagulants in coagulation-flocculation of wastewater: A review. **Journal of Cleaner Production**, v. 345, p. 131133, 2022. Disponível em: https://doi.org/10.1016/J.JCLEPRO.2022.131133. Acesso em: 14 set. 2022.

ADETUNJI, A. I.; OLANIRAN, A. O. Treatment of industrial oily wastewater by advanced technologies: a review. **Applied Water Science**, v. 11, n. 6, p. 98, 2021. Disponível em: https://doi.org/10.1007/s13201-021-01430-4

AHMAD, T.; GURIA, C. Progress in the modification of polyvinyl chloride (PVC) membranes: A performance review for wastewater treatment. **Journal of Water Process Engineering**, v. 45, p. 102466, 2022. Disponível em: https://doi.org/10.1016/J.JWPE.2021.102466. Acesso em: 21 fev. 2023.

AHMAD, T.; GURIA, C.; MANDAL, A. A review of oily wastewater treatment using ultrafiltration membrane: A parametric study to enhance the membrane performance. **Journal of Water Process Engineering**, v. 36, p. 101289, 2020. Disponível em: https://doi.org/10.1016/J.JWPE.2020.101289. Acesso em: 21 fev. 2023.

ALKAYA, E.; DEMIRER, G. N. Greening of production in metal processing industry through process modifications and improved management practices. **Resources, Conservation and Recycling**, v. 77, p. 89–96, 2013. Disponível em: https://doi.org/10.1016/J.RESCONREC.2013.06.004. Acesso em: 30 mar. 2020.

BAI, J.; ZHOU, B. Titanium Dioxide Nanomaterials for Sensor Applications. **Chemical Reviews**, v. 114, n. 19, p. 10131–10176, 2014. Disponível em: https://doi.org/10.1021/cr400625j

BAIG, N.; SALHI, B.; SAJID, M.; ALJUNDI, I. H. Recent Progress in Microfiltration/Ultrafiltration Membranes for Separation of Oil and Water Emulsions. **Chemical Record**, n. 202100320, 2022. Disponível em: https://doi.org/10.1002/tcr.202100320

BAIG, U.; WAHEED, A. An efficient and simple strategy for fabricating a polypyrrole decorated ceramic-polymeric porous membrane for purification of a variety of oily wastewater streams. **Environmental Research**, v. 219, p. 114959, 2023. Disponível em: https://doi.org/10.1016/J.ENVRES.2022.114959. Acesso em: 12 jan. 2023.

BAKER, R. W. Overview of Membrane Science and Technology. *In*: **Membrane Technology and Applications**. 3. ed. Chichester: John Wiley & Sons, Ltd, 2012 a. (Wiley Online Books). p. 1–14. *E-book*. Disponível em: https://doi.org/doi:10.1002/9781118359686.ch1

BAKER, R. W. Membrane Transport Theory. *In*: **Membrane Technology and Applications**. 3. ed. Chichester: John Wiley & Sons, Ltd, 2012 b. (Wiley Online Books). p. 15–96. *E-book*. Disponível em: https://doi.org/doi:10.1002/9781118359686.ch2

BAO, Z.; CHEN, D.; LI, N.; XU, Q.; LI, H.; HE, J.; LU, J. Superamphiphilic and underwater superoleophobic membrane for oil/water emulsion separation and organic dye degradation. **Journal of Membrane Science**, v. 598, p. 117804, 2020. Disponível em: https://doi.org/https://doi.org/10.1016/j.memsci.2019.117804

BARRIOS-ESTRADA, C.; ROSTRO-ALANIS, M. de J.; PARRA, A. L.; BELLEVILLE, M. P.; SANCHEZ-MARCANO, J.; IQBAL, H. M. N.; PARRA-SALDÍVAR, R. Potentialities

of active membranes with immobilized laccase for Bisphenol A degradation. **International Journal of Biological Macromolecules**, v. 108, p. 837–844, 2018. Disponível em: https://doi.org/10.1016/j.ijbiomac.2017.10.177

BENZ, M.; EULER, W. B.; GREGORY, O. J. The Role of Solution Phase Water on the Deposition of Thin Films of Poly(vinylidene fluoride). **Macromolecules**, v. 35, n. 7, p. 2682–2688, 2002. Disponível em: https://doi.org/10.1021/ma011744f

BHATTACHARYA, A.; MISRA, B. N. Grafting: a versatile means to modify polymers: Techniques, factors and applications. **Progress in Polymer Science**, v. 29, n. 8, p. 767–814, 2004. Disponível em: https://doi.org/10.1016/J.PROGPOLYMSCI.2004.05.002. Acesso em: 2 abr. 2020.

BORJIGIN, B.; LIU, lixue; YU, L.; XU, L.; ZHAO, C.; WANG, J. Influence of incorporating beta zeolite nanoparticles on water permeability and ion selectivity of polyamide nanofiltration membranes. **Journal of Environmental Sciences**, v. 98, p. 77–84, 2020. Disponível em: https://doi.org/10.1016/J.JES.2020.04.010. Acesso em: 7 jan. 2023.

BURZIO, L. A.; WAITE, J. H. Cross-Linking in Adhesive Quinoproteins: Studies with Model Decapeptides. **Biochemistry**, v. 39, n. 36, p. 11147–11153, 2000. Disponível em: https://doi.org/10.1021/bi0002434

BYRAPPA, K.; ADSCHIRI, T. Hydrothermal technology for nanotechnology. **Progress in Crystal Growth and Characterization of Materials**, v. 53, n. 2, p. 117–166, 2007. Disponível em: https://doi.org/10.1016/j.pcrysgrow.2007.04.001

CAÑIZARES, P.; LOBATO, J.; PAZ, R.; RODRIGO, M. A.; SÁEZ, C. Advanced oxidation processes for the treatment of olive-oil mills wastewater. **Chemosphere**, v. 67, n. 4, p. 832–838, 2007. Disponível em: https://doi.org/10.1016/J.CHEMOSPHERE.2006.10.064. Acesso em: 30 mar. 2020.

CARDOSO, A. R. T.; AMBROSI, A.; DI LUCCIO, M.; HOTZA, D. Membranes for separation of CO2/CH4 at harsh conditions. **Journal of Natural Gas Science and Engineering**, v. 98, p. 104388, 2022. Disponível em: https://doi.org/10.1016/J.JNGSE.2021.104388. Acesso em: 14 set. 2022.

CASQUEIRA, R. G.; TOREM, M. L.; KOHLER, H. M. The removal of zinc from liquid streams by electroflotation. **Minerals Engineering**, v. 19, n. 13, p. 1388–1392, 2006. Disponível em: https://doi.org/10.1016/J.MINENG.2006.02.001. Acesso em: 30 mar. 2020.

CHEN, D. *et al.* Photocatalytic degradation of organic pollutants using TiO2-based photocatalysts: A review. **Journal of Cleaner Production**, v. 268, p. 121725, 2020 a. Disponível em: https://doi.org/10.1016/J.JCLEPRO.2020.121725. Acesso em: 7 set. 2022.

CHEN, M.; HEIJMAN, S. G. J.; RIETVELD, L. C. State-of-the-Art Ceramic Membranes for Oily Wastewater Treatment: Modification and Application. **Membranes**, v. 11, n. 11, p. 888, 2021. Disponível em: https://doi.org/10.3390/membranes11110888

CHEN, Y.; XIE, A.; CUI, J.; LANG, J.; LI, C.; YAN, Y.; DAI, J. Flower-like visible light driven antifouling membrane with robust regeneration for high efficient oil/water separation. **Journal of the Taiwan Institute of Chemical Engineers**, v. 106, p. 138–147, 2020 b. Disponível em: https://doi.org/https://doi.org/10.1016/j.jtice.2019.10.022

CHEN, Y. Y.; XIE, A. T.; CUI, J. Y.; LANG, J. H.; YAN, Y. S.; LI, C. X.; DAI, J. D. UV-Driven Antifouling Paper Fiber Membranes for Efficient Oil-Water Separation. **Industrial & Engineering Chemistry Research**, v. 58, n. 13, p. 5186–5194, 2019. Disponível em: https://doi.org/10.1021/acs.iecr.8b05930

CHENG, D. S.; ZHANG, Y. L.; BAI, X.; LIU, Y. H.; DENG, Z. M.; WU, J. H.; BI, S. G.; RAN, J. H.; CAI, G. M.; WANG, X. Mussel-inspired fabrication of superhydrophobic cotton fabric for oil/water separation and visible light photocatalytic. **Cellulose**, v. 27, n. 9, p. 5421–5433, 2020. Disponível em: https://doi.org/10.1007/s10570-020-03149-y

COCA, J.; GUTIÉRREZ, G.; BENITO, J. M. Treatment of oily wastewater. *In*: COCA-PRADOS, J.; GUTIÉRREZ-CERVELLÓ, G. (org.). **Water Purification and Management**. *[S. l.]*: Springer Science & Business Media, 2011. Disponível em: https://doi.org/10.1007/978-90-481-9775-0

COCA, J.; GUTIÉRREZ, G.; BENITO, J. M. Treatment of oily wastewater by membrane hybrid processes. *In*: **Economics sustainability and environmental protection in mediterranean countries through clean manufacturing methods**. 1. ed. Dordrecht:

Springer Netherlands, 2013. p. 155. Disponível em: https://doi.org/10.1007/978-94-007-5079-1

COELHO, L. L.; GRAO, M.; POMONE, T.; RATOVA, M.; KELLY, P.; WILHELM, M.; MOREIRA, R. de F. P. M. Photocatalytic microfiltration membranes produced by magnetron sputtering with self-cleaning capabilities. **Thin Solid Films**, v. 747, p. 139143, 2022. Disponível em: https://doi.org/https://doi.org/10.1016/j.tsf.2022.139143

COLLINS, A. W.; ELANGO, V.; CURTIS, D.; RODRIGUE, M.; PARDUE, J. H. Biogeochemical controls on biodegradation of buried oil along a coastal headland beach. **Marine Pollution Bulletin**, v. 154, p. 111051, 2020. Disponível em: https://doi.org/10.1016/J.MARPOLBUL.2020.111051

DA SILVA, A. F. V.; CESCA, K.; AMBROSI, A.; ZIN, G.; DI LUCCIO, M.; OLIVEIRA, J. V. An expedite facile method for modification of PVDF membranes with polydopamine and TiO2 to improve water permeation. **Materials Letters**, p. 132611, 2022. Disponível em: https://doi.org/10.1016/J.MATLET.2022.132611. Acesso em: 14 jun. 2022.

DA SILVA, A. F. V.; FAGUNDES, A. P.; MACUVELE, D. L. P.; DE CARVALHO, E. F. U.; DURAZZO, M.; PADOIN, N.; SOARES, C.; RIELLA, H. G. Green synthesis of zirconia nanoparticles based on Euclea natalensis plant extract: Optimization of reaction conditions and evaluation of adsorptive properties. **Colloids and Surfaces A: Physicochemical and Engineering Aspects**, v. 583, p. 123915, 2019. Disponível em: https://doi.org/10.1016/J.COLSURFA.2019.123915. Acesso em: 30 out. 2019.

DALSIN, J. L.; HU, B.-H.; LEE, B. P.; MESSERSMITH, P. B. Mussel Adhesive Protein Mimetic Polymers for the Preparation of Nonfouling Surfaces. **Journal of the American Chemical Society**, v. 125, n. 14, p. 4253–4258, 2003. Disponível em: https://doi.org/10.1021/ja0284963

DANKEAW, A.; GUALANDRIS, F.; SILVA, R. H.; SCIPIONI, R.; HANSEN, K. K.; KSAPABUTR, B.; ESPOSITO, V.; MARANI, D. Highly porous Ce-W-TiO2 free-standing electrospun catalytic membranes for efficient de-NOx via ammonia selective catalytic

reduction. **Environmental Science: Nano**, v. 6, n. 1, p. 94–104, 2019. Disponível em: https://doi.org/10.1039/c8en01046c

DELLA VECCHIA, N. F.; AVOLIO, R.; ALFÈ, M.; ERRICO, M. E.; NAPOLITANO, A.; D'ISCHIA, M. Building-Block Diversity in Polydopamine Underpins a Multifunctional Eumelanin-Type Platform Tunable Through a Quinone Control Point. **Advanced Functional Materials**, v. 23, n. 10, p. 1331–1340, 2013. Disponível em: https://doi.org/https://doi.org/10.1002/adfm.201202127

DJAOUED, Y.; BADILESCU, S.; ASHRIT, P. V; BERSANI, D.; LOTTICI, P. P.; ROBICHAUD, J. Study of Anatase to Rutile Phase Transition in Nanocrystalline Titania Films. **Journal of Sol-Gel Science and Technology**, v. 24, p. 255–264, 2002.

DONG, H.; ZENG, G.; TANG, L.; FAN, C.; ZHANG, C.; HE, X.; HE, Y. An overview on limitations of TiO2-based particles for photocatalytic degradation of organic pollutants and the corresponding countermeasures. **Water Research**, v. 79, p. 128–146, 2015. Disponível em: https://doi.org/10.1016/j.watres.2015.04.038

DONG, L.; TONG, X.; LI, X.; ZHOU, J.; WANG, S.; LIU, B. Some developments and new insights of environmental problems and deep mining strategy for cleaner production in mines. **Journal of Cleaner Production**, v. 210, p. 1562–1578, 2019. Disponível em: https://doi.org/https://doi.org/10.1016/j.jclepro.2018.10.291

DU, C.; SONG, Y.; HAN, X.; XIAO, S. Insights into the key components of bacterial assemblages in typical process units of oily wastewater treatment plants. **Environmental Research**, v. 180, p. 108889, 2020. Disponível em: https://doi.org/10.1016/J.ENVRES.2019.108889. Acesso em: 12 jan. 2023.

EMAMJOMEH, M. M.; SIVAKUMAR, M. Review of pollutants removed by electrocoagulation and electrocoagulation/flotation processes. **Journal of Environmental Management**, v. 90, n. 5, p. 1663–1679, 2009. Disponível em: https://doi.org/10.1016/J.JENVMAN.2008.12.011

ESPÍNDOLA, J. C.; CRISTÓVÃO, R. O.; MENDES, A.; BOAVENTURA, R. A. R.; VILAR, V. J. P. Photocatalytic membrane reactor performance towards oxytetracycline

removal from synthetic and real matrices: Suspended vs immobilized TiO2-P25. **Chemical Engineering Journal**, v. 378, p. 122114, 2019. Disponível em: https://doi.org/10.1016/J.CEJ.2019.122114. Acesso em: 14 set. 2022.

ESTRADA-VILLEGAS, G. M.; BUCIO, E. Comparative study of grafting a polyampholyte in a fluoropolymer membrane by gamma radiation in one or two-steps. **Radiation Physics and Chemistry**, v. 92, p. 61–65, 2013. Disponível em: https://doi.org/10.1016/J.RADPHYSCHEM.2013.07.015

FARHAN HANAFI, M.; SAPAWE, N. A review on the water problem associate with organic pollutants derived from phenol, methyl orange, and remazol brilliant blue dyes. **Materials Today: Proceedings**, v. 31, p. A141–A150, 2020. Disponível em: https://doi.org/10.1016/J.MATPR.2021.01.258. Acesso em: 2 fev. 2023.

FENG, Q. Y.; ZHAN, Y. Q.; YANG, W.; SUN, A.; DONG, H. Y.; CHIAO, Y. H.; LIU, Y. C.; CHEN, X. M.; CHEN, Y. W. Bi-functional super-hydrophilic/underwater super-oleophobic 2D lamellar Ti3C2Tx MXene/poly (arylene ether nitrile) fibrous composite membrane for the fast purification of emulsified oil and photodegradation of hazardous organics. **Journal of Colloid And Interface Science**, v. 612, p. 156–170, 2022. Disponível em: https://doi.org/10.1016/j.jcis.2021.12.160

FUJISHIMA, A.; HONDA, K. Electrochemical Photolysis of Water at a Semiconductor Electrode. **Nature**, v. 238, n. 5358, p. 37–38, 1972. Disponível em: https://doi.org/10.1038/238037a0

GAUR, S. S.; JAGADEESAN, H. Titanium Dioxide (TiO2) based photocatalysis for textile wastewater treatment – its applications and biosafety – A Review. **International Journal of Mecanical Engineering**, v. 6, n. February, p. 564–582, 2022.

GHIMIRE, N.; WANG, S. Biological Treatment of Petrochemical Wastewater. *In*: **Petroleum Chemicals - Recent Insight**. *[S. l.]*: IntechOpen, 2019. Disponível em: https://doi.org/10.5772/intechopen.79655

GIANNETTI, E. Semi-crystalline fluorinated polymers. **Polymer International**, v. 50, n. 1, p. 20–10, 2001. Disponível em: https://doi.org/10.1002/1097-0126(200101)50:1<10::AID-PI614>3.0.CO;2-W

GILL, F. L.; KUPERAN VISWANATHAN, K.; ZAINI, M.; KARIM, A. The Critical Review of the Pollution Haven Hypothesis. **International Journal of Energy Economics and Policy** |, v. 8, n. 1, p. 167–174, 2018. Disponível em: http:www.econjournals.com

GOH, P. S.; ONG, C. S.; NG, B. C. Applications of Emerging Nanomaterials for Oily Wastewater Treatment. *In*: **Nanotechnology in Water and Wastewater Treatment**. *[S. l.]*: Elsevier, 2019. p. 101–113. Disponível em: https://doi.org/10.1016/B978-0-12-813902-8.00005-8

GOH, P. S.; ONG, C. S.; NG, B. C.; ISMAIL, A. F. Applications of Emerging Nanomaterials for Oily Wastewater Treatment. *In*: **Nanotechnology in Water and Wastewater Treatment: Theory and Applications**. 1. ed. *[S. l.]*: Elsevier, 2019. p. 101–113. Disponível em: https://doi.org/10.1016/B978-0-12-813902-8.00005-8

GOLSHENAS, A.; SADEGHIAN, Z.; ASHRAFIZADEH, S. N. Performance evaluation of a ceramic-based photocatalytic membrane reactor for treatment of oily wastewater. **Journal of Water Process Engineering**, v. 36, p. 101186, 2020. Disponível em: https://doi.org/https://doi.org/10.1016/j.jwpe.2020.101186

GOODARZI, F.; ZENDEHBOUDI, S. A Comprehensive Review on Emulsions and Emulsion Stability in Chemical and Energy Industries. **The Canadian Journal of Chemical Engineering**, v. 97, n. 1, p. 281–309, 2019. Disponível em: https://doi.org/https://doi.org/10.1002/cjce.23336

GU, Y.; FAVIER, I.; PRADEL, C.; GIN, D. L.; LAHITTE, J.-F.; NOBLE, R. D.; GÓMEZ, M.; REMIGY, J.-C. High catalytic efficiency of palladium nanoparticles immobilized in a polymer membrane containing poly(ionic liquid) in Suzuki–Miyaura cross-coupling reaction. **Journal of Membrane Science**, v. 492, p. 331–339, 2015. Disponível em: https://doi.org/10.1016/J.MEMSCI.2015.05.051

GUO, D.; XIAO, Y.; LI, T.; ZHOU, Q.; SHEN, L.; LI, R.; XU, Y.; LIN, H. Fabrication of high-performance composite nanofiltration membranes for dye wastewater treatment: mussel-inspired layer-by-layer self-assembly. **Journal of Colloid and Interface Science**, v. 560, p. 273–283, 2020 a. Disponível em: https://doi.org/https://doi.org/10.1016/j.jcis.2019.10.078

GUO, F.; ZHAO, J.; LI, F.; KONG, D.; GUO, H.; WANG, X.; HU, H.; ZONG, L.; XU, J. Polar crystalline phases of PVDF induced by interaction with functionalized boron nitride nanosheets. **CrystEngComm**, v. 22, n. 37, p. 6207–6215, 2020 b. Disponível em: https://doi.org/10.1039/D0CE01001D

HALIM, A.; ERNAWATI, L.; ISMAYATI, M.; MARTAK, F.; ENOMAE, T. Bioinspired cellulose-based membranes in oily wastewater treatment. **Frontiers of Environmental Science & Engineering**, v. 16, n. 7, p. 94, 2021. Disponível em: https://doi.org/10.1007/s11783-021-1515-2

HAN, F.; KAMBALA, V. S. R.; SRINIVASAN, M.; RAJARATHNAM, D.; NAIDU, R. Tailored titanium dioxide photocatalysts for the degradation of organic dyes in wastewater treatment: A review. **Applied Catalysis A: General**, v. 359, n. 1, p. 25–40, 2009. Disponível em: https://doi.org/https://doi.org/10.1016/j.apcata.2009.02.043

HASSANSHAHI, N.; HU, G.; LI, J. Application of Ionic Liquids for Chemical Demulsification: A Review. **Molecules**, v. 25, n. 21, p. 4915, 2020. Disponível em: https://doi.org/10.3390/molecules25214915

HE, Z.; MILLER, D. J.; KASEMSET, S.; PAUL, D. R.; FREEMAN, B. D. The effect of permeate flux on membrane fouling during microfiltration of oily water. **Journal of Membrane Science**, v. 525, p. 25–34, 2017. Disponível em: https://doi.org/10.1016/J.MEMSCI.2016.10.002. Acesso em: 17 nov. 2021.

HOMOCIANU, M.; PASCARIU, P. High-performance photocatalytic membranes for water purification in relation to environmental and operational parameters. **Journal of Environmental Management**, v. 311, p. 114817, 2022. Disponível em: https://doi.org/10.1016/j.jenvman.2022.114817

HOU, X. Anaerobic xylose fermentation by Spathaspora passalidarum. **Applied Microbiology and Biotechnology**, v. 94, n. 1, p. 205–214, 2012. Disponível em: https://doi.org/10.1007/s00253-011-3694-4

HU, L.; WANG, Z.; HU, Y.; LIU, Y.; ZHANG, S.; ZHOU, Y.; ZHANG, Y.; LIU, Y.; LI, B. The preparation of Janus Cu(OH)2@Cu2O/Cu mesh and application in purification of oily wastewater. **Materials Research Bulletin**, v. 126, p. 110815, 2020. Disponível em: https://doi.org/https://doi.org/10.1016/j.materresbull.2020.110815

HUANG, S.; RAS, R. H. A.; TIAN, X. Antifouling membranes for oily wastewater treatment: Interplay between wetting and membrane fouling. **Current Opinion in Colloid and Interface Science**, v. 36, p. 90–109, 2018. Disponível em: https://doi.org/10.1016/j.cocis.2018.02.002

IKHSAN, S. N. W.; YUSOF, N.; AZIZ, F.; MISDAN, N.; ISMAIL, A. F.; LAU, W.-J.; JAAFAR, J.; SALLEH, W. N. W.; HAIROM, N. H. H. Efficient separation of oily wastewater using polyethersulfone mixed matrix membrane incorporated with halloysite nanotube-hydrous ferric oxide nanoparticle. **Separation and Purification Technology**, v. 199, n. September 2017, p. 161–169, 2018. Disponível em: https://doi.org/10.1016/j.seppur.2018.01.028

ISIAKA, A. A.; OLANIRAN, A. O. Treatment of industrial oily wastewater by advanced technologies: a review. **Applied Water Science**, Heidelberg, v. 11, n. 6, 2021. Disponível em: https://doi.org/http://dx.doi.org/10.1007/s13201-021-01430-4

ISMAEL, M. A review on graphitic carbon nitride (g-C3N4) based nanocomposites: Synthesis, categories, and their application in photocatalysis. **Journal of Alloys and Compounds**, v. 846, p. 156446, 2020. Disponível em: https://doi.org/10.1016/J.JALLCOM.2020.156446. Acesso em: 20 jul. 2022.

JAFARI, B.; ABBASI, M.; HASHEMIFARD, S. A. Development of new tubular ceramic microfiltration membranes by employing activated carbon in the structure of membranes for treatment of oily wastewater. **Journal of Cleaner Production**, v. 244, p. 118720, 2020. Disponível em: https://doi.org/10.1016/J.JCLEPRO.2019.118720. Acesso em: 14 set. 2022.

JAGABA, A. H.; KUTTY, S. R. M.; HAYDER, G.; LATIFF, A. A. A.; AZIZ, N. A. A.; UMARU, I.; GHALEB, A. A. S.; ABUBAKAR, S.; LAWAL, I. M.; NASARA, M. A. Sustainable use of natural and chemical coagulants for contaminants removal from palm oil mill effluent: A comparative analysis. **Ain Shams Engineering Journal**, v. 11, n. 4, p. 951–960, 2020. Disponível em: https://doi.org/10.1016/J.ASEJ.2020.01.018. Acesso em: 14 set. 2022.

JAMALY, S.; GIWA, A.; HASAN, S. W. Recent improvements in oily wastewater treatment: Progress, challenges, and future opportunities. **Journal of Environmental Sciences**, v. 37, p. 15–30, 2015 a. Disponível em: https://doi.org/10.1016/J.JES.2015.04.011

JAMALY, S.; GIWA, A.; HASAN, S. W. Recent improvements in oily wastewater treatment: Progress, challenges, and future opportunities. **Journal of Environmental Sciences**, v. 37, p. 15–30, 2015 b. Disponível em: https://doi.org/10.1016/J.JES.2015.04.011. Acesso em: 7 jan. 2023.

JEGANATHAN, J.; BASSI, A.; NAKHLA, G. Pre-treatment of high oil and grease pet food industrial wastewaters using immobilized lipase hydrolyzation. **Journal of Hazardous Materials**, v. 137, n. 1, p. 121–128, 2006. Disponível em: https://doi.org/10.1016/J.JHAZMAT.2005.11.106

KAJITVICHYANUKUL, P.; NGUYEN, V. H.; BOONUPARA, T.; PHAN THI, L. A.; WATCHARENWONG, A.; SUMITSAWAN, S.; UDOMKUN, P. Challenges and effectiveness of nanotechnology-based photocatalysis for pesticides-contaminated water: A review. **Environmental Research**, v. 212, p. 113336, 2022. Disponível em: https://doi.org/10.1016/J.ENVRES.2022.113336. Acesso em: 12 jan. 2023.

KAMEYA, Y.; YABE, H. Optical and Superhydrophilic Characteristics of TiO2 Coating with Subwavelength Surface Structure Consisting of Spherical Nanoparticle Aggregates. **Coatings**, v. 9, n. 9, p. 547, 2019. Disponível em: https://doi.org/10.3390/coatings9090547

KANAN, S.; MOYET, M. A.; ARTHUR, R. B.; PATTERSON, H. H. Recent advances on TiO_2 -based photocatalysts toward the degradation of pesticides and major organic

pollutants from water bodies. **Catalysis Reviews**, v. 62, n. 1, p. 1–65, 2020. Disponível em: https://doi.org/10.1080/01614940.2019.1613323

KHADER, E. H.; MOHAMMED, T. H. J.; MIRGHAFFARI, N. Use of Natural Coagulants for Removal of COD, Oil and Turbidity from Produced Waters in the Petroleum Industry. **Journal of Petroleum & Environmental Biotechnology**, v. 09, n. 03, 2018. Disponível em: https://doi.org/10.4172/2157-7463.1000374

KHOUNI, I.; LOUHICHI, G.; GHRABI, A.; MOULIN, P. Efficiency of a coagulation/flocculation–membrane filtration hybrid process for the treatment of vegetable oil refinery wastewater for safe reuse and recovery. **Process Safety and Environmental Protection**, v. 135, p. 323–341, 2020. Disponível em: https://doi.org/10.1016/J.PSEP.2020.01.004

KIM, J.; VAN DER BRUGGEN, B. The use of nanoparticles in polymeric and ceramic membrane structures: Review of manufacturing procedures and performance improvement for water treatment. **Environmental Pollution**, v. 158, n. 7, p. 2335–2349, 2010. Disponível em: https://doi.org/10.1016/J.ENVPOL.2010.03.024

KONSTANTINOU, I. K.; ALBANIS, T. A. TiO2-assisted photocatalytic degradation of azo dyes in aqueous solution: kinetic and mechanistic investigations: A review. **Applied Catalysis B: Environmental**, v. 49, n. 1, p. 1–14, 2004. Disponível em: https://doi.org/https://doi.org/10.1016/j.apcatb.2003.11.010

KOPPÁNY, F. *et al.* Enhancement of Hydrophilicity of Nano-Pitted TiO2 Surface Using Phosphoric Acid Etching. **Nanomaterials**, v. 13, n. 3, p. 511, 2023. Disponível em: https://doi.org/10.3390/nano13030511

KOVÁCS, I.; VERÉB, G.; KERTÉSZ, S.; HODÚR, C.; LÁSZLÓ, Z. Fouling mitigation and cleanability of TiO2 photocatalyst-modified PVDF membranes during ultrafiltration of model oily wastewater with different salt contents. **Environmental Science and Pollution Research**, v. 25, n. 35, p. 34912–34921, 2018. Disponível em: https://doi.org/10.1007/s11356-017-0998-7

KUMARI, P.; BAHADUR, N.; DUMÉE, L. F. Photo-catalytic membrane reactors for the remediation of persistent organic pollutants – A review. **Separation and Purification Technology**, v. 230, p. 115878, 2020. Disponível em: https://doi.org/10.1016/J.SEPPUR.2019.115878

LAI, T.; SHEN, L.; ZHANG, M.; HE, Y.; LIN, H. Effects of Van Der Waals Surface Energy on Membrane Fouling in a Submerged Membrane Bioreactor (MBR). **Current Environmental Engineering**, v. 2, n. 1, p. 50–55, 2015. Disponível em: https://doi.org/10.2174/2212717802011508311505 41

LANCEROS-MÉNDEZ, S.; MANO, J. F.; COSTA, A. M.; SCHMIDT, V. H. FTIR and DSC studies of mechanically deformed β-PVDF films. **Journal of Macromolecular Science, Part B**, v. 40, n. 3–4, p. 517–527, 2001. Disponível em: https://doi.org/10.1081/MB-100106174

LEE, H.; DELLATORE, S. M.; MILLER, W. M.; MESSERSMITH, P. B. Mussel-Inspired Surface Chemistry for Multifunctional Coatings. **Science**, v. 318, n. 5849, p. 426–430, 2007. Disponível em: https://doi.org/10.1126/science.1147241

LEFEBVRE, O.; MOLETTA, R. Treatment of organic pollution in industrial saline wastewater: A literature review. **Water Research**, v. 40, n. 20, p. 3671–3682, 2006. Disponível em: https://doi.org/10.1016/J.WATRES.2006.08.027. Acesso em: 14 set. 2022.

LEITE, M. J. L.; RAMALHO MARQUES, I.; PRONER, M.; H. H. ARAÚJO, P.; AMBROSI, A.; DI LUCCIO, M. Catalytically active membranes for esterification: A review. **Chinese Journal of Chemical Engineering**, 2022. Disponível em: https://doi.org/10.1016/J.CJCHE.2022.03.009. Acesso em: 14 set. 2022.

LI, J.; SUN, Y.; ZHANG, L.; XIAO, X.; YANG, N.; ZHANG, L.; YANG, X.; PENG, F.; JIANG, B. Visible-light induced CoMoO4@Bi2MoO6 heterojunction membrane with attractive photocatalytic property and high precision separation toward oil-in-water emulsion. **Separation and Purification Technology**, v. 277, p. 119568, 2021. Disponível em: https://doi.org/https://doi.org/10.1016/j.seppur.2021.119568

LI, L.; LIU, Z.; ZHANG, Q.; MENG, C.; ZHANG, T.; ZHAI, J. Underwater superoleophobic porous membrane based on hierarchical TiO2 nanotubes: multifunctional integration of oil–water separation, flow-through photocatalysis and self-cleaning. **Journal of Materials Chemistry A**, v. 3, n. 3, p. 1279–1286, 2015. Disponível em: https://doi.org/10.1039/C4TA04699D

LI, N.; CHEN, G. Y.; ZHAO, J. H.; YAN, B. B.; CHENG, Z. J.; MENG, L. J.; CHEN, V. Self-cleaning PDA/ZIF-67@PP membrane for dye wastewater remediation with peroxymonosulfate and visible light activation. **Journal of Membrane Science**, v. 591, 2019. Disponível em: https://doi.org/10.1016/j.memsci.2019.117341

LI, X.; SOTTO, A.; LI, J.; VAN DER BRUGGEN, B. Progress and perspectives for synthesis of sustainable antifouling composite membranes containing in situ generated nanoparticles. **Journal of Membrane Science**, v. 524, p. 502–528, 2017. Disponível em: https://doi.org/10.1016/J.MEMSCI.2016.11.040. Acesso em: 13 jun. 2022.

LI, Z.; HE, H.; LIANG, Y.; OUYANG, L.; ZHANG, T. C.; YUAN, S. Photocatalytically Driven Self-Cleaning and Underwater Superoleophobic Copper Mesh Modified with Hierarchical Bi2WO6@CuO Nanowires for Oil/Water Separation. **Industrial & Engineering Chemistry Research**, v. 59, n. 37, p. 16450–16461, 2020. Disponível em: https://doi.org/10.1021/acs.iecr.0c03101

LIANG, H.; ESMAEILI, H. Application of nanomaterials for demulsification of oily wastewater: A review study. **Environmental Technology & Innovation**, v. 22, p. 101498, 2021. Disponível em: https://doi.org/10.1016/j.eti.2021.101498

LIRA, J. O. B.; RIELLA, H. G.; PADOIN, N.; SOARES, C. CFD + DoE optimization of a flat plate photocatalytic reactor applied to NOx abatement. **Chemical Engineering and Processing - Process Intensification**, v. 154, p. 107998, 2020. Disponível em: https://doi.org/https://doi.org/10.1016/j.cep.2020.107998

LIU, F.; HASHIM, N. A.; LIU, Y.; ABED, M. R. M.; LI, K. Progress in the production and modification of PVDF membranes. **Journal of Membrane Science**, v. 375, n. 1–2, p. 1–27,

2011. Disponível em: https://doi.org/10.1016/J.MEMSCI.2011.03.014. Acesso em: 4 out. 2022.

LIU, R.; FU, X.; WANG, C.; DAWSON, G. Dopamine Surface Modification of Trititanate Nanotubes: Proposed In-Situ Structure Models. **Chemistry – A European Journal**, v. 22, n. 17, p. 6071–6074, 2016. Disponível em: https://doi.org/https://doi.org/10.1002/chem.201600075

LIU, Y. C.; YU, Z. X.; LI, X. H.; SHAO, L. Y.; ZENG, H. J. Super hydrophilic composite membrane with photocatalytic degradation and self-cleaning ability based on LDH and g-C3N4. **Journal of Membrane Science**, v. 617, 2021. Disponível em: https://doi.org/10.1016/j.memsci.2020.118504

LIU, Y.; SU, Y.; CAO, J.; GUAN, J.; ZHANG, R.; HE, M.; FAN, L.; ZHANG, Q.; JIANG, Z. Antifouling, high-flux oil/water separation carbon nanotube membranes by polymer-mediated surface charging and hydrophilization. **Journal of Membrane Science**, v. 542, p. 254–263, 2017. Disponível em: https://doi.org/10.1016/J.MEMSCI.2017.08.018. Acesso em: 28 nov. 2021.

LOH, A.; SHANKAR, R.; HA, S. Y.; AN, J. G.; YIM, U. H. Suspended particles enhance biodegradation of oil in sea. **Science of The Total Environment**, v. 685, p. 324–331, 2019. Disponível em: https://doi.org/10.1016/J.SCITOTENV.2019.05.390

LU, W.; DUAN, C.; LIU, C.; ZHANG, Y.; MENG, X.; DAI, L.; WANG, W.; YU, H.; NI, Y. A self-cleaning and photocatalytic cellulose-fiber- supported "Ag@AgCl@MOF- cloth'' membrane for complex wastewater remediation. **Carbohydrate Polymers**, v. 247, p. 116691, 2020. Disponível em: https://doi.org/https://doi.org/10.1016/j.carbpol.2020.116691

LUO, J.; CHEN, W.; SONG, H.; LIU, J. Fabrication of hierarchical layer-by-layer membrane as the photocatalytic degradation of foulants and effective mitigation of membrane fouling for wastewater treatment. **Science of The Total Environment**, v. 699, p. 134398, 2020. Disponível em: https://doi.org/10.1016/J.SCITOTENV.2019.134398. Acesso em: 13 jun. 2022.

LYNGE, M. E.; SCHATTLING, P.; STÄDLER, B. Recent developments in poly(dopamine)-based coatings for biomedical applications. **Nanomedicine**, v. 10, n. 17, p. 2725–2742, 2015. Disponível em: https://doi.org/10.2217/nnm.15.89

MA, F.-X.; HAO, B.; XI, X.-Y.; WANG, R.; MA, P.-C. Aggregation-induced demulsification technology for the separation of highly emulsified oily wastewater produced in the petrochemical industry. **Journal of Cleaner Production**, v. 374, p. 134017, 2022. Disponível em: https://doi.org/10.1016/J.JCLEPRO.2022.134017. Acesso em: 13 set. 2022.

MA, W.; LI, Y.; GAO, S.; CUI, J.; QU, Q.; WANG, Y.; HUANG, C.; FU, G. Self-Healing and Superwettable Nanofibrous Membranes with Excellent Stability toward Multifunctional Applications in Water Purification. **ACS Applied Materials & Interfaces**, v. 12, n. 20, p. 23644–23654, 2020 a. Disponível em: https://doi.org/10.1021/acsami.0c05701

MA, W.; LI, Y.; ZHANG, M.; GAO, S.; CUI, J.; HUANG, C.; FU, G. Biomimetic Durable Multifunctional Self-Cleaning Nanofibrous Membrane with Outstanding Oil/Water Separation, Photodegradation of Organic Contaminants, and Antibacterial Performances. **ACS Applied Materials & Interfaces**, v. 12, n. 31, p. 34999–35010, 2020 b. Disponível em: https://doi.org/10.1021/acsami.0c09059

MA, Y.; WANG, X.; JIA, Y.; CHEN, X.; HAN, H.; LI, C. Titanium Dioxide-Based Nanomaterials for Photocatalytic Fuel Generations. **Chemical Reviews**, v. 114, n. 19, p. 9987–10043, 2014. Disponível em: https://doi.org/10.1021/cr500008u

MA, Y.; ZHANG, Y.; ZHU, X.; LU, N.; LI, C.; YUAN, X.; QU, J. Photocatalytic degradation and rate constant prediction of chlorophenols and bisphenols by H3PW12O40/GR/TiO2 composite membrane. **Environmental Research**, v. 188, p. 109786, 2020 c. Disponível em: https://doi.org/10.1016/J.ENVRES.2020.109786. Acesso em: 12 jan. 2023.

MAGNONE, E.; HWANG, J. Y.; SHIN, M. C.; ZHUANG, X.; LEE, J. I.; PARK, J. H. Al2O3-Based Hollow Fiber Membranes Functionalized by Nitrogen-Doped Titanium Dioxide for Photocatalytic Degradation of Ammonia Gas. **Membranes**, v. 12, n. 7, p. 693, 2022. Disponível em: https://doi.org/10.3390/membranes12070693

MALLAKPOUR, S.; NIKKHOO, E. Surface modification of nano-TiO2 with trimellitylimido-amino acid-based diacids for preventing aggregation of nanoparticles. **Advanced Powder Technology**, v. 25, n. 1, p. 348–353, 2014. Disponível em: https://doi.org/10.1016/j.apt.2013.05.017

MALTOS, R. A.; REGNERY, J.; ALMARAZ, N.; FOX, S.; SCHUTTER, M.; CATH, T. J.; VERES, M.; CODAY, B. D.; CATH, T. Y. Produced water impact on membrane integrity during extended pilot testing of forward osmosis – reverse osmosis treatment. **Desalination**, v. 440, p. 99–110, 2018. Disponível em: https://doi.org/10.1016/J.DESAL.2018.02.029. Acesso em: 17 nov. 2021.

MAMMA, D.; GERONTAS, S.; PHILIPPOPOULOS, C. J.; CHRISTAKOPOULOS, P.; MACRIS, B. J.; KEKOS, D. Combined Photo-Assisted and Biological Treatment of Industrial Oily Wastewater. **Journal of Environmental Science and Health - Part A Toxic/Hazardous Substances and Environmental Engineering**, v. 39, n. 3, p. 729–740, 2004. Disponível em: https://doi.org/10.1081/ESE-120027738

MARQUES, I. R.; ZIN, G.; PRANDO, L. T.; BRETANHA, C. C.; PRONER, M. C.; RIGO, E.; REZZADORI, K.; DA COSTA, C.; DI LUCCIO, M. Deposition of Dopamine and Polyethyleneimine on Polymeric Membranes: Improvement of Performance of Ultrafiltration Process. **Macromolecular Research**, v. 28, n. 12, p. 1091–1097, 2020. Disponível em: https://doi.org/10.1007/s13233-020-8156-3

MEHMOOD, C. T.; WAHEED, H.; TAN, W.; XIAO, Y. Photocatalytic quorum quenching: A new antifouling and in-situ membrane cleaning strategy for an external membrane bioreactor coupled to UASB. **Journal of Environmental Chemical Engineering**, v. 9, n. 4, p. 105470, 2021. Disponível em: https://doi.org/10.1016/J.JECE.2021.105470. Acesso em: 14 set. 2022.

MENG, A.; CHENG, B.; TAN, H.; FAN, J.; SU, C.; YU, J. TiO2/polydopamine S-scheme heterojunction photocatalyst with enhanced CO2-reduction selectivity. **Applied Catalysis B: Environmental**, v. 289, p. 120039, 2021. Disponível em: https://doi.org/10.1016/J.APCATB.2021.120039. Acesso em: 22 fev. 2023.

MIKLOS, D. B.; REMY, C.; JEKEL, M.; LINDEN, K. G.; DREWES, J. E.; HÜBNER, U. Evaluation of advanced oxidation processes for water and wastewater treatment – A critical review. **Water Research**, v. 139, p. 118–131, 2018. Disponível em: https://doi.org/10.1016/J.WATRES.2018.03.042

MINELLA, M.; FAGA, M. G.; MAURINO, V.; MINERO, C.; PELIZZETTI, E.; COLUCCIA, S.; MARTRA, G. Effect of Fluorination on the Surface Properties of Titania P25 Powder: An FTIR Study. **Langmuir**, v. 26, n. 4, p. 2521–2527, 2010. Disponível em: https://doi.org/10.1021/la902807g

MOKHBI, Y.; KORICHI, M.; AKCHICHE, Z. Combined photocatalytic and Fenton oxidation for oily wastewater treatment. **Applied Water Science**, v. 9, n. 2, p. 35, 2019. Disponível em: https://doi.org/10.1007/s13201-019-0916-x

MOZIA, S. Photocatalytic membrane reactors (PMRs) in water and wastewater treatment. A review. **Separation and Purification Technology**, v. 73, n. 2, p. 71–91, 2010. Disponível em: https://doi.org/10.1016/J.SEPPUR.2010.03.021. Acesso em: 19 jul. 2022.

MOZIA, S.; MORAWSKI, A. W.; MOLINARI, R.; PALMISANO, L.; LODDO, V. Photocatalytic membrane reactors: Fundamentals, membrane materials and operational issues. *In*: **Handbook of Membrane Reactors**. 1. ed. *[S. l.]*: Elsevier, 2013. v. 2, p. 236–295. Disponível em: https://doi.org/10.1533/9780857097347.1.236

MULINARI, J. *et al.* Catalytic membranes for the treatment of oily wastewater. *In*: SHAH, M. P.; RODRIGUEZ-COUTO, S. (org.). **Membrane-Based Hybrid Processes for Wastewater Treatment**. 1. ed. Cambridge: Elsevier, 2021. p. 73–95. Disponível em: https://doi.org/10.1016/b978-0-12-823804-2.00026-4. Acesso em: 27 jun. 2021.

MULINARI, J.; AMBROSI, A.; FENG, Y.; HE, Z.; HUANG, X.; LI, Q.; DI LUCCIO, M.; HOTZA, D.; OLIVEIRA, J. V. Polydopamine-assisted one-step immobilization of lipase on α-alumina membrane for fouling control in the treatment of oily wastewater. **Chemical Engineering Journal**, v. 459, p. 141516, 2023. Disponível em: https://doi.org/10.1016/J.CEJ.2023.141516. Acesso em: 2 fev. 2023.

MULINARI, J.; AMBROSI, A.; INNOCENTINI, M. D. de M.; FENG, Y.; LI, Q.; DI LUCCIO, M.; HOTZA, D.; OLIVEIRA, J. V. Lipase immobilization on alumina membranes using a traditional and a nature-inspired method for active degradation of oil fouling. **Separation and Purification Technology**, v. 287, p. 120527, 2022. Disponível em: https://doi.org/https://doi.org/10.1016/j.seppur.2022.120527

MULINARI, J.; OLIVEIRA, J. V.; HOTZA, D. Lipase immobilization on ceramic supports: An overview on techniques and materials. **Biotechnology Advances**, v. 42, p. 107581, 2020. Disponível em: https://doi.org/10.1016/j.biotechadv.2020.107581

NASCIMBÉN SANTOS, É.; LÁSZLÓ, Z.; HODÚR, C.; ARTHANAREESWARAN, G.; VERÉB, G. Photocatalytic membrane filtration and its advantages over conventional approaches in the treatment of oily wastewater: A review. **Asia-Pacific Journal of Chemical Engineering**, v. 15, n. 5, p. e2533, 2020. Disponível em: https://doi.org/https://doi.org/10.1002/apj.2533

NASKAR, M.; DAS, B.; PAL, D.; SARKAR, D. Performance of Intermeshed Spinning Basket Membrane Module in Ultrafiltration of Oil-Water Emulsion. **Water Conservation Science and Engineering**, v. 3, n. 4, p. 279–287, 2018. Disponível em: https://doi.org/10.1007/s41101-018-0056-4

NASROLLAHI, N.; GHALAMCHI, L.; VATANPOUR, V.; KHATAEE, A. Photocatalytic-membrane technology: a critical review for membrane fouling mitigation. **Journal of Industrial and Engineering Chemistry**, v. 93, p. 101–116, 2021. Disponível em: https://doi.org/10.1016/J.JIEC.2020.09.031. Acesso em: 2 fev. 2023.

NI, M.; LEUNG, M. K. H.; LEUNG, D. Y. C.; SUMATHY, K. A review and recent developments in photocatalytic water-splitting using TiO2 for hydrogen production. **Renewable and Sustainable Energy Reviews**, v. 11, n. 3, p. 401–425, 2007. Disponível em: https://doi.org/https://doi.org/10.1016/j.rser.2005.01.009

ONG, C. S.; LAU, W. J.; GOH, P. S.; NG, B. C.; ISMAIL, A. F. Investigation of submerged membrane photocatalytic reactor (sMPR) operating parameters during oily wastewater

treatment process. **Desalination**, v. 353, p. 48–56, 2014. Disponível em: https://doi.org/10.1016/J.DESAL.2014.09.008. Acesso em: 2 abr. 2020.

OSEGHE, E. O.; NDUNGU, P. G.; JONNALAGADDA, S. B. Synthesis of mesoporous Mn/TiO2 nanocomposites and investigating the photocatalytic properties in aqueous systems. **Environmental Science and Pollution Research**, v. 22, n. 1, p. 211–222, 2015. Disponível em: https://doi.org/10.1007/S11356-014-3356-Z. Acesso em: 13 mar. 2022.

OYMACI, P.; NIJMEIJER, K.; BORNEMAN, Z. Development of Polydopamine Forward Osmosis Membranes with Low Reverse Salt Flux. **Membranes**, v. 10, n. 5, p. 94, 2020. Disponível em: https://doi.org/10.3390/membranes10050094

PADMANABHAN, N. T.; THOMAS, N.; LOUIS, J.; MATHEW, D. T.; GANGULY, P.; JOHN, H.; PILLAI, S. C. Graphene coupled TiO2 photocatalysts for environmental applications: A review. **Chemosphere**, v. 271, p. 129506, 2021. Disponível em: https://doi.org/10.1016/J.CHEMOSPHERE.2020.129506. Acesso em: 20 jul. 2022.

PAIMAN, S. H.; RAHMAN, M. A.; UCHIKOSHI, T.; MD NORDIN, N. A. H.; ALIAS, N. H.; ABDULLAH, N.; ABAS, K. H.; OTHMAN, M. H. D.; JAAFAR, J.; ISMAIL, A. F. In situ growth of α-Fe2O3 on Al2O3/YSZ hollow fiber membrane for oily wastewater. **Separation and Purification Technology**, v. 236, p. 116250, 2020. Disponível em: https://doi.org/https://doi.org/10.1016/j.seppur.2019.116250

PENG, D.; LI, W.; LIANG, X.; ZHENG, L.; GUO, X. Enzymatic preparation of hydrophobic biomass with one-pot synthesis and the oil removal performance. **Journal of Environmental Sciences**, v. 124, p. 105–116, 2023. Disponível em: https://doi.org/10.1016/J.JES.2021.10.019. Acesso em: 7 jan. 2023.

PINTOR, A. M. A.; VILAR, V. J. P.; BOTELHO, C. M. S.; BOAVENTURA, R. A. R. Oil and grease removal from wastewaters: Sorption treatment as an alternative to state-of-the-art technologies. A critical review. **Chemical Engineering Journal**, v. 297, p. 229–255, 2016. Disponível em: https://doi.org/10.1016/J.CEJ.2016.03.121

PRAMODA, K. P.; MOHAMED, A.; PHANG, I. Y.; LIU, T. Crystal transformation and thermomechanical properties of poly(vinylidene fluoride)/clay nanocomposites. **Polymer International**, v. 54, n. 1, p. 226–232, 2005. Disponível em: https://doi.org/10.1002/pi.1692

PRAVEEN, P.; VIRUTHAGIRI, G.; MUGUNDAN, S.; SHANMUGAM, N. Structural, optical and morphological analyses of pristine titanium di-oxide nanoparticles - Synthesized via sol-gel route. **Spectrochimica Acta - Part A: Molecular and Biomolecular Spectroscopy**, v. 117, p. 622–629, 2014. Disponível em: https://doi.org/10.1016/j.saa.2013.09.037

PRONER, M. C.; RAMALHO MARQUES, I.; AMBROSI, A.; REZZADORI, K.; DA COSTA, C.; ZIN, G.; TRES, M. V; DI LUCCIO, M. Impact of MWCO and Dopamine/Polyethyleneimine Concentrations on Surface Properties and Filtration Performance of Modified Membranes. **Membranes**, v. 10, n. 9, 2020. Disponível em: https://doi.org/10.3390/membranes10090239

PUTATUNDA, S.; BHATTACHARYA, S.; SEN, D.; BHATTACHARJEE, C. A review on the application of different treatment processes for emulsified oily wastewater. **International Journal of Environmental Science and Technology**, v. 16, n. 5, p. 2525–2536, 2019. Disponível em: https://doi.org/10.1007/s13762-018-2055-6

QADIR, D.; MUKHTAR, H.; KEONG, L. K. Mixed Matrix Membranes for Water Purification Applications. **Separation and Purification Reviews**, v. 46, n. 1, p. 62–80, 2017. Disponível em: https://doi.org/10.1080/15422119.2016.1196460

QU, F. *et al.* Hierarchically superhydrophilic poly(vinylidene fluoride) membrane with self-cleaning fabricated by surface mineralization for stable separation of oily wastewater. **Journal of Membrane Science**, v. 640, p. 119864, 2021. Disponível em: https://doi.org/https://doi.org/10.1016/j.memsci.2021.119864

RAMASUNDARAM, S.; YOON, S.; KIM, K. J.; PARK, C. Preferential Formation of Electroactive Crystalline Phases in Poly(vinylidene fluoride)/Organically Modified Silicate Nanocomposites. **J Polym Sci Part B: Polym Phys**, v. 46, p. 2173–2187, 2008. Disponível em: https://doi.org/10.1002/polb.21550

RANA, D.; BAG, K.; BHATTACHARYYA, S. N.; MANDAL, B. M. **Miscibility of Poly(styrene-co-butyl acrylate) with Poly(ethyl methacrylate): Existence of Both UCST and LCSTJ Polym Sci B: Polym Phys**. *[S. l.: s. n.]*.

RANA, D.; MANDAL, B. M.; BHATTACHARYYA, S. N. Analogue Calorimetric Studies of Blends of Poly(vinyl ester)s and Polyacrylates. **Macromolecules**, v. 29, p. 1579–1583, 1996.

RAWINDRAN, H.; LIM, J.-W.; GOH, P.-S.; SUBRAMANIAM, M. N.; ISMAIL, A. F.; RADI BIN NIK M DAUD, N. M.; REZAEI-DASHT ARZHANDI, M. Simultaneous separation and degradation of surfactants laden in produced water using PVDF/TiO2 photocatalytic membrane. **Journal of Cleaner Production**, v. 221, p. 490–501, 2019. Disponível em: https://doi.org/10.1016/J.JCLEPRO.2019.02.230

REHMAN, S.; ULLAH, R.; BUTT, A. M.; GOHAR, N. D. Strategies of making TiO2 and ZnO visible light active. **Journal of Hazardous Materials**, v. 170, n. 2–3, p. 560–569, 2009. Disponível em: https://doi.org/10.1016/J.JHAZMAT.2009.05.064. Acesso em: 19 jul. 2022.

RIAZ, S.; PARK, S.-J. An overview of TiO2-based photocatalytic membrane reactors for water and wastewater treatments. **Journal of Industrial and Engineering Chemistry**, v. 84, p. 23–41, 2020. Disponível em: https://doi.org/https://doi.org/10.1016/j.jiec.2019.12.021

ROBERTSON, S. J.; MCGILL, W. B.; MASSICOTTE, H. B.; RUTHERFORD, P. M. Petroleum hydrocarbon contamination in boreal forest soils: a mycorrhizal ecosystems perspective. **Biological Reviews**, v. 82, n. 2, p. 213–240, 2007. Disponível em: https://doi.org/10.1111/j.1469-185X.2007.00012.x

SALEM, F.; THIEMANN, T. Produced Water from Oil and Gas Exploration—Problems, Solutions and Opportunities. **Journal of Water Resource and Protection**, v. 14, n. 02, p. 142–185, 2022. Disponível em: https://doi.org/10.4236/jwarp.2022.142009

SAMUEL, O.; OTHMAN, M. H. D.; KAMALUDIN, R.; KURNIAWAN, T. A.; LI, T.; DZINUN, H.; IMTIAZ, A. Treatment of oily wastewater using photocatalytic membrane

reactors: A critical review. **Journal of Environmental Chemical Engineering**, v. 10, n. 6, p. 108539, 2022. Disponível em: https://doi.org/10.1016/j.jece.2022.108539

SAWALHA, H.; ALSHARABATY, R.; SARSOUR, S.; AL-JABARI, M. Wastewater from leather tanning and processing in Palestine: Characterization and management aspects. **Journal of Environmental Management**, v. 251, p. 109596, 2019. Disponível em: https://doi.org/10.1016/J.JENVMAN.2019.109596. Acesso em: 14 set. 2022.

SAWUNYAMA, L.; OYEWO, O. A.; SEHERI, N.; ONJEFU, S. A.; ONWUDIWE, D. C. Metal oxide functionalized ceramic membranes for the removal of pharmaceuticals in wastewater. **Surfaces and Interfaces**, v. 38, p. 102787, 2023. Disponível em: https://doi.org/10.1016/j.surfin.2023.102787

SHAH BUDDIN, M. M. H.; AHMAD, A. L.; ABD KHALIL, A. T.; PUASA, S. W. A review of demulsification technique and mechanism for emulsion liquid membrane applications. **Journal of Dispersion Science and Technology**, v. 43, n. 6, p. 910–927, 2022. Disponível em: https://doi.org/10.1080/01932691.2020.1845962

SHAH, L. A.; MALIK, T.; SIDDIQ, M.; HALEEM, A.; SAYED, M.; NAEEM, A. TiO2 nanotubes doped poly(vinylidene fluoride) polymer membranes (PVDF/TNT) for efficient photocatalytic degradation of brilliant green dye. **Journal of Environmental Chemical Engineering**, v. 7, n. 5, p. 103291, 2019. Disponível em: https://doi.org/10.1016/J.JECE.2019.103291

SHAH, V.; PRASETYA, N.; LI, K. Polydopamine modification of high-performance PVDF ultrafiltration membranes prepared by the combined crystallisation and diffusion (CCD) method. **Journal of Membrane Science**, v. 635, p. 119538, 2021. Disponível em: https://doi.org/10.1016/J.MEMSCI.2021.119538. Acesso em: 30 mar. 2023.

SHALABY, M. S.; SOŁOWSKI, G.; ABBAS, W. Recent Aspects in Membrane Separation for Oil/Water Emulsion. **Advanced Materials Interfaces**, v. 8, n. 20, 2021. Disponível em: https://doi.org/10.1002/ADMI.202100448. Acesso em: 18 jul. 2022.

SHARMA, S.; KUMAR, R.; RAIZADA, P.; AHAMAD, T.; ALSHEHRI, S. M.; NGUYEN, V.-H.; THAKUR, S.; NGUYEN, C. C.; KIM, S. Y.; LE, Q. van; SINGH, P. An overview on

recent progress in photocatalytic air purification: Metal-based and metal-free photocatalysis. **Environmental Research**, v. 214, p. 113995, 2022. Disponível em: https://doi.org/https://doi.org/10.1016/j.envres.2022.113995

SHARON, M.; MODI, F.; SHARON, M. Titania based nanocomposites as a photocatalyst: A review. **AIMS Materials Science**, v. 3, n. 3, p. 1236–1254, 2016. Disponível em: https://doi.org/10.3934/matersci.2016.3.1236

SHIRAISHI, Y.; HIRAI, T. Selective organic transformations on titanium oxide-based photocatalysts. **Journal of Photochemistry and Photobiology C: Photochemistry Reviews**, v. 9, n. 4, p. 157–170, 2008. Disponível em: https://doi.org/https://doi.org/10.1016/j.jphotochemrev.2008.05.001

SHIRAZI, S.; LIN, C. J.; CHEN, D. Inorganic fouling of pressure-driven membrane processes - A critical review. **Desalination**, v. 250, n. 1, p. 236–248, 2010. Disponível em: https://doi.org/10.1016/j.desal.2009.02.056

SILVA, F. L.; PINHEIRO, J. C.; LEITE, M. J. L.; PRONER, M. C.; DA SILVA, A. F. V.; FREIRE, D. M. G.; TREICHEL, H.; AMBROSI, A.; DI LUCCIO, M. Influence of different PEG/salt aqueous two-phase system on the extraction of 2,3-butanediol. **Preparative Biochemistry & Biotechnology**, v. 52, n. 9, p. 1051–1059, 2022. Disponível em: https://doi.org/10.1080/10826068.2022.2028635

SINGH GAUR, S.; JAGADEESAN, H. Titanium Dioxide (TiO2) based photocatalysis for textile wastewater treatment-its applications and biosafety-A Review. **International Journal of Mechanical Engineering**, v. 6, n. 3, p. 974–5823, 2021.

SINGH, R.; HANKINS, N. P. Introduction to Membrane Processes for Water Treatment. **Emerging Membrane Technology for Sustainable Water Treatment**, p. 15–52, 2016. Disponível em: https://doi.org/10.1016/B978-0-444-63312-5.00002-4. Acesso em: 3 ago. 2022.

SUBRAMANIAM, M. N.; GOH, P. S.; LAU, W. J.; ISMAIL, A. F. Exploring the potential of photocatalytic dual layered hollow fiber membranes incorporated with hybrid titania nanotube-boron for agricultural wastewater reclamation. **Separation and Purification**

Technology, v. 275, p. 119136, 2021. Disponível em: https://doi.org/https://doi.org/10.1016/j.seppur.2021.119136

SUN, F.; LI, T. T.; REN, H. T.; SHIU, B. C.; PENG, H. K.; LIN, J. H.; LOU, C. W. Dopamine-decorated lotus leaf-like PVDF/TiO2 membrane with underwater superoleophobic for highly efficient oil-water separation. **Process Safety and Environmental Protection**, v. 147, p. 788–797, 2021 a. Disponível em: https://doi.org/10.1016/j.psep.2021.01.006

SUN, F.; LI, T. T.; REN, H. T.; SHIU, B. C.; PENG, H. K.; LIN, J. H.; LOU, C. W. Multi-scaled, hierarchical nanofibrous membrane for oil/water separation and photocatalysis: Preparation, characterization and properties evaluation. **Progress In Organic Coatings**, v. 152, 2021 b. Disponível em: https://doi.org/10.1016/j.porgcoat.2020.106125

SUN, W.; SHI, J.; CHEN, C.; LI, N.; XU, Z.; LI, J.; LV, H.; QIAN, X.; ZHAO, L. A review on organic–inorganic hybrid nanocomposite membranes: a versatile tool to overcome the barriers of forward osmosis. **RSC Advances**, v. 8, n. 18, p. 10040–10056, 2018. Disponível em: https://doi.org/10.1039/C7RA12835E

SUNDAR, K. P.; KANMANI, S. Progression of Photocatalytic reactors and it's comparison: A Review. **Chemical Engineering Research and Design**, v. 154, p. 135–150, 2020. Disponível em: https://doi.org/10.1016/J.CHERD.2019.11.035

TANG, C. Y.; CHONG, T. H.; FANE, A. G. Colloidal interactions and fouling of NF and RO membranes: A review. **Advances in Colloid and Interface Science**, v. 164, n. 1–2, p. 126–143, 2011. Disponível em: https://doi.org/10.1016/J.CIS.2010.10.007. Acesso em: 28 nov. 2021.

TANSEL, B.; SEVIMOGLU, O. Coalescence and size distribution characteristics of oil droplets attached on flocs after coagulation. **Water, Air, and Soil Pollution**, v. 169, n. 1–4, p. 293–302, 2006. Disponível em: https://doi.org/10.1007/s11270-006-3110-3

TANUDJAJA, H. J.; CHEW, J. W. Assessment of oil fouling by oil-membrane interaction energy analysis. **Journal of Membrane Science**, v. 560, p. 21–29, 2018. Disponível em: https://doi.org/10.1016/J.MEMSCI.2018.05.008. Acesso em: 28 nov. 2021.

TANUDJAJA, H. J.; HEJASE, C. A.; TARABARA, V. V.; FANE, A. G.; CHEW, J. W. Membrane-based separation for oily wastewater: A practical perspective. **Water Research**, v. 156, p. 347–365, 2019. Disponível em: https://doi.org/10.1016/J.WATRES.2019.03.021

TAVAKOLI, A.; SOHRABI, M.; KARGARI, A. A review of methods for synthesis of nanostructured metals with emphasis on iron compounds. **Chemical Papers**, v. 61, n. 3, p. 151–170, 2007. Disponível em: https://doi.org/10.2478/s11696-007-0014-7

TETTEH, E. K.; RATHILAL, S.; ASANTE-SACKEY, D.; CHOLLOM, M. N. Prospects of Synthesized Magnetic TiO2-Based Membranes for Wastewater Treatment: A Review. **Materials**, v. 14, n. 13, p. 3524, 2021. Disponível em: https://doi.org/10.3390/ma14133524

THEOPHANIDES, S. M. E.-T. Preparation and Characterization of PVDF/PMMA/Graphene Polymer Blend Nanocomposites by Using ATR-FTIR Technique. *In*: **Infrared Spectroscopy**. Rijeka: IntechOpen, 2012. p. Ch. 10. *E-book*. Disponível em: https://doi.org/10.5772/36497

VALE DE MACEDO, G. H. R.; CHAGAS, V. L.; CRUZ DOS SANTOS, M. H.; COSTA DOS SANTOS, G. D.; BAZÁN, J. M. N.; ZAGMIGNAN, A.; CARVALHO, E. M.; MENDONÇA DE MIRANDA, R. de C.; TEIXEIRA, C. S.; NASCIMENTO DA SILVA, L. C. Development and characterization of alginate-derived crosslinked hydrogel membranes incorporated with ConA and gentamicin for wound dressing applications. **Biochemical Engineering Journal**, v. 187, p. 108664, 2022. Disponível em: https://doi.org/10.1016/J.BEJ.2022.108664. Acesso em: 9 fev. 2023.

VASCONCELOS, D. C. L.; COSTA, V. C.; NUNES, E. H. M.; SABIONI, A. C. S.; GASPARON, M.; VASCONCELOS, W. L. Infrared Spectroscopy of Titania Sol-Gel Coatings on 316L Stainless Steel. **Materials Sciences and Applications**, v. 02, n. 10, p. 1375–1382, 2011. Disponível em: https://doi.org/10.4236/msa.2011.210186

VATANPARAST, H.; EFTEKHARI, M.; JAVADI, A.; MILLER, R.; BAHRAMIAN, A. Influence of hydrophilic silica nanoparticles on the adsorption layer properties of non-ionic surfactants at water/heptane interface. **Journal of Colloid and Interface Science**, v. 545, p.

242–250, 2019. Disponível em: https://doi.org/10.1016/J.JCIS.2019.03.047. Acesso em: 30 mar. 2023.

VATANPOUR, V.; MADAENI, S. S.; KHATAEE, A. R.; SALEHI, E.; ZINADINI, S.; MONFARED, H. A. TiO2 embedded mixed matrix PES nanocomposite membranes: Influence of different sizes and types of nanoparticles on antifouling and performance. **Desalination**, v. 292, p. 19–29, 2012. Disponível em: https://doi.org/10.1016/J.DESAL.2012.02.006

VENKATESH, K.; ARTHANAREESWARAN, G.; BOSE, A. C.; KUMAR, P. S. Hydrophilic hierarchical carbon with TiO2 nanofiber membrane for high separation efficiency of dye and oil-water emulsion. **Separation and Purification Technology**, v. 241, p. 116709, 2020. Disponível em: https://doi.org/https://doi.org/10.1016/j.seppur.2020.116709

VO, L. T.; GIANNELIS, E. P. Compatibilizing poly(vinylidene fluoride)/nylon-6 blends with nanoclay. **Macromolecules**, v. 40, n. 23, p. 8271–8276, 2007. Disponível em: https://doi.org/10.1021/ma071508q

WANG, D. *et al.* Stabilization mechanism and chemical demulsification of water-in-oil and oil-in-water emulsions in petroleum industry: A review. **Fuel**, v. 286, p. 119390, 2021. Disponível em: https://doi.org/10.1016/J.FUEL.2020.119390. Acesso em: 14 set. 2022.

WANG, J.; WANG, X.; ZHAO, S.; SUN, B.; WANG, Z.; WANG, J. Robust superhydrophobic mesh coated by PANI/TiO2 nanoclusters for oil/water separation with high flux, self-cleaning, photodegradation and anti-corrosion. **Separation and Purification Technology**, v. 235, p. 116166, 2020 a. Disponível em: https://doi.org/https://doi.org/10.1016/j.seppur.2019.116166

WANG, M.; GAO, Q.; ZHANG, M.; ZHANG, M.; ZHANG, Y.; HU, J.; WU, G. In-situ formation of durable akaganeite (β-FeOOH) nanorods on sulfonate-modified poly(ethylene terephthalate) fabric for dual-functional wastewater treatment. **Journal of Hazardous Materials**, v. 386, p. 121647, 2020 b. Disponível em: https://doi.org/https://doi.org/10.1016/j.jhazmat.2019.121647

WANG, Q.; CUI, J.; XIE, A.; LANG, J.; LI, C.; YAN, Y. PVDF composite membrane with robust UV-induced self-cleaning performance for durable oil/water emulsions separation. **Journal of the Taiwan Institute of Chemical Engineers**, v. 110, p. 130–139, 2020 c. Disponível em: https://doi.org/10.1016/j.jtice.2020.02.024

WANG, Q.; GAO, Q.; AL-ENIZI, A. M.; NAFADY, A.; MA, S. Recent advances in MOF-based photocatalysis: environmental remediation under visible light. **Inorganic Chemistry Frontiers**, v. 7, n. 2, p. 300–339, 2020 d. Disponível em: https://doi.org/10.1039/C9QI01120J

WANG, Q. X.; YU, Z. X.; LIU, Y. C.; ZHU, X. M.; LONG, R. X.; LI, X. Y. Co-intercalation of TiO2 and LDH to reduce graphene oxide photocatalytic composite membrane for purification of dye wastewater. **Applied Clay Science**, v. 216, 2022. Disponível em: https://doi.org/10.1016/j.clay.2021.106359

WANG, T.; QIBLAWEY, H.; JUDD, S.; BENAMOR, A.; NASSER, M. S.; MOHAMMADIAN, A. Fabrication of high flux nanofiltration membrane via hydrogen bonding based co-deposition of polydopamine with poly(vinyl alcohol). **Journal of Membrane Science**, v. 552, p. 222–233, 2018. Disponível em: https://doi.org/10.1016/J.MEMSCI.2018.02.009. Acesso em: 26 ago. 2022.

WANG, Y.; ZHANG, Y.; WANG, J. Nano spinel CoFe2O4 deposited diatomite catalytic separation membrane for efficiently cleaning wastewater. **Journal of Membrane Science**, v. 615, p. 118559, 2020. Disponível em: https://doi.org/https://doi.org/10.1016/j.memsci.2020.118559

WANG, Z.; YANG, H. C.; HE, F.; PENG, S.; LI, Y.; SHAO, L.; DARLING, S. B. Mussel-Inspired Surface Engineering for Water-Remediation Materials. **Matter**, v. 1, n. 1, p. 115–155, 2019. Disponível em: https://doi.org/10.1016/J.MATT.2019.05.002. Acesso em: 26 ago. 2022.

WEI, X.; ZHANG, S.; HAN, Y.; WOLFE, F. A. Treatment of petrochemical wastewater and produced water from oil and gas. **Water Environment Research**, v. 91, n. 10, p. 1025–1033, 2019. Disponível em: https://doi.org/10.1002/wer.1172

WU, C.-H. Comparison of azo dye degradation efficiency using UV/single semiconductor and UV/coupled semiconductor systems. **Chemosphere**, v. 57, n. 7, p. 601–608, 2004. Disponível em: https://doi.org/10.1016/j.chemosphere.2004.07.008

WU, P.; JIANG, L. Y.; HE, Z.; SONG, Y. Treatment of metallurgical industry wastewater for organic contaminant removal in China: status, challenges, and perspectives. **Environmental Science: Water Research & Technology**, v. 3, n. 6, p. 1015–1031, 2017. Disponível em: https://doi.org/10.1039/C7EW00097A

XIA, P.; LIU, M.; CHENG, B.; YU, J.; ZHANG, L. Dopamine Modified g-C $_3$ N $_4$ and Its Enhanced Visible-Light Photocatalytic H $_2$ -Production Activity. **ACS Sustainable Chemistry & Engineering**, v. 6, n. 7, p. 8945–8953, 2018. Disponível em: https://doi.org/10.1021/acssuschemeng.8b01300

XU, Q.; YU, J.; ZHANG, J.; ZHANG, J.; LIU, G. Cubic anatase TiO2 nanocrystals with enhanced photocatalytic CO2 reduction activity. **Chemical Communications**, v. 51, n. 37, p. 7950–7953, 2015. Disponível em: https://doi.org/10.1039/C5CC01087J

XUE, J.; XU, M.; GAO, J.; ZONG, Y.; WANG, M.; MA, S. Multifunctional porphyrinic Zr-MOF composite membrane for high-performance oil-in-water separation and organic dye adsorption/photocatalysis. **Colloids and Surfaces A: Physicochemical and Engineering Aspects**, v. 628, p. 127288, 2021. Disponível em: https://doi.org/https://doi.org/10.1016/j.colsurfa.2021.127288

YAACOB, N.; GOH, P. S.; ISMAIL, A. F.; NAZRI, N. A. M.; NG, B. C.; ABIDIN, M. N. Z.; YOGARATHINAM, L. T. ZrO2–TiO2 incorporated pvdf dual-layer hollow fiber membrane for oily wastewater treatment: Effect of air gap. **Membranes**, v. 10, n. 6, p. 1–18, 2020. Disponível em: https://doi.org/10.3390/MEMBRANES10060124. Acesso em: 13 abr. 2022.

YAN, Z.; ZHANG, Y.; YANG, H.; FAN, G.; DING, A.; LIANG, H.; LI, G.; REN, N.; VAN DER BRUGGEN, B. Mussel-inspired polydopamine modification of polymeric membranes for the application of water and wastewater treatment: A review. **Chemical Engineering Research and Design**, v. 157, p. 195–214, 2020. Disponível em: https://doi.org/10.1016/J.CHERD.2020.03.011. Acesso em: 26 ago. 2022.

YANG, D.; YANG, Y.; XIA, J. Hydrological cycle and water resources in a changing world: A review. **Geography and Sustainability**, v. 2, n. 2, p. 115–122, 2021. Disponível em: https://doi.org/10.1016/J.GEOSUS.2021.05.003. Acesso em: 2 fev. 2023.

YANG, F.; GUO, Z. Fabrication of inorganic-organic hybrid TiO2@PDA@CuO composite nanoparticles and its special wettable, gas sensing and photocatalytic behaviors. **Materials Letters**, v. 217, p. 320–323, 2018. Disponível em: https://doi.org/10.1016/J.MATLET.2018.01.122. Acesso em: 22 fev. 2023.

YANG, J.; WANG, L.; XIE, A.; DAI, X.; YAN, Y.; DAI, J. Facile surface coating of metal-tannin complex onto PVDF membrane with underwater Superoleophobicity for oil-water emulsion separation. **Surface and Coatings Technology**, v. 389, n. November 2019, p. 125630, 2020. Disponível em: https://doi.org/10.1016/j.surfcoat.2020.125630

YANG, W.; LIU, C.; CHEN, Y. Stability of Polydopamine Coatings on Gold Substrates Inspected by Surface Plasmon Resonance Imaging. **Langmuir**, v. 34, n. 12, p. 3565–3571, 2018. Disponível em: https://doi.org/10.1021/acs.langmuir.7b03143. Acesso em: 21 fev. 2023.

YIN, H.; ZHAO, J.; LI, Y. Q.; HUANG, L. L.; ZHANG, H.; CHEN, L. H. A novel Pd decorated polydopamine-SiO2/PVA electrospun nanofiber membrane for highly efficient degradation of organic dyes and removal of organic chemicals and oils. **Journal of Cleaner Production**, v. 275, 2020. Disponível em: https://doi.org/10.1016/j.jclepro.2020.122937

YU, J.; FAN, J.; ZHAO, L. Dye-sensitized solar cells based on hollow anatase TiO2 spheres prepared by self-transformation method. **Electrochimica Acta**, v. 55, n. 3, p. 597–602, 2010. Disponível em: https://doi.org/https://doi.org/10.1016/j.electacta.2009.09.021

YU, J.; LOW, J.; XIAO, W.; ZHOU, P.; JARONIEC, M. Enhanced Photocatalytic CO2-Reduction Activity of Anatase TiO2 by Coexposed {001} and {101} Facets. **Journal of the American Chemical Society**, v. 136, n. 25, p. 8839–8842, 2014. Disponível em: https://doi.org/10.1021/ja5044787

YU, L.; HAN, M.; HE, F. A review of treating oily wastewater. **Arabian Journal of Chemistry**, v. 10, p. S1913–S1922, 2017. Disponível em: https://doi.org/10.1016/J.ARABJC.2013.07.020

YU, S.; ZHENG, W.; YU, W.; ZHANG, Y.; JIANG, Q.; ZHAO, Z. Formation mechanism of β-phase in PVDF/CNT composite prepared by the sonication method. **Macromolecules**, v. 42, n. 22, p. 8870–8874, 2009. Disponível em: https://doi.org/10.1021/ma901765j

YU, Z.; MIN, X.; LI, F.; YIN, D.; PENG, Y.; ZENG, G. A mussel-inspired method to fabricate a novel reduced graphene oxide/Bi12O17Cl2 composites membrane for catalytic degradation and oil/water separation. **Polymers for Advanced Technologies**, v. 30, n. 1, p. 101–109, 2019. Disponível em: https://doi.org/10.1002/pat.4448

YUE, R.-Y.; GUAN, J.; ZHANG, C.-M.; YUAN, P.-C.; LIU, L.-N.; ZAHEER AFZAL, M.; WANG, S.-G.; SUN, X.-F. Photoinduced superwetting membranes for separation of oil-in-water emulsions. **Separation and Purification Technology**, v. 241, p. 116536, 2020. Disponível em: https://doi.org/https://doi.org/10.1016/j.seppur.2020.116536

ZENG, G.; WEI, K.; YANG, D.; YAN, J.; ZHOU, K.; PATRA, T.; SENGUPTA, A.; CHIAO, Y.-H. Improvement in performance of PVDF ultrafiltration membranes by co-incorporation of dopamine and halloysite nanotubes. **Colloids and Surfaces A: Physicochemical and Engineering Aspects**, v. 586, p. 124142, 2020. Disponível em: https://doi.org/https://doi.org/10.1016/j.colsurfa.2019.124142

ZHANG, D.; WANG, G.; ZHI, S.; XU, K.; ZHU, L.; LI, W.; ZENG, Z.; XUE, Q. Superhydrophilicity and underwater superoleophobicity TiO2\Al2O3 composite membrane with ultra low oil adhesion for highly efficient oil-in-water emulsions separation. **Applied Surface Science**, v. 458, n. February, p. 157–165, 2018. Disponível em: https://doi.org/10.1016/j.apsusc.2018.07.052

ZHANG, L.; YANG, J.; ZHAO, X.; XIAO, X.; SUN, F.; ZUO, X.; NAN, J. Small-molecule surface-modified bismuth-based semiconductors as a new class of visible-light-driven photocatalytic materials: Structure-dependent photocatalytic properties and

photosensitization mechanism. **Chemical Engineering Journal**, v. 380, p. 122546, 2020. Disponível em: https://doi.org/10.1016/J.CEJ.2019.122546. Acesso em: 20 jul. 2022.

ZHANG, L.-P.; LIU, Z.; FARAJ, Y.; ZHAO, Y.; ZHUANG, R.; XIE, R.; JU, X.-J.; WANG, W.; CHU, L.-Y. High-flux efficient catalytic membranes incorporated with iron-based Fenton-like catalysts for degradation of organic pollutants. **Journal of Membrane Science**, v. 573, p. 493–503, 2019. Disponível em: https://doi.org/10.1016/J.MEMSCI.2018.12.032

ZHU, M.; LIU, Y.; CHEN, M.; SADRZADEH, M.; XU, Z.; GAN, D.; HUANG, Z.; MA, L.; YANG, B.; ZHOU, Y. Robust superhydrophilic and underwater superoleophobic membrane optimized by Cu doping modified metal-organic frameworks for oil-water separation and water purification. **Journal of Membrane Science**, v. 640, p. 119755, 2021. Disponível em: https://doi.org/https://doi.org/10.1016/j.memsci.2021.119755

ZIN, G.; WU, J.; REZZADORI, K.; PETRUS, J. C. C.; DI LUCCIO, M.; LI, Q. Modification of hydrophobic commercial PVDF microfiltration membranes into superhydrophilic membranes by the mussel-inspired method with dopamine and polyethyleneimine. **Separation and Purification Technology**, v. 212, p. 641–649, 2019. Disponível em: https://doi.org/https://doi.org/10.1016/j.seppur.2018.10.014

ZIOUI, D.; SALAZAR, H.; AOUDJIT, L.; MARTINS, P. M. Photocatalytic polymeric nanocomposite membrane towards oily wastewater. **Preprints**, n. April, p. 1–11, 2019. Disponível em: https://doi.org/10.20944/preprints201904.0060.v1

ZONG, Y. Q.; MA, S. S.; XUE, J. J.; GU, J. D.; WANG, M. X. Bifunctional NiAlFe LDH-coated membrane for oil-in-water emulsion separation and photocatalytic degradation of antibiotic. **Science of The Total Environment**, v. 751, 2021. Disponível em: https://doi.org/10.1016/j.scitotenv.2020.141660

APPENDIX A (Supplementary material chapter 3)

Figure A1. Permeate flux vs pressure for all membranes tested in this study.

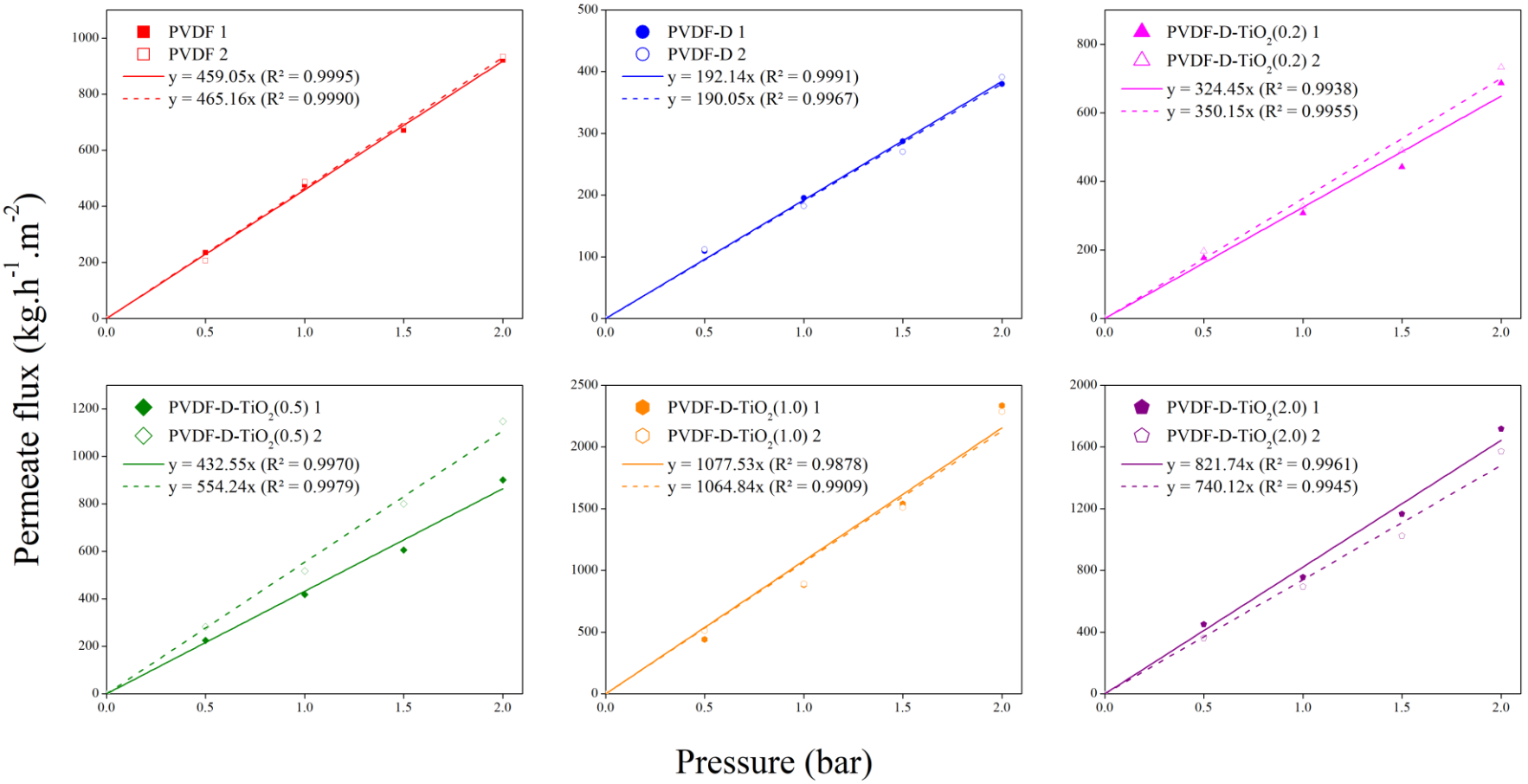

APPENDIX B (Supplementary material chapter 4)

Figure B1. Droplet size determined by a LUMiSizer dispersion analyzer.

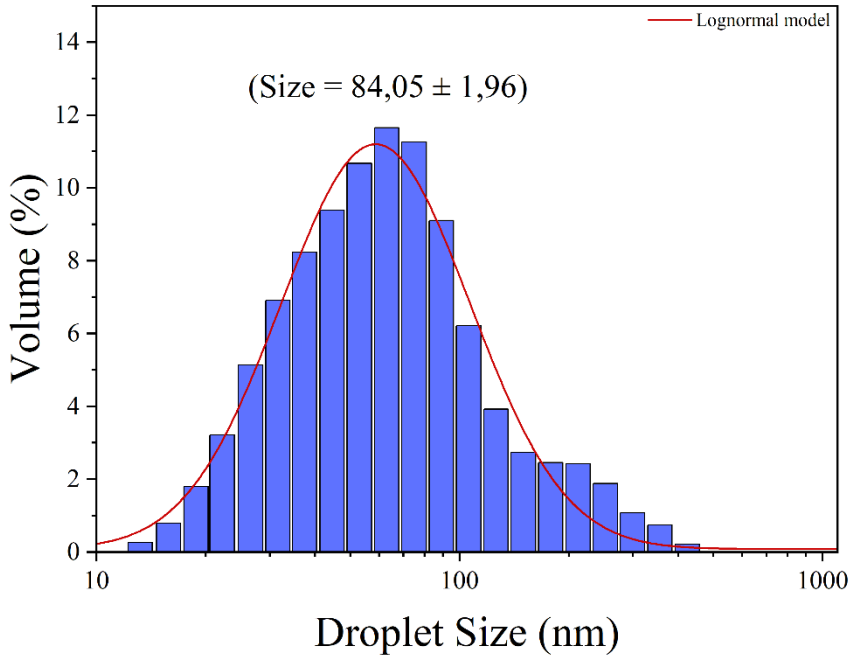

Figure B2. UV-vis spectra for membrane stability at different pHs and images of solutions after 12 hours of exposure.

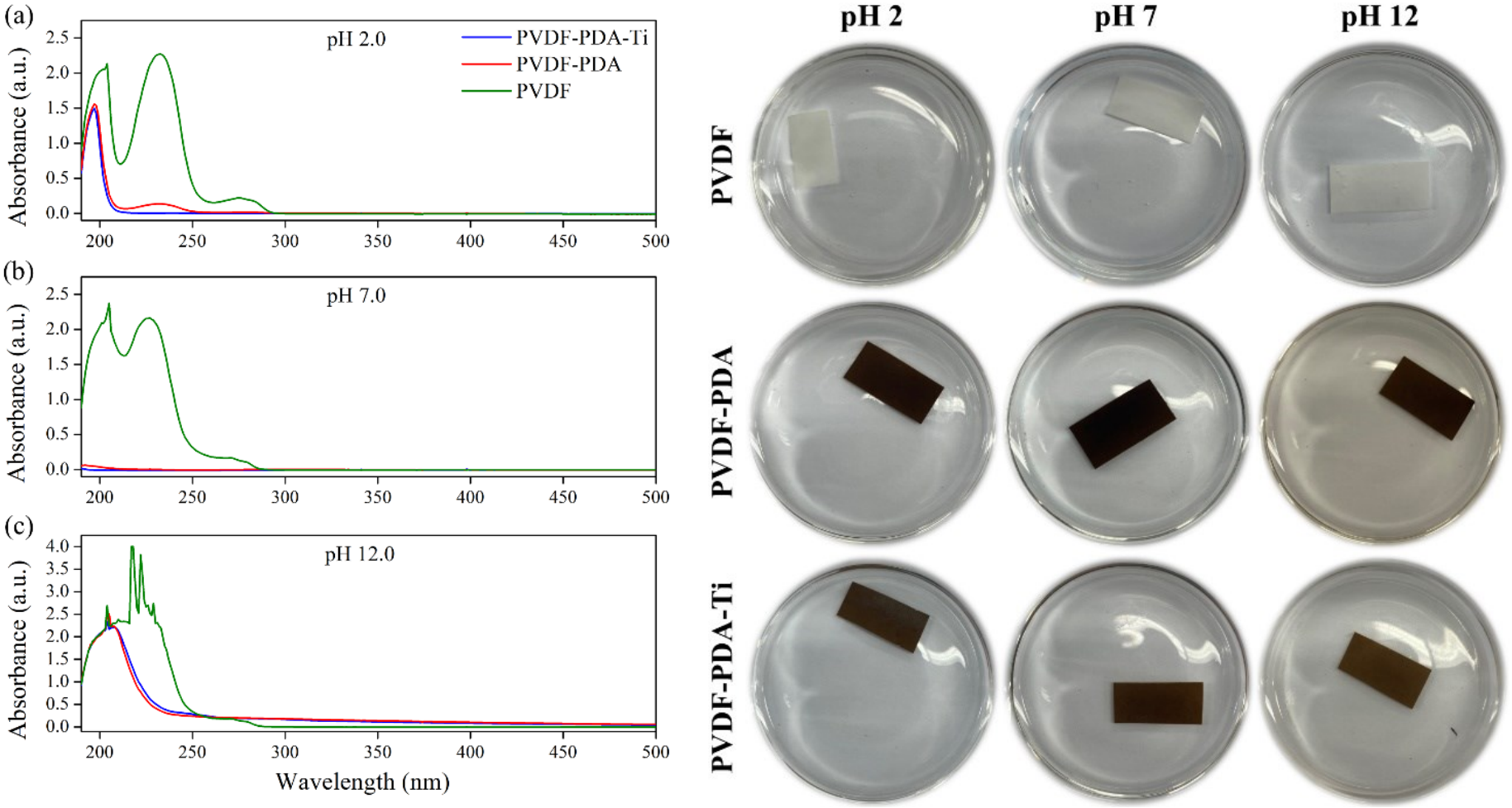

Figure B3. Images of all membranes obtained through the different conditions evaluated in the work.

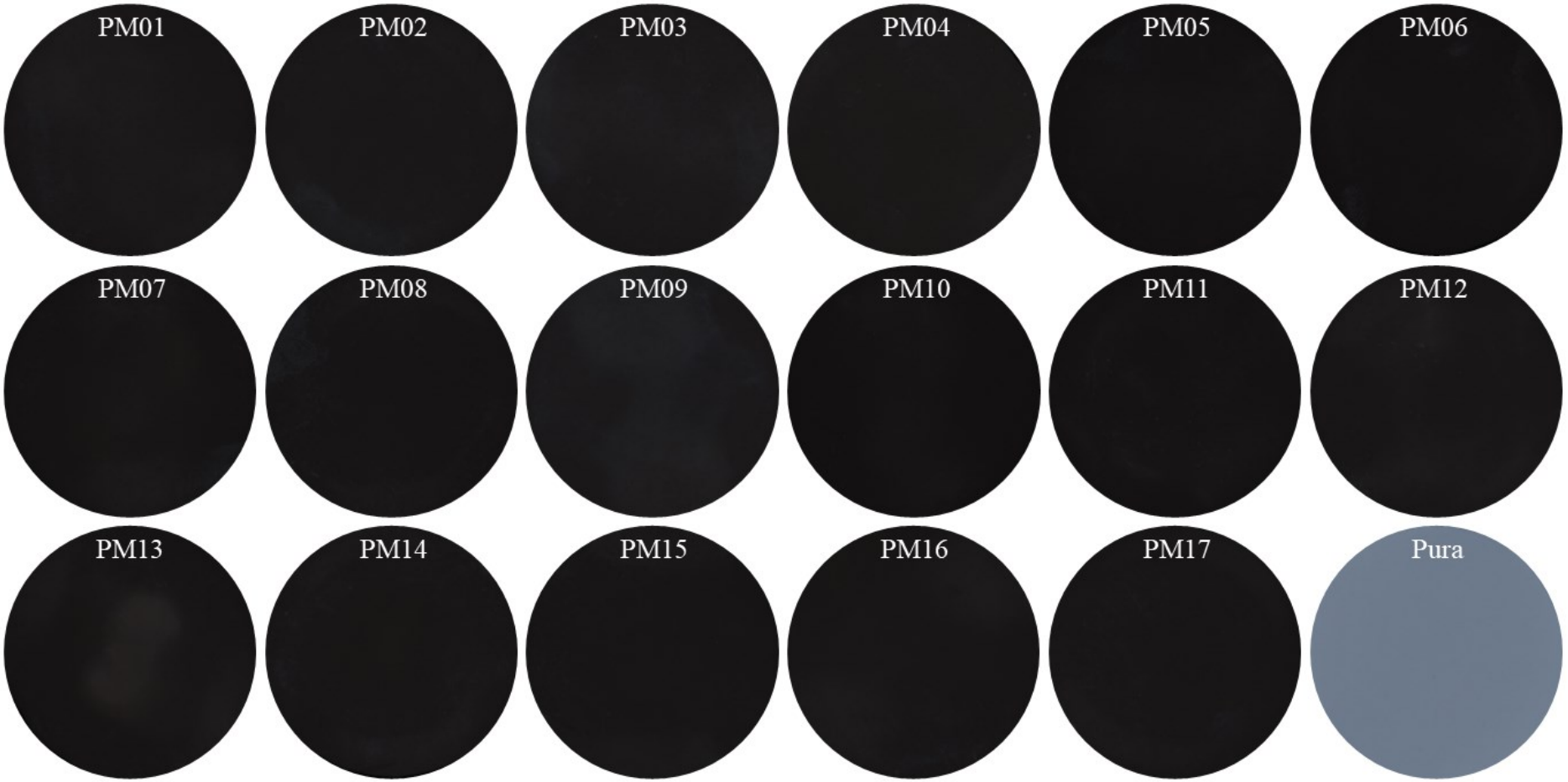

* The photographs were taken using a high-end professional camera, ensuring excellent quality and accuracy. To ensure uniformity and minimize the effects of lighting variations, all the images were captured under consistent lighting conditions.

Table B1. Coded matrix for experimental design and responses.

Essay	X_1-DA concentration (g L^{-1})	X_2-TiO_2 amount (%)	X_3-Agitation (rpm)	Water permeance (kg h^{-1} bar^{-1} m^{-2})	TOC rejection (%)	Degradation (%)
1	1.0	1.0	120.0	714.53	84.55	95.5
2	1.0	1.0	160.0	558.82	82.71	89.7
3	1.0	2.0	120.0	757.38	84.15	97.3
4	1.0	2.0	160.0	593.62	85.40	93.0
5	2.0	1.0	120.0	804.18	83.95	65.0
6	2.0	1.0	160.0	791.83	81.29	60.5
7	2.0	2.0	120.0	540.30	79.64	71.8
8	2.0	2.0	160.0	830.22	80.78	65.7
9	0.7	1.5	140.0	708.33	82.09	96.8
10	2.3	1.5	140.0	758.35	82.75	52.0
11	1.5	0.7	140.0	709.06	81.46	59.6
12	1.5	2.3	140.0	731.78	88.82	90.1
13	1.5	1.5	106.4	673.13	83.78	71.2
14	1.5	1.5	173.6	723.52	80.47	80.0
15	1.5	1.5	140.0	777.64	77.80	64.1
16	1.5	1.5	140.0	761.17	75.61	66.0
17	1.5	1.5	140.0	732.26	75.73	68.1

Table B2. Analysis of variance (ANOVA) for the Water permeance, TOC rejection, and MB degradation of membranes in the experimental design (CCRD).

Water permeance	SS	DF	MS	F	p
(1) DA concentration (g L^{-1})(L)	13308.0	1	13308.01	25.22	0.04*
DA concentration (g L^{-1})(Q)	1609.3	1	1609.32	3.05	0.22
(2) TiO_2 amount (%)(L)	880.5	1	880.51	1.67	0.33
TiO_2 amount (%)(Q)	3074.7	1	3074.71	5.83	0.14
(3) Agitation (rpm)(L)	134.4	1	134.42	0.25	0.66
Agitation (rpm)(Q)	6671.1	1	6671.09	12.64	0.07
1L by 2L	11486.2	1	11486.16	21.77	0.04*
1L by 3L	44556.8	1	44556.83	84.44	0.01*
2L by 3L	10819.8	1	10819.78	20.51	0.05*
Lack of Fit	18907.2	5	3781.43	7.17	0.13
Pure Error	1055.3	2	527.66		
Total SS	108984.6	16			R^2=0.8168
TOC rejection	SS	DF	MS	F	p
(1) DA concentration (g L^{-1})(L)	7.39	1	7.39	4.88	0.16
DA concentration (g L^{-1})(Q)	42.85	1	42.85	28.28	0.03*
(2) TiO_2 amount (%)(L)	7.09	1	7.09	4.68	0.16
TiO_2 amount (%)(Q)	95.48	1	95.48	63.02	0.02*
(3) Agitation (rpm)(L)	4.32	1	4.32	2.85	0.23
Agitation (rpm)(Q)	38.37	1	38.37	25.33	0.04*
1L by 2L	6.30	1	6.30	4.16	0.18
1L by 3L	0.11	1	0.11	0.07	0.81
2L by 3L	5.92	1	5.92	3.91	0.19
Lack of Fit	33.22	5	6.64	4.39	0.20
Pure Error	3.03	2	1.52		
Total SS	184.60	16			R^2=0.8036
MB degradation	SS	DF	MS	F	p
(1) DA concentration (g L^{-1})(L)	2586.55	1	2586.55	662.32	0.00*
DA concentration (g L^{-1})(Q)	172.56	1	172.56	44.19	0.02*
(2) TiO_2 amount (%)(L)	341.81	1	341.81	87.52	0.01*
TiO_2 amount (%)(Q)	185.69	1	185.69	47.55	0.02*
(3) Agitation (rpm)(L)	2.56	1	2.56	0.65	0.50
Agitation (rpm)(Q)	210.14	1	210.14	53.81	0.02*
1L by 2L	6.09	1	6.09	1.56	0.34
1L by 3L	0.02	1	0.02	0.00	0.95
2L by 3L	0.01	1	0.01	0.00	0.97
Lack of Fit	312.33	5	62.47	15.99	0.06
Pure Error	7.81	2	3.91		
Total SS	3615.20	16			R^2=0.9115

*$p < 0.05$ – Significative factors.